Surface Plasmon Resonance Sensors for Detection of Chemical and Biological Species

Ji Homola

Chem. Rev., **2008**, 108 (2), 462-493 • DOI: 10.1021/cr068107d

Surface Plasmon Resonance Sensors for Detection of Chemical and Biological Species

Jiří Homola†

Institute of Photonics and Electronics ASCR, Chaberská 57, 182 51 Prague 8, Czech Republic

Received May 31, 2007

Contents

† Telephone +420 266 773 448; fax +420 284 681 534; e-mail homola@ufe.cz.

1. Introduction

Optical sensors based on excitation of surface plasmons, commonly referred to as surface plasmon resonance (SPR) sensors, belong to the group of refractometric sensing devices including the resonant mirror sensor,[1,2] the grating coupler sensor,[3−5] the integrated optical Mach−Zehnder interferometer,[6,7] the integrated Young interferometer,[8,9] and the white light interferometer,[10,11] which measure changes in the refractive index occurring in the field of an electromagnetic wave supported by the optical structure of the sensor.

Since the first demonstration of surface plasmon resonance for the study of processes at the surfaces of metals[12] and sensing of gases[13] in the early 1980s, SPR sensors have made vast advances in terms of both development of the technology and its applications. SPR biosensors have become a central tool for characterizing and quantifying biomolecular interactions. Moreover, development of SPR sensors for detection of chemical and biological species has gained considerable momentum, and the number of publications reporting applications of SPR biosensors for detection of analytes related to medical diagnostics, environmental monitoring, and food safety and security has been rapidly growing. Over the past decade, thousands of research papers on SPR biosensors have been published. SPR biosensors, as one of the main optical biosensor technologies, have been also extensively featured in biosensor books[14−17] and reviews.[18−26] Review articles[27−30] and books[31] focused on SPR biosensor technology have also been published.

10.1021/cr068107d CCC: $71.00
Published on Web 01/30/2008

Jiří Homola received his M.S. degree in physical engineering in 1988 from the Czech Technical University, Prague, Czech Republic, and his Ph.D. degree from the Academy of Sciences of the Czech Republic in 1993. Since then, he has been with the Institute of Photonics and Electronics, Prague, Czech Republic. From 1997 to 2002, he was with the Department of Electrical Engineering, University of Washington, Seattle, since 2001 as a Research Associate Professor. He is currently Head of Photonics Division and Chairman of Department of Optical Sensors at the Institute of Photonics and Electronics, Prague, and Affiliate Associate Professor at the University of Washington, Seattle. Dr. Homola is a Member of the Editorial Board of *Sensors and Actuators B* (Elsevier) and Associate Editor of the *Journal of Sensors* (Hindawi). He has served on technical committees of numerous scientific conferences and is a Member of the Permanent Steering Committees of Advanced Study Course on Optical Chemical Sensors and Europt(r)ode Conference Series. He is also a Member of the NATO CBP Advisory Panel. He received the Otto Wichterle Prize, Czech Republic, in 2003, and the Roche Diagnostics Prize for Sensor Technology, Germany, in 2006. Dr. Homola has edited 2 books, 3 book chapters, and 60 research papers in scientific journals and presented over 100 research papers at international conferences. His research interests are in biophotonics, guided-wave photonics, optical sensors, and biosensors.

This paper reviews advances in SPR sensor technology and its applications since the year 2000. The review focuses on SPR sensors employing conventional (unlocalized) surface plasmons propagating along planar structures and their applications for detection of chemical and biological species. Aspects related to applications of SPR method for the study of biomolecules and their interactions are outside the scope of this review.

2. Surface Plasmons on Planar Structures

The first observation of surface plasmons was made in 1902 by Wood, who reported anomalies in the spectrum of light diffracted on a metallic diffraction grating.[32] Fano has proven that these anomalies are associated with the excitation of electromagnetic surface waves on the surface of the diffraction grating.[33] In 1968 Otto demonstrated that the drop in the reflectivity in the attenuated total reflection (ATR) method is due to the excitation of surface plasmons.[34] In the same year, Kretschmann and Raether observed excitation of surface plasmons in another configuration of the attenuated total reflection method.[35] These pioneering works of Otto, Kretschmann, and Raether established a convenient method for the excitation of surface plasmons and their investigation and ushered surface plasmons into modern optics. Fundamentals of surface plasmons can be found in numerous review articles and books.[36−39]

2.1. Surface Plasmons on Metal−Dielectric Interface

The simplest geometry in which a surface plasmon can exist consists of a semi-infinite metal with a complex

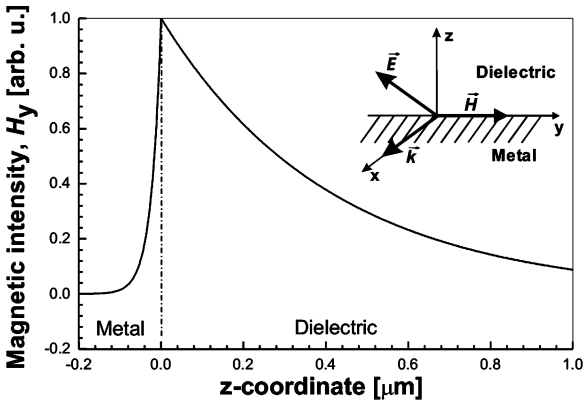

Figure 1. Spatial distribution of the magnetic intensity for a surface plasmon at the interface between gold and a dielectric ($n_d = 1.328$) in the direction perpendicular to the interface, $\lambda = 850$ nm.

permittivity, $\epsilon_m = \epsilon'_m + i\epsilon''_m$, and a semi-infinite dielectric with permittivity, $\epsilon_d = \epsilon'_d + i\epsilon''_d$, where ϵ'_j and ϵ''_j are real and imaginary parts of ϵ_j (j is m or d). Analysis of Maxwell's equations with appropriate boundary conditions suggests that this structure can support only a single guided mode of electromagnetic field—a surface plasmon. Surface plasmon is a transversally magnetic (TM) mode, and therefore its vector of intensity of magnetic field lies in the plane of metal−dielectric interface and is perpendicular to the direction of propagation. If we use such a Cartesian system of coordinates that the metal occupies the region $z < 0$ and the surface plasmon propagates along the x-axis, the vector of magnetic intensity $\vec{H}$ of the surface plasmon can be written as

$$\vec{H}_j = (0,H_y,0)_j = (0,1,0)A\exp[-\alpha_j z + i(\beta x - \omega t)] \quad (1)$$

where ω is the angular frequency, t is time, β is the propagation constant, $\alpha_j = \sqrt{\beta^2 - (\omega/c)^2\epsilon_j}$, where j is either m for metal or d for dielectric, and $i = \sqrt{-1}$. The vector of the electric field is perpendicular to the vector of the magnetic intensity and can be calculated from Maxwell's equations and eq 1. A typical profile of the magnetic field of a surface plasmon is shown in Figure 1. The intensity of the magnetic field reaches its maximum at the metal−dielectric interface and decays into both the metal and dielectric. The field decay in the direction perpendicular to the metal−dielectric interface is characterized by the penetration depth, which is defined as the distance from the interface at which the amplitude of the field decreases by a factor of e (where e is the base of the natural logarithm). The penetration depth depends on the wavelength and permittivities of the materials involved. Penetration depth into the dielectric for a surface plasmon propagating along the interface of gold and a dielectric with $n_d = 1.32$ increases with wavelength and ranges from 100 to 600 nm in the wavelength region from 600 to 1000 nm.[31]

The propagation constant of a surface plasmon at a metal−dielectric interface can be expressed as

$$\beta_{SP} = \frac{\omega}{c}\sqrt{\frac{\epsilon_d\epsilon_m}{\epsilon_d + \epsilon_m}} = \frac{2\pi}{\lambda}\sqrt{\frac{\epsilon_d\epsilon_m}{\epsilon_d + \epsilon_m}} \quad (2)$$

where c is the speed of light in a vacuum and λ is the wavelength in a vacuum.[36,37] If the structure is lossless ($\epsilon''_m = \epsilon''_d = 0$), eq 2 represents a guided mode only if the

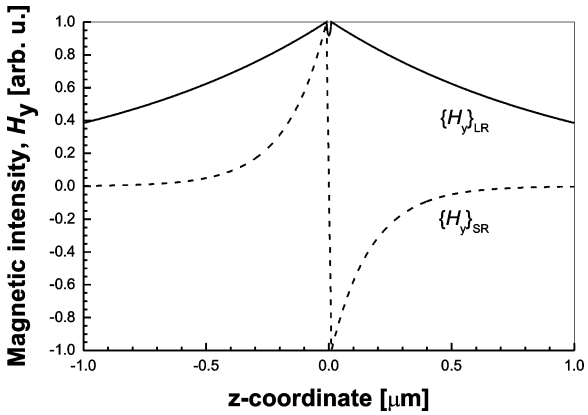

Figure 2. Spatial distribution of the magnetic intensity of symmetric and antisymmetric surface plasmons propagating along a thin gold film ($\epsilon_m = -30.5 + i\,1.6$, thickness = 20 nm) embedded between two identical dielectrics ($n_d = 1.328$), $\lambda = 850$ nm.

permittivities ϵ'_m and ϵ'_d are of opposite signs and $\epsilon'_m < -\epsilon'_d$. As the permittivity of dielectric materials is usually positive, this requires that the real part of the permittivity of the metal is negative. Metals such as gold, silver, and aluminum exhibit a negative real part of permittivity in the visible and near-infrared regions of the spectrum. These metals also exhibit a considerable imaginary part of the permittivity, which causes the propagation constant of a surface plasmon to have a nonzero imaginary part. The imaginary part of the propagation constant is associated with the attenuation of the surface plasmon in the direction of propagation.[36,37] The propagation constant is related to the effective index n_{ef} and attenuation b as

$$n_{ef} = \frac{c}{\omega}\mathrm{Re}\{\beta_{SP}\},\ b = \frac{0.2}{\ln 10}\mathrm{Im}\{\beta_{SP}\} \qquad (3)$$

where Re{ } and Im{ } denote the real and imaginary parts of a complex number, respectively; the attenuation b is in dBcm^{-1} if β is given in m^{-1}.

2.2. Long-Range and Short-Range Surface Plasmons

A planar structure consisting of a thick metal film sandwiched between two semi-infinite dielectrics supports two independent surface plasmons at the opposite boundaries of the metal film. If the metal film is thin, coupling between the surface plasmons at opposite boundaries of the metal film can occur, giving rise to mixed modes of electromagnetic field—symmetric and antisymmetric surface plasmons. Characteristics of these surface plasmons can be found from Maxwell's equations and appropriate boundary conditions.[40−42] The symmetric surface plasmon exhibits a propagation constant and attenuation, which both increase with increasing metal film thickness.[31] The propagation constant and attenuation of the antisymmetric surface plasmon decrease with increasing thickness of the metal film. The symmetric surface plasmon exhibits a lower attenuation than its antisymmetric counterpart, and therefore it is referred to as a long-range surface plasmon, whereas the antisymmetric mode is referred to as a short-range surface plasmon.[40,41]

Figure 2 shows the distribution of magnetic intensity of the symmetric and antisymmetric surface plasmons propagating along a thin gold film surrounded by two identical dielectrics. The profiles of magnetic intensity of symmetric and antisymmetric plasmons are symmetric or antisymmetric

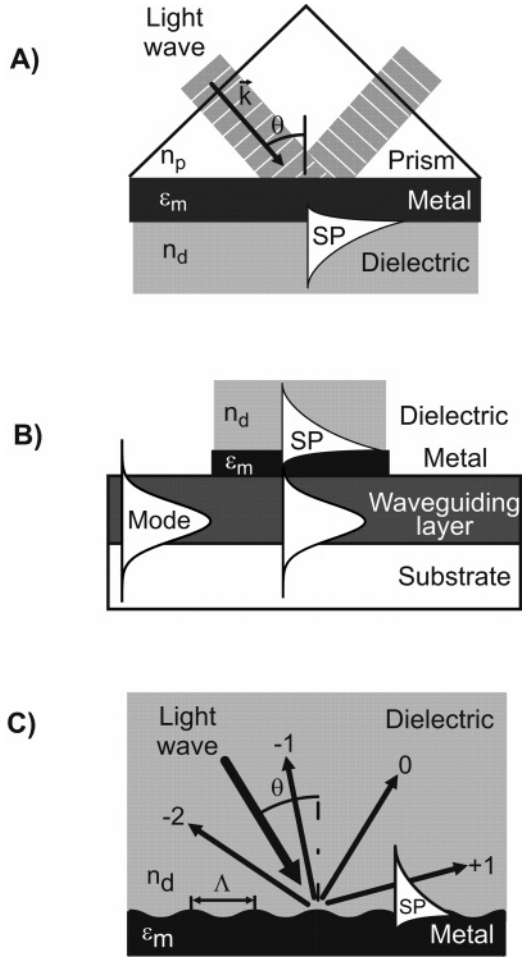

Figure 3. Coupling of light to a surface plasmon via (A) prism coupler, (B) waveguide coupler, and (C) grating coupler.

with respect to the center of the metal. The field of the symmetric surface plasmon penetrates much more deeply into the dielectric medium than the field of the antisymmetric surface plasmon or the field of a conventional surface plasmon at a single metal−dielectric interface (Figure 1).

2.3. Optical Excitation of Surface Plasmons

A light wave can couple to a surface plasmon at a metal−dielectric interface if the component of light's wavevector that is parallel to the interface matches the propagation constant of the surface plasmon. As the propagation constant of a surface plasmon at a metal−dielectric interface is larger than the wavenumber of the light wave in the dielectric, surface plasmons cannot be excited directly by light incident onto a smooth metal surface. The wavevector of light can be increased to match that of the surface plasmon by the attenuated total reflection or diffraction. This enhancement and subsequently the coupling between light and a surface plasmon are performed in a coupling device (coupler). The most common couplers used in SPR sensors include a prism coupler, a waveguide coupler, and a grating coupler (Figure 3).

Prism couplers represent the most frequently used method for optical excitation of surface plasmons.[35−37] In the Kretschmann configuration of the attenuated total reflection (ATR) method (Figure 3A),[35] a light wave passes through a high refractive index prism and is totally reflected at the base of the prism, generating an evanescent wave penetrating a

thin metal film. The evanescent wave propagates along the interface with the propagation constant, which can be adjusted to match that of the surface plasmon by controlling the angle of incidence. Thus, the matching condition

$$\frac{2\pi}{\lambda} n_p \sin(\theta) = \mathrm{Re}\{\beta_{SP}\} \quad (4)$$

can be fulfilled, allowing the evanescent wave to be coupled to the surface plasmon. θ denotes the angle of incidence, n_p denotes the refractive index of the prism ($n_p > n_d$), and β_{SP} denotes the propagation constant of the surface plasmon. Surface plasmons can be also excited by a light wave guided in an optical waveguide. This approach is illustrated in Figure 3B. Light propagates in a waveguide in the form of guided modes. The electromagnetic field of a guided mode is concentrated in the waveguiding layer, and a portion of the field propagates, as an evanescent wave, in the low-refractive index medium surrounding the waveguiding layer. When light enters the region of the waveguide containing a metal layer, the evanescent wave excites a surface plasmon at the outer boundary of the metal layer. The coupling condition for the guided mode and the surface plasmon is fulfilled when the propagation constants of the two waves are equal

$$\beta_{mode} = \mathrm{Re}\{\beta_{SP}\} \quad (5)$$

where β_{mode} denotes the propagation constant of the waveguide mode. Another approach to optical excitation of surface plasmons is based on the diffraction of light in a grating coupler (Figure 3C). In this method, a light wave is incident from the dielectric medium on a metallic grating. The diffracted light can couple to a surface plasmon if the momentum of diffracted light parallel to the grating surface is equal to the propagation constant of the surface plasmon

$$\frac{2\pi}{\lambda} n_d \sin\theta + m\frac{2\pi}{\Lambda} = \pm\mathrm{Re}\{\beta^{SP}\} \quad (6)$$

where m is an integer and denotes the diffraction order and λ is the grating period.[43]

In the process of optical excitation of surface plasmon, a portion of the energy of the light wave is transferred into the energy of a surface plasmon and dissipated in the metal film, which results in a drop of intensity of the light wave. In addition to the change in the intensity, the light wave exciting a surface plasmon undergoes a change in phase.[31]

3. Fundamentals of SPR Sensors

3.1. SPR Sensors

In principle, SPR sensors are thin-film refractometers that measure changes in the refractive index occurring at the surface of a metal film supporting a surface plasmon. A surface plasmon excited by a light wave propagates along the metal film, and its evanescent field probes the medium (sample) in contact with the metal film. A change in the refractive index of the dielectric gives rise to a change in the propagation constant of the surface plasmon, which through the coupling condition (eqs 4−6) alters the characteristics of the light wave coupled to the surface plasmon (e.g., coupling angle, coupling wavelength, intensity, phase). On the basis of which characteristic of the light wave modulated by a surface plasmon is measured, SPR sensors are classified as sensors with angular, wavelength, intensity, or phase modulation.[31]

In SPR sensors with angular modulation, a monochromatic light wave is used to excite a surface plasmon. The strength of coupling between the incident wave and the surface plasmon is observed at multiple angles of incidence, typically by employing a convergent light beam. The excitation of surface plasmons is observed as a dip in the angular spectrum of reflected light. The angle of incidence yielding the strongest coupling is measured and used as a sensor output.[44] In SPR sensors with wavelength modulation, a surface plasmon is excited by a collimated light wave containing multiple wavelengths, typically a beam of polychromatic light. The excitation of surface plasmons is observed as a dip in the wavelength spectrum of reflected light. The wavelength yielding the strongest coupling is measured and used as a sensor output.[45] SPR sensors with intensity modulation are based on measuring the strength of the coupling between the light wave and the surface plasmon at a single angle of incidence and wavelength, and the intensity of light wave serves as a sensor output.[13] In SPR sensors with phase modulation the shift in phase of the light wave coupled to the surface plasmon is measured at a single angle of incidence and wavelength of the light wave and used as a sensor output.[46]

3.2. SPR Affinity Biosensors

SPR affinity biosensors are sensing devices which consist of a biorecognition element that recognizes and is able to interact with a selected analyte and an SPR transducer, which translates the binding event into an output signal. The biorecognition elements are immobilized in the proximity of the surface of a metal film supporting a surface plasmon. Analyte molecules in a liquid sample in contact with the SPR sensor bind to the biorecognition elements, producing an increase in the refractive index at the sensor surface, which is optically measured (section 3.1).

The change in the refractive index produced by the capture of biomolecules depends on the concentration of analyte molecules at the sensor surface and the properties of the molecules. If the binding occurs within a thin layer at the sensor surface of thickness h, the sensor response is proportional to the binding-induced refractive index change, which can be expressed as

$$\Delta n = \left(\frac{dn}{dc}\right)\frac{\Gamma}{h} \quad (7)$$

where (dn/dc) denotes the refractive index increment of the analyte molecules (typically 0.1−0.3 mL/g[47,48]) and Γ denotes the surface concentration in mass/area.[49]

3.3. Performance Considerations

The main performance characteristics of SPR (bio)sensors include sensitivity, linearity, resolution, accuracy, reproducibility, dynamic range, and limit of detection.[31]

3.3.1. Sensitivity

Sensor sensitivity is the ratio of the change in sensor output to the change in the quantity to be measured (e.g., concentration of analyte). The sensitivity of an SPR affinity biosensor depends on two factors—sensitivity of the sensor output (e.g., resonant angle or wavelength) to the refractive index and efficiency of the conversion of the binding to a change in

the refractive index (section 3.2).[31] The sensitivity of an SPR sensor to a refractive index S_{RI} can be expressed as a product of two terms

$$S_{RI} = \frac{\delta Y}{\delta n_{ef}} \frac{\delta n_{ef}}{\delta n_d} \quad (8)$$

where Y denotes sensor output. The first term describes the sensitivity of sensor output to the effective index of a surface plasmon and depends on the method of excitation of surface plasmons and the used modulation approach. The second term describes the sensitivity of the effective index of a surface plasmon to refractive index and is *independent* of the modulation method and the method of excitation.[31]

In general, the sensitivity of the effective index of a surface plasmon to refractive index depends on the distribution of the refractive index change. Homola and Piliarik used the perturbation theory[50] to calculate the sensitivity of the effective index to the refractive index for two limiting cases: (i) the change in the refractive index that occurs within the whole sample and (ii) the change in the refractive index that occurs only within a very short distance from the sensor surface.[31] They showed that the sensitivity of the effective index of a surface plasmon to bulk refractive index change can be expressed as

$$\left(\frac{\delta n_{ef}}{\delta n_d}\right)_B = \frac{{n_{ef}}^3}{{n_d}^3} > 1 \quad (9)$$

and therefore is always larger than the sensitivity of a free space plane wave in the infinite dielectric medium, which is equal to 1.[31] The sensitivity of the effective index of a surface plasmon to surface refractive index change occurring within a layer with a thickness h can be, assuming $h \ll L_{pd} = 1/\mathrm{Re}\{\alpha_d\}$ and $|\epsilon'_m| \gg \epsilon''_m$, written as

$$\left(\frac{\delta n_{ef}}{\delta n_d}\right)_S = 2\left(\frac{\delta n_{ef}}{\delta n_d}\right)_B \frac{h}{L_{pd}} \quad (10)$$

This suggests that the surface refractive index sensitivity is proportional to the bulk refractive index sensitivity and the ratio of the thickness of the layer within which the surface refractive index change occurs and the penetration depth of the surface plasmon, L_{pd}. As the penetration depth of a surface plasmon on gold increases with increasing wavelength, the surface refractive index sensitivity of the effective index decreases with the wavelength more quickly than the bulk refractive index sensitivity.[31]

3.3.2. Resolution

Resolution is a key performance characteristic of an SPR sensor and ultimately limits another important performance characteristic of an SPR affinity biosensor—the limit of detection (LOD). The resolution of an SPR sensor is defined as the smallest change in the bulk refractive index that produces a detectable change in the sensor output. The magnitude of sensor output change that can be detected depends on the level of uncertainty of the sensor output—the output noise. The resolution of an SPR sensor, r_{RI}, is typically expressed in terms of the standard deviation of noise of the sensor output, σ_{so}, translated to the refractive index of bulk medium, $r_{RI} = \sigma_{so}/S_{RI}$, where S_{RI} is the bulk refractive index sensitivity.

SPR sensors of all the modulation approaches need to measure the intensity of the light wave coupled to a surface plasmon to determine the sensor output. Therefore, their resolution is limited by the noise in the intensity of the detected light. Dominant sources of noise are the fluctuations in the light intensity emitted by the light source, shot noise associated with photon statistics, and noise in conversion of the light intensity into electric signal by the detector.[31] To reduce the noise, light intensities are averaged. The averaging involves either averaging of time series of intensity from the same detector (time averaging) or averaging of intensities from multiple detectors (e.g., of a two-dimensional array) measured at a single time (spatial averaging). The time averaging reduces the noise in the intensity of light by a factor of $\sqrt{M}$, where M is the number of averaged intensities. The spatial averaging used in spectroscopic SPR sensors (averaged spectra are measured in several rows of a 2D detector[51,52]) or intensity-modulated sensors (averaged area of a 2D detector forms a signal of one measuring channel[53−55]) is less efficient, as the light fluctuations affect all of the measured intensities in the same way and therefore cannot be eliminated by the spatial averaging.

The noise in the light intensity is translated to sensor output noise by a data processing algorithm used to generate the sensor output. Although various methods for processing data from spectroscopic SPR sensors have been developed (centroid method,[56,57] polynomial fitting,[58,59] and optimal linear data analysis[60]), the noise in angular or wavelength spectra was found to transform to the noise in the sensor output in a similar fashion.[61]

Piliarik and Homola investigated the propagation of noise through the centroid data processing algorithm and demonstrated that the noise of the centroid method can be expressed as

$$\sigma_{RI} = K\frac{1}{\sqrt{N}} \frac{\sigma_{th}}{d} \frac{w}{S_{RI}} \quad (11)$$

where N is the number of intensities used for the calculation of the centroid, σ_{th} is the total intensity noise at the threshold, d is the difference of intensities at the SPR dip minimum and at the threshold, w is the width of the dip, S_{RI} is the bulk refractive index sensitivity of the sensor, and K is a factor depending on the relative contributions of the sources of noise.[31] As follows from eq 11, the noise in the sensor output is mainly determined by the ratio of the noise in the light intensity at the threshold and the depth of the SPR dip. The ratio w/S_{RI} depends only weakly on the choice of coupler and modulation and therefore has only a minor effect on the sensor resolution.[31] Although the analysis was performed for the spectroscopic sensors ($N > 1$), it can be extended to intensity-modulated SPR sensors ($N = 1$). Equation 11 also explains why spectroscopic SPR sensors typically exhibit better resolution than their intensity-based counterparts—the N values in spectroscopic SPR sensors are typically of the order of 100,[62−64] which improves resolution by an order of magnitude. Another important conclusion is that in the intensity-modulated SPR sensor σ_{RI} is proportional to σ_{th}/I, which for most kinds of noise decreases with increasing intensity of light.

Ran and Lipson performed theoretical and experimental comparisons of resolution of intensity and phase modulation-based SPR sensors.[65] They demonstrated that under identical noise conditions, the performances of SPR sensors based on

intensity and phase modulations are comparable. This is due to the facts that in phase modulation-based sensors not the phase but the intensity of a light beam (produced by interference) is measured and that the configurations providing higher phase sensitivity to the refractive index exhibit highest absorption and consequently worse signal-to-noise ratios. They also demonstrated that the refractive index resolution can be improved for both the modulation approaches if the intensity of light coupled to the surface plasmon and received by the detector is increased,[65] which is consistent with the results of Piliarik and Homola.[31]

3.3.3. Limit of Detection and Minimum Resolvable Surface Coverage

In the field of SPR sensors, the term resolution usually refers to a bulk refractive index resolution. On the other hand, the limit of detection (LOD) is usually defined as the concentration of analyte that produces sensor output corresponding to 3 standard deviations of sensor output measured for a blank sample.[66] The ultimate LOD can be predicted only when the parameters of the interaction between the analyte and biorecognition element and mass transport to the sensor surface are known. However, the smallest detectable surface concentration (minimum resolvable surface coverage) can be determined independently of these factors.

The minimum resolvable change of molecular mass captured by the biorecognition elements σ_Γ depends on the sensor sensitivity and the noise in the sensor output:

$$\sigma_\Gamma = \frac{\sigma_{SO} \quad h}{S_h \left(\frac{\partial n}{\partial c}\right)_{vol}} \tag{12}$$

$(\partial n/\partial c)_{vol}$ denotes the volume refractive index increment of the molecular concentration, and S_h denotes the refractive index sensitivity of sensor output to a refractive index change within the sensitive layer of a thickness h. For thicknesses much smaller than the penetration depth of the surface plasmon (see eq 10), the following relationship between the bulk refractive index resolution and the resolution of surface coverage can be written:

$$\sigma_\Gamma = \sigma_{RI} \frac{L_{pd}}{2\left(\frac{\partial n}{\partial c}\right)_{vol}} \tag{13}$$

For an SPR sensor operating at the wavelength of 760 nm ($L_{pd} = 320$ nm) and a typical analyte with a refractive index increment $(\partial n/\partial c)_{vol} = 0.18 cm^3/g$ (DNA or BSA[48]), eq 13 suggests that a refractive index resolution of $\sigma_{RI} = 10^{-6}$ RIU corresponds to a surface coverage resolution of $\sigma_\Gamma = 0.91$ pg/mm^2.

4. Advances in SPR Biosensor Technology

An SPR affinity biosensor consists of a biorecognition element and an SPR transducer. The core of the transducer is an optical platform in which a surface plasmon is optically excited and interrogated and the binding between a biorecognition element (e.g., antibody) immobilized on the surface of the transducer and target analyte in a liquid sample is measured. An SPR biosensor also incorporates a fluidic system that usually consists of a flow cell or cuvette confining the sample at the sensing surface and a sample-handling system for sample collection and preparation.

In the following sections, recent advances in the two most critical elements of the SPR biosensor technology—optical platforms and biorecognition elements and their immobilization—are reviewed.

4.1. Optical Platforms Used in SPR Sensors

4.1.1. SPR Sensors Based on Prism Couplers

Most of the SPR sensors developed to date, including the first reported SPR sensor,[13] use a prism coupler to couple light to a surface plasmon. Prism coupling is convenient and can be realized with simple and conventional optical elements. Moreover, it can be readily combined with any type of modulation.

Sensors Based on Intensity Modulation. Research into SPR sensors with intensity modulation focuses mainly on the two important aspects—improving performance (sensitivity, resolution) and increasing throughput.

To increase the sensitivity of intensity-modulated SPR sensors, Lechuga's group proposed an approach based on combination of the magneto-optic activity of magnetic materials and a surface plasmon resonance in a special multilayer structure.[67] They demonstrated an improvement in sensitivity by a factor of 3 compared to a conventional intensity-modulated SPR sensor and a refractive index resolution of 5×10^{-6} RIU.[67]

A typical example of a high-throughput SPR sensor is the SPR imaging.[68,69] In a typical SPR imaging configuration, a beam of monochromatic light passes through a prism coupler and is made incident on a thin metal film at an angle of incidence close to the coupling angle. The intensity of reflected light depends on the strength of the coupling between the incident light and the surface plasmon and therefore can be correlated with the distribution of the refractive index at the surface of the metal film.[68,69]

Corn's group has researched SPR imaging for over a decade. In their earlier works, they employed a HeNe laser as a source of illumination.[69] However, a highly coherent light source generated images with parasitic interference patterns that were disturbing SPR measurements. In 1997 they improved their SPR imaging instrument by introducing an incoherent light source and a NIR narrow band-pass filter.[70] Using this approach, they detected hybridization of short (18-base) oligonucleotides at concentrations as low as 10 nM[71] (this was estimated to correspond to a refractive index resolution in the 10^{-5} RIU range). The use of a white light source and a bandpass filter was also advocated by Yager's group.[72] They demonstrated that by tilting the interference filter, an operating wavelength of the SPR imaging sensor can be tuned.[72] Later they demonstrated that their SPR imaging instrument operating at a wavelength of 853 nm can provide a refractive index resolution of 3×10^{-5} RIU.[55] In 2005 Corn's group reported SPR imaging with a special multilayer structure supporting long-range surface plasmons; however, the use of long-range surface plasmons led only to minor sensitivity improvements of 20% (experiment) and 40% (theory) compared to the conventional SPR imaging.[73]

A dual-wavelength SPR imaging system was reported by Zybin et al.[74] In their SPR sensor, they used two sequentially switched-on laser diodes, and the intensities of the reflected light at the two different wavelengths were measured and

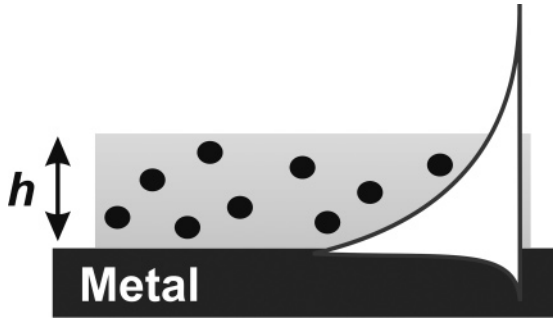

Figure 4. Concept of SPR biosensing.

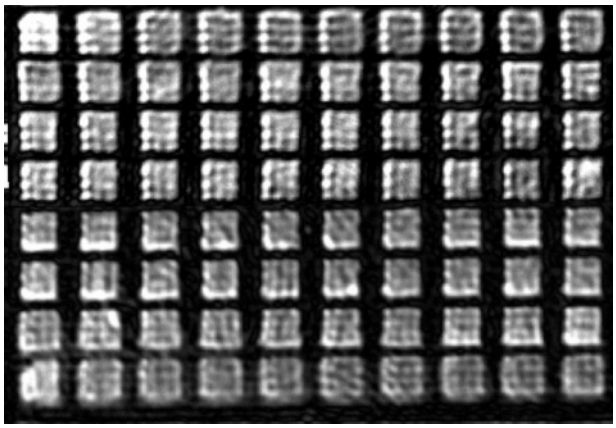

Figure 5. Typical image obtained with an SPR imaging sensor with a polarization control. Bright rectangles correspond to areas of an SPR chip (300 × 300 μm) covered with a monolayer of albumin molecules formed on the surface of gold by microspotting.

the sensor output was defined as the difference of these two signals. A refractive index resolution of 2×10^{-6} RIU was achieved when the signal was averaged over a large beam diameter (6 mm^2).

Campbell's group reported an SPR imaging system with a controllable angle of incidence.[75,76] This feature allows SPR images to be acquired sequentially at different angles of incidence and selection of the optimum angle of incidence for the SPR measurements. With a HeNe laser as a source of light, their sensor was able to measure simultaneously in 120 sensing channels with a refractive index resolution of 2×10^{-5} RIU. Recently, they claimed an improvement in sensor resolution down to 5×10^{-6} RIU.[77]

Recently, Piliarik et al. investigated SPR imaging with an elliptically polarized light[78] and concluded that a change in the polarization of light induced by the coupling of light to a surface plasmon can be exploited to significantly improve the sensitivity and operating range of SPR imaging sensors. In addition, this approach, as illustrated in Figure 5, provides high-contrast SPR images (with a low background), which are well suited for automated image analysis.

Homola's group developed an SPR imaging approach based on polarization contrast and excitation of surface plasmons on spatially patterned multilayers.[53] In this configuration a prism coupler with an SPR chip containing a spatially patterned multilayer structure was placed between two crossed polarizers. The output polarizer blocked all of the light reflected from the (inactive) areas outside the sensing areas, generating high-contrast images. Two types of SPR multilayers with opposite sensitivities to refractive index were employed, and the output signal was defined as a ratio of the intensities generated from the two neighboring multilayers. This sensor was shown to be able to detect refractive index changes down to 2×10^{-6} RIU and to detect short oligonucleotides (23-mers) at concentrations as low as 100 pM.[79]

Currently, commercial SPR imaging instruments are available from GWC Technologies, Inc.[80] (Madison, WI), Lumera[81] (Bothell, WA),[29] IBIS Technologies (Hengelo, The Netherlands),[82] and SPRi-Array from GenOptics (Orsay, France).[83]

Sensors Based on Spectroscopy of Surface Plasmons. In sensors based on spectroscopy of surface plasmons, the angular or wavelength spectrum of a light wave coupled to a surface plasmon is measured and sensor output is related to a change in the angular or wavelength position of the SPR dip.

In the early 1990s, an angular modulation-based SPR sensor consisting of a light-emitting diode (LED), a glass prism, and a detector array with imaging optics was introduced.[58,84,85] A divergent beam produced by the LED was collimated and focused by means of a cylindrical lens to produce a wedge-shaped beam of light, which was used to illuminate a thin gold film on the back of a glass prism containing several sensing areas (channels). The imaging optics consisted of one imaging and one cylindrical lens ordered in such a way that the angular spectrum of each sensor channel was projected on separate rows of the array detector.[86−88] This design has been adopted by Biacore and resulted in a family of commercial SPR sensors with high performance (resolution down to 1×10^{-7}RIU) and multiple sensing channels (up to four).

In 2004, Thirstrup et al. integrated several optical elements into a single sensor chip.[63] In this approach, the cylindrical focusing optics utilized to create a beam of a desired angular span was replaced by a diffraction grating of a special design incorporated into the sensing element.[89,90] A wide parallel light beam was diffracted by the focusing grating and focused into a small spot on the SPR measuring surface. The reflected light followed a similar path, producing a parallel beam with an angular spectrum superimposed across the beam. A two-dimensional photodetector was used to measure the angular spectrum of the reflected light for several parallel channels. This design offered a compact SPR platform with a resolution of about 5×10^{-7} RIU.[89]

An SPR sensor with wavelength modulation and parallel channel architecture was reported by Homola's group.[91] In this sensor, a polychromatic light from a halogen lamp was collimated into a large-diameter parallel beam, which was launched in a prism coupler. The light reflected from different sensing channels was collected by different output collimators coupled and transmitted to different inputs of a spectrograph. The SPR sensor of this design was demonstrated to be able to resolve refractive index changes down to 2×10^{-7} RIU.[62]

An SPR sensor with wavelength division multiplexing (WDM) of sensing channels was proposed by Homola et al.[92] In this approach, signals from multiple surface plasmons excited in different areas of a sensing surface are encoded into different regions of the spectrum of the light wave. Two configurations of WDMSPR sensors have been developed.[93,94] In the first configuration, a wide parallel beam of polychromatic light is made incident onto a sensing surface consisting of a thin gold film, a part of which is coated with a thin dielectric film. As the presence of the thin dielectric film shifts the coupling wavelength to a longer wavelength

(compared to the bare gold), the reflected light exhibits two dips associated with the excitation of surface plasmons in the area with and without the overlayer.[93] The second configuration of WDMSPR sensor employs a special prism coupler in which a polychromatic light is sequentially incident on different areas of the sensing surface at different angles of incidence. Due to the different angles of incidence, the surface plasmons in different regions are excited with different wavelengths of the incident light.[94] Therefore, the spectrum of transmitted light contains multiple dips associated with surface plasmons in different areas of the sensing surface. The WDMSPR approach was combined with the parallel architecture, yielding an eight-channel SPR sensor with a resolution around 1×10^{-6} RIU.[94]

An optical sensor based on spectroscopy of long-range surface plasmons was reported by Nenninger et al.[95] In that work, a long-range surface plasmon was excited on a special multilayer structure consisting of a glass substrate, a Teflon AF layer, and a thin gold layer. A resolution as low as 2×10^{-7} RIU was achieved.[95] Most recently, Homola's group demonstrated an improved configuration for excitation of long-range surface plasmons and demonstrated an SPR sensor with a resolution as low as 3×10^{-8} RIU.[96]

Development of portable/mobile SPR sensor platforms suitable for deployment in the field presents an important direction in SPR sensor research. Several miniaturized SPR optical platforms based on spectroscopy of surface plasmons have been developed. A concept of the miniature SPR sensor based on integration of all electro-optical components in a monolithic platform developed by Texas Instruments in the mid-1990s[97] was further advanced by researchers at Texas Instruments and the University of Washington. The Spreeta 2000 SPR sensor (Texas Instruments, USA) consists of a plastic prism molded onto a microelectronic platform containing an infrared LED and a linear diode array detector. The LED emits a diverging beam that passes through a polarizer and strikes the sensor surface at a range of angles. The angle at which light is reflected from this surface toward a detector varies with the location on the surface. The initial version of this platform exhibited a refractive index resolution of 5×10^{-6} RIU.[98] Baseline noise and smoothness of response of this sensor were investigated by Chinowsky et al.,[99] who showed that the baseline noise established under constant conditions was $<2 \times 10^{-7}$ RIU; however, the sensor response to a gradual change in the refractive index revealed departures from the expected sensor output of about 8×10^{-5} RIU. A portable SPR instrument based on the Spreeta 2000 design was reported by Naimushin et al.[100] Their instrument incorporated temperature stabilization and was demonstrated to provide a refractive index resolution of 3×10^{-6} RIU. Recently, an SPR instrument based on two Texas Instruments Spreeta devices was adopted for deployment in a surrogate unmanned aerial vehicle and applied for detection of airborne analytes.[101] Another compact, portable SPR sensor platform was developed by Kawazumi et al.[52] Their system was also based on angular modulation and Kretschamnn geometry. A line-shape light beam from an LED was focused on the sensing surface using a cylindrical lens. Two-dimensional Fourier transform images of the reflected light were measured with a compact CCD camera. SPR measurements were carried out at a fixed angle, and the resonance angles were obtained by analyzing the two-dimensional images. The system provided four independent sensing channels and a refractive index resolution of 10^{-4} RIU.[52]

Nowadays numerous SPR sensors based on spectroscopy of surface plasmons are commercially available. They include Biacore systems from Biacore (now part of GE Healthcare, USA),[88] Spreeta sensor from Texas Instruments (Dallas, TX),[102] Multiskop system from Optrel (Kleinmachnow, Germany),[103] SR 7000 platforms from Reichert Analytical Instruments (Depew, NY),[104] Plasmonic from Hofmann Sensorsysteme (Wallenfels, Germany),[105] Autolab Esprit and Springle SPR systems from Eco Chemie (Utrecht, The Netherlands),[106] SPR-20 from DKK-TOA Corp. (Tokyo, Japan),[107] BIOSUPLAR 6 from Analytical μ-Systems (Sinzing, Germany),[108] and Sensia β-SPR Research Platform (Madrid, Spain).[109]

SPR Sensors Based on Phase Modulation. The research group of Nikitin demonstrated two SPR sensor platforms based on interferometry.[110,111] The first approach was based on the interference of the TM-polarized signal beam with the TE-polarized reference beam,[110] whereas the second method was based on a Mach−Zehnder interferometer combining TM-polarized signal and reference beams.[111] This configuration was demonstrated in two modes: (a) phase contrast (Zernike phase contrast) increasing the sensor sensitivity and (b) "fringe mode", in which there was a definite angle between the interfering beams and a pattern of interference fringes was superimposed on the image of the surface. Local variations in the phase of the signal beam resulted in bending and moving of the interference fringes. A refractive index resolution was on the order of 10^{-7} RIU.[111] At the same time as Nikitin et al. published their work,[111] a similar configuration of SPR sensor based on the Mach−Zehnder interferometer was reported by Notcovich et al.[112] They used their system for measurement of the refractive index of gases and demonstrated a refractive index resolution on the order of 10^{-6} RIU.[112]

Wu et al. proposed a phase-modulation SPR sensor based on common-path, heterodyne interferometry.[113] Two acousto-optic modulators were used to split the incoming laser light from a HeNe laser into two linearly orthogonally polarized beams with a frequency difference of 60 kHz. These two light beams were merged into one beam by a polarization beam splitter. One portion of the beam was directed to a detector while the other was coupled into an SPR prism coupler. The TE and TM components of light reflected from a thin layer of gold on the base of the prism were recombined using a polarizer, and the output beam was received by a detector. SPR-induced phase shift was determined by an electronic phase meter (lock-in amplifier). The refractive index resolution of this design was estimated to be 2×10^{-7} RIU.[113]

Alieva and Konopsky developed an SPR sensor based on interference between a surface plasmon supported on a metal film and a bulk wave propagating at grazing angle in the flow cell just above the surface of metal.[114] This approach suppresses the sensitivity of the SPR method to variations in the refractive index of a liquid sample, which in SPR biosensors interfere with binding measurements.

Naraoka and Kajikawa reported a phase-modulation SPR sensor based on a rotating analyzer method.[115] In their approach, a linearly polarized light from a semiconductor laser was coupled to an SPR prism coupler and reflectivity was detected while the rotational angle of the analyzer was scanned. The phase difference between the TE and TM

components of the reflected light were determined from the dependence of the reflectivity on the angle of analyzer. The refractive index resolution of their system was estimated to be below 2×10^{-7} RIU.[115]

In recent years, SPR sensors with phase modulation have been extensively studied by the researchers at the Chinese University of Hong Kong and City University of Hong Kong. In 2002 Ho et al. reported an SPR sensor based on the Mach−Zehnder interferometer.[116] In that work, an optical beam from an unpolarized HeNe laser passed through a prism coupler and the TM-polarized component of the beam excited surface plasmons in two parallel sensing channels, one filled with a sample and the other with a reference solution. TE and TM polarization components of the output beam were split by a polarizing beam splitter. The optical path for TE polarization was modulated by means of a piezoelectric actuator. Finally, TM polarization was converted to TE polarization by a half-waveplate, and the two beams were recombined. The shift between the interference patterns for the measuring and reference sensing channels was measured. Resolution of this sensor was estimated to be about 3×10^{-6} RIU.[116] An alternative configuration of an SPR sensor with phase modulation was reported by Wu et al. in 2004.[117] In this configuration, one Mach−Zehnder interferometer performed independent interference of TE and TM polarized components of a signal beam emerging from a prism coupler and a reference beam. Subsequently, the output TE and TM beams were separated in a Wollaston prism and directed to two separate detectors. A piezoelectric actuator modulated the optical path in a reference arm of the interferometer, producing a periodic intensity modulation in both TE and TM polarizations. The interference patterns for TE and TM polarizations were processed to reduce the noise and compensate for instabilities in the setup,[118] and the sensor output was determined as a mutual shift of the two patterns. Resolution of the sensor was estimated to be 5.5×10^{-8} RIU.[117] Another SPR sensor based on measuring the phase difference between TE and TM polarization components of light beam was reported by Ho et al.[119] They used a single beam and a photoelastic phase modulator to introduce a carrier frequency so that the phase can be determined by measuring the relative amplitude of the first harmonic signal. Resolution of the sensor was determined to be 1.2×10^{-6} RIU.[119] In 2007, a phase modulation-based SPR sensor employing a Michelson interferometer was reported by Yuan et al.[120] They used a Michelson interferometer with an SPR prism coupler inserted in one arm of the interferometer. This arrangement allows the TM-polarized component of the light beam to incur a 2-fold phase shift compared with that in the Mach−Zehnder interferometer. Therefore, the sensitivity of the Michelson interferometer-based SPR sensor was twice as high as that of the SPR sensor with the Mach−Zehnder interferometer. This improvement was demonstrated in a single experimental system incorporating both Michelson and Mach−Zehnder interferometers in which the refractive index resolutions were established to be 7.7×10^{-7} and 1.5×10^{-6} RIU, respectively.[120]

4.1.2. SPR Sensors Based on Grating Couplers

Grating couplers have not been used in SPR sensors as widely as the prism couplers. However, their compatibility with mass production (in particular, replication into plastic) makes a grating coupler an attractive approach for fabrication of low-cost SPR sensing structures.

In 2001 Brockman and Fernandez presented an SPR imaging device based on grating coupling.[121] In this approach, a collimated monochromatic light beam (wavelength = 860 nm) was made incident onto a plastic chip with a gold-coated diffraction grating. An array of 400 sensing channels (spot diameter = 250 μm) was prepared on the chip by means of spatially resolved functionalization. Upon reflection from the chip, the light was projected onto a two-dimensional CCD array.[121] This concept was further developed by HTS Biosystems (Hopkinton, MA).[122] In 2005, Biacore International AB acquired the FLEXChip technology from HTS Biosystems.

Another high-throughput SPR sensor based on grating coupling was reported by Homola's group.[64] This approach was based on angular spectroscopy of surface plasmons on an array of diffraction gratings. A collimated beam of monochromatic light was focused with a cylindrical lens on a row of gold-coated diffraction gratings and reflected under nearly normal incidence. The angular spectra were transformed back to a collimated beam by means of a focusing lens and projected onto a two-dimensional CCD detector. Different rows of gratings were read sequentially by moving the beam splitter and cylindrical lens with respect to the sensor chip. A refractive index resolution of 5×10^{-6} RIU was achieved for simultaneous measurements in over 200 sensing channels.[64]

Homola's group reported an SPR sensor based on simultaneous spectroscopy of multiple surface plasmons on a multidiffractive grating.[123] A polychromatic light beam was made incident onto a special metallic grating with a grating profile composed of multiple harmonics. The reflected light contained multiple SPR dips, one for each grating period. The use of multiple surface plasmons of different field profiles can provide more detailed information about the refractive index distribution at the sensor surface. This approach was illustrated in a model experiment in which three-surface plasmon spectroscopy was used to determine background refractive index variations and changes in the thickness and refractive index of a bovine serum albumin (BSA) multilayer.[123] Recently, an SPR sensor based on two-plasmon spectroscopy on a bi-diffractive grating was investigated in terms of its ability to distinguish contributions to sensor response due to refractive index changes at the sensor surface (i.e., binding) and due to refractive index changes in the whole sample. Theoretical analysis yielding an estimate of an error of such decomposition was reported.[124] Recently, Homola's group reported an SPR biosensor using both long-range and short-range surface plasmons excited simultaneously on a diffraction grating of a special design.[125] This approach offers several interesting features such as extended probe depth of the long-range surface plasmon and ability to distinguish sensor response caused by bulk and surface refractive index changes. The sensor was demonstrated to be able to detect changes in the refractive index as small as 3.5×10^{-6} RIU.[125]

An SPR sensor based on angular spectroscopy of surface plasmons was reported by Unfricht et al. in 2005.[126] In their configuration, an LED source was moved by an angle encoder along an arc centered on the chip in order to change the incident angle. The light reflected from the chip surface was detected using a CCD camera that captured sequential images across the range of interrogated angles, and the coupling angle was measured.[126]

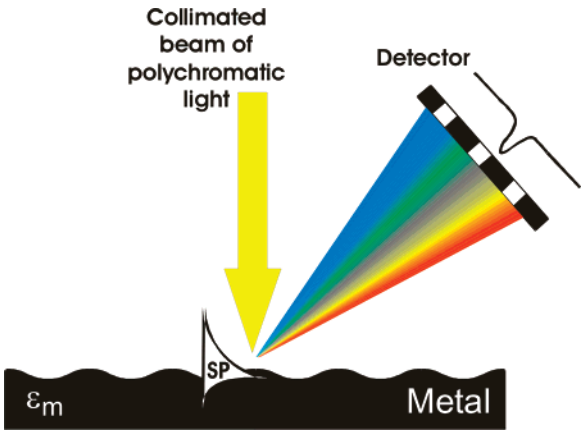

Figure 6. Concept of SPR sensor based on simultaneous excitation of surface plasmons by a polychromatic light and the dispersion of light on a special grating coupler.[127]

A new approach to the development of sensors based on spectroscopy of surface plasmons on diffractive gratings was reported by Telezhnikova and Homola.[127] A collimated beam of polychromatic light was made incident on a special diffraction grating. A portion of incident light was coupled to a surface plasmon at the metal−dielectric interface via the second order of diffraction. Simultaneously, the light diffracted into the first diffraction order was dispersed and the light components of different wavelengths were directed to different areas of a position-sensitive detector (Figure 6). The coupling of light into a surface plasmon resulted in a drop in the intensity of diffracted light, which was observed as a narrow dip in the spectrum of diffracted light.[127] A refractive index resolution of this sensor was established at 3×10^{-7} RIU.

In 2007, Chien et al. reported an SPR sensor in which light was coupled into a metal−dielectric waveguide by a subwavelength grating.[128] In this configuration, white light was made incident on the waveguiding layer through the grating structure and was coupled to a surface plasmon supported by a thin metal film. An SPR dip was observed in the spectrum of reflected light. A refractive index resolution of this sensor was established at 1×10^{-6} RIU.[128]

4.1.3. SPR Sensor Based on Waveguide Couplers

Fiber optic SPR sensors present the highest degree of miniaturization of SPR sensors. The first fiber optic SPR sensors were reported in the early 1990s.[129−131] In SPR sensors based on side-polished single-mode optical fibers, a fundamental mode of the fiber couples to a surface plasmon at the outer surface of a metal layer deposited on a side-polished region of the fiber. The coupling results in attenuation of a transmitted light at a fixed wavelength (intensity-modulated SPR sensor) or a characteristic dip in the spectrum of transmitted light (wavelength-modulated SPR sensor). The main challenge for obtaining a stable performance is the sensitivity of polarization of light guided in the fiber to deformations of the fiber. The deformations generate changes in the strength of coupling between the light and a surface plasmon and thus interfere with SPR measurements. In 1999 Homola's group reported an intensity-modulated fiber optic SPR sensor with a resolution better than 2×10^{-5} RIU.[132] Later, they reported a wavelength-modulated version of this sensor with resolutions of 5×10^{-7} RIU (no deformations) and 3×10^{-5} RIU (under moderate deformations).[133] In 2003 the sensitivity of the sensor to deformation of the fiber was dramatically reduced by the introduction of polarization-maintaining fibers. An SPR sensor based on a side-polished polarization-maintaining fiber was demonstrated to exhibit a refractive index resolution of 2×10^{-6} RIU.[134]

Chiu et al. reported a fiber optic SPR sensor based on a D-shape optical fiber and heterodyne interferometry.[135] Their sensor measured refractive index changes down to 2×10^{-6} RIU. In 2007 Lin et al. extended this approach to multimode fibers and reported an SPR sensor with wavelength modulation based on a side-polished multimode optical fiber.[136] The sensor was shown to be able to resolve refractive index changes as small as 3×10^{-6} RIU.

An integrated optical SPR sensor with intensity modulation and one sensing channel and one reference channel was reported by Mouvet et al.[137] The signal from the sensing channel was normalized to the signal from the reference channel, resulting in an increased stability and a refractive index resolution of 5×10^{-5} RIU.[138] A wavelength modulation-based integrated optical SPR sensor was reported by Homola's group. The sensor was demonstrated to provide a refractive index resolution as low as 1×10^{-6} RIU.[139] An SPR sensor based on a strip waveguide consisting of a germanium-doped silicon dioxide waveguiding layer on a silicon substrate and wavelength modulation was reported by Huang et al.[140] Their sensor exhibited a sensitivity similar to that reported in ref 139.

In conventional waveguide-based SPR sensors, the resonant coupling between a surface plasmon and a waveguide mode occurs for refractive indices of sample considerably higher than the refractive index of a typical aqueous sample. Various approaches to control the operating range of waveguide-based SPR sensor, so that it includes aqueous environments, were proposed. They include an integrated optical waveguide fabricated in low refractive index glass,[141] a buffer layer,[142] or a high refractive index overlayer.[143] Skorobogatiy and Kabashin proposed to overcome this limitation of conventional waveguides by employing a photonic-crystal waveguide.[144] In their paper, they theoretically demonstrated the feasibility of a photonic crystal waveguide-based SPR sensor using a single-mode photonic crystal waveguide in which the effective index of a mode confined in the waveguiding layer can be made considerably smaller than the refractive index of the waveguiding layer material, enabling phase matching with a surface plasmon at any wavelength.[144]

Debackere et al. proposed an interferometric SPR sensor consisting of a silicon-on-insulator (SOI) waveguide and a thin metal layer.[145] In their design, a mode guided by a thin silicon film excited two surface plasmons on opposite sides of a thin metal film. These two modes propagated side by side over a short distance (10 μm) and were recombined in a waveguide mode at the end of the metal film. The transmitted intensity depended on the mutual phase delay of the two interfering surface plasmons. As the propagation constant of the surface plasmon propagating at the outer boundary was sensitive to the refractive index of the adjacent medium (sample), changes in the refractive index of sample could be measured by measuring changes in the intensity of transmitted light. As this sensor is based on interference rather than phase-matching, the operating range of the sensor can be conveniently controlled by the geometry of the device.[145]

Wang et al. reported an alternative approach to integrated optical SPR sensing based on electro-optical modulation.[146]

Their sensor consisted of titanium-diffused channel waveguide in a lithium niobate substrate in which the propagation constant of a mode was modulated by voltage applied between the electrodes on two sides of the waveguiding layer. In the amplitude modulation mode, the intensity of transmitted light was measured as the electrode voltage was scanned and the slope of the intensity−voltage dependence was correlated with the amount of analyte captured at the sensor surface. The same approach was demonstrated for the wavelength modulation mode in which the resonant wavelength was measured.[146]

4.2. Biorecognition Elements and Their Immobilization

In SPR affinity biosensors, one of the interacting molecules (biorecognition element or target molecule) is immobilized on the solid surface of the SPR sensor and the other is contained in a liquid sample. Which of the molecules is immobilized depends on the used detection format (section 5.1)—in direct, sandwich, and competitive detection formats, the molecule that needs to be immobilized is a biorecognition element; in the inhibition detection format, the immobilized molecules is the target molecule or its derivative. The choice of appropriate biorecognition elements and immobilization method is of critical importance with direct impact on key performance characteristics of the sensor such as sensitivity, specificity, and LOD.

4.2.1. Biorecognition Elements

Various kinds of biorecognition elements have been employed in affinity SPR biosensors. Antibodies remain by far the most frequently used biorecognition element. They offer high affinity and specificity against target analyte. Moreover, antibodies against numerous target molecules are now commercially available. Development of high-quality antibodies is, however, a rather expensive and laborious process.[147] Recently, single-chain antibody fragments (scFvs) have been also used as biorecognition elements.[148] Biotinylated scFv fragments expressed in yeast can be spotted on streptavidin-coated sensor surfaces directly from cell supernatant without the need of purification.[149] Another type of biorecognition element that has been employed in SPR sensors are peptides. In comparison with antibodies, peptides, in general, are inexpensive, more stable, and easier to manipulate. However, peptides sometimes lack high affinity and specificity against the target. In SPR biosensors, peptides have been applied mainly for the detection of antibodies, for example, antibodies against hepatitis G,[150] herpes simplex virus type 1 and type 2,[151] and Epstein−Barr virus,[152] and for the detection of heavy metals.[153] Recently, aptamers emerged as another promising type of biomolecular recognition element for SPR biosensors.[154,155] DNA or RNA aptamers are single-stranded oligonucleotide sequences, which can be produced to bind to various molecular targets such as small molecules, proteins, nucleic acids, and even cells, tissues, and organisms.[155,156] Moreover, the synthesis of aptamers is straightforward and reproducible.

4.2.2. Immobilization of Biorecognition Elements

In SPR biosensors, one of the interacting molecules (mostly biorecognition element) is immobilized on the sensor surface. The surface chemistry has to be designed in such a way that it enables immobilization of a sufficient number of biorecognition elements on the sensing surface while minimizing the nonspecific binding to the surface. In addition, biorecognition elements need to be immobilized on the sensor surface without affecting their biological activity. In principle, the molecules can be immobilized either on the surface or in a three-dimensional matrix. Although immobilization on surfaces is more straightforward to perform, the number of accessible biorecognition elements is limited by the capacity of the surface (too high density of immobilized biorecognition elements can lead to lower response due to sterical hindrance). Immobilization in a three-dimensional matrix typically provides more binding sites than immobilization on the surface and a better environment for the preservation of immobilized molecules during prolonged storage.[157] The most widely used three-dimensional matrix for immobilization of molecules in a structured environment is the carboxymethylated dextran.[158]

For two-dimensional (surface) immobilization of biorecognition elements on the sensing (gold) surface, self-assembled monolayers (SAMs) of alkanethiolates or disulfides have been widely used.[159] To provide a desired surface concentration of biomolecular recognition elements and a nonfouling background, mixed SAMs of long-chained (n = 12 and higher) alkanethiolates terminated with a functional group for further attachment of biomolecular recognition elements and oligo(ethylene glycol)-terminated shorter-chained alkanethiolates for a nonfouling background have been developed.[160,161]

The main approaches to immobilization of molecules to the surface of SPR sensors are based on physical absorption and hydrophobic and electrostatic interactions,[162] covalent coupling,[158] and attachment of tagged molecules by a site-specific non-covalent interaction between the tag and an immobilized capture molecule via biotin−avidin[163] or histidine-chelated metal ion[164] interaction or DNA hybridization.[165] A more detailed account of immobilization methods is given in refs 31 and 166.

As proteins represent the class of molecules that are most frequently used as biorecognition elements, the following section is dedicated to the immobilization of proteins. The most commonly used approach to the immobilization of proteins is via a covalent bond formed between the nucleophilic functional groups supplied by amino acids (e.g., amino groups, lysine; thiol groups, cysteine) of the protein and electrophilic groups (e.g., activated carboxyls, aldehydes) on the sensor surface.[158,167] The covalent immobilization is stable; however, as proteins typically contain many functional groups, immobilization via these functional groups results in random orientation of immobilized proteins. Moreover, simultaneous immobilization via multiple functional groups may restrict conformational flexibility of the protein and impair its function. Another approach to the immobilization of proteins is based on biochemical affinity reaction. The most common example of this approach is the immobilization based on avidin−biotin chemistry. In this immobilization method, protein avidin (or a closely related streptavidin) is immobilized on the sensing surface (covalently or via pre-immobilized biotin) and provides binding sites for subsequent attachment of a biotin-conjugated protein. The protein can be biotinylated by various methods targeting different groups on the protein. Orientation of the immobilized proteins depends on the orientation of avidin/streptavidin molecules, the biotinylation method used, and the properties of the protein. Alternatively, antibodies can be immobilized via

interaction between the F_c region of the antibody and protein A or protein G. This method provides good access to the binding site of the antibody, located on the Fab variable region; however, to control orientation of the antibody, the orientation of protein A itself needs to be controlled.[168] Recently, DNA-directed immobilization of antibodies has been described.[165] This approach takes advantage of DNA chip technology, which provides an exceptionally stable pattern of single-stranded DNA (ssDNA) sequences and uses it for the immobilization of proteins conjugated with complementary ssDNA sequences via DNA hybridization. This approach provides an elegant and flexible platform both for SPR sensors with a limited number of sensing channels and for high-throughput screening SPR systems. The drawback of this method is that it requires that the protein is conjugated with ssDNA.[165] Another bioaffinity immobilization method is based on the interaction between histidine-tagged protein and chelated metal ions, for example, nitrilotriacetic acid (NTA) immobilized on the surface and loaded with bivalent metal cations.[164] NTA can be attached to the sensing surface covalently via acetic group using EDC/NHS chemistry.[169] Recombinant proteins with affinity tags can be produced by genetic engineering. As the tag can be placed at a defined position on the protein, this approach allows site-specific and thus highly ordered protein immobilization. Moreover, the binding between chelated metal ions and histidine is reversible and the immobilized protein can be released by introduction of a competing ligand (e.g., imidazole) or a chelation agent (e.g., ethylenediaminetetraacetic acid, EDTA). Whereas reusability of the surface is one of the main advantages of this immobilization method, the main drawback is the low affinity of the His-tag to an individual chelator. In 2005 Piehler's group expanded this immobilization technique by designing supramolecular entities binding to oligohistidine tags with high affinity and stability.[170] They designed supramolecular multivalent chelator heads (MCH) containing multiple NTA moieties and investigated their binding with hexahistidine (H6)- and decahistidine (H10)-tagged molecules. It was demonstrated that the binding stability of the complex increases with an increasing number of NTA moieties. An improvement of the stability of the chelator−oligohistidine complex by 4 orders of magnitude compared to that of mono-NTA was achieved.[170] Tinazli et al. developed multivalent metal-chelating thiols for attachment of histidine-tagged proteins to the surface of SPR sensors via SAMs.[171] Dramatically improved stability of protein binding by these multivalent chelator surfaces was observed compared to mono-NTA/His(6) tag interaction. Regenerability of the surface (removal of the protein) using EDTA was also demonstrated.[171] Immobilization and arraying of histidine-tagged proteins by combining molecular and surface multivalency was demonstrated by Valiokas et al.[172] They employed SAMs formed by triethylene glycol-terminated alkyl thiols[171] functionalized with either a single NTA moiety (mono-NTA) or a chelator head group containing two NTA moieties (bis-NTA). The process of immobilization of proteins was observed with SPR imaging.[172]

Immobilization of peptides can follow strategies similar to those developed for proteins, including electrostatic attraction and amine- or thiol-based covalent coupling. The most straightforward approach to the immobilization of oligonucleotides is based on the use of biotinylated derivatives.[173] Small molecules with functional groups (aliphatic amines, thiols, aldehydes, or carboxylic groups) can be covalently linked to suitable corresponding groups on the sensor surface. Small molecules without suitable functional groups need to be derivatized.[174] To deliver molecular recognition elements to different areas of the SPR sensor surface, the immobilization chemistry needs to be spatially controlled. For instance, Campbell's group demonstrated the microspotting of double-stranded DNA on gold for SPR microscopy using two approaches.[175] Both methods use streptavidin and biotinylated oligonucleotides. In the first method, the robotic microspotter was used to deliver nanoliter droplets of dsDNAs onto a uniform layer of streptavidin. In the second method, a streptavidin layer was also microspotted on a mixed-alkanethiolate SAM and, subsequently, microspots of dsDNA were added using microspotting. Homola's group compared the microspotting technique with the conventional flow-through in situ functionalization.[79] In their study, the spatially resolved functionalization based on microspotting applied to immobilization of short oligonucleotides was shown to provide a surface concentration of oligonucleotide probes of about 2.2×10^{12} oligonucleotides per cm^2, which was higher by 80% than the surface coverage provided by the flow-through functionalization method.[79]

4.2.3. Nonfouling Surfaces

As the adsorption of proteins is of major concern in numerous important biomedical and biological applications (biocompatible materials for prostheses, tissue engineering, cell culturing, implantable devices, microarrays, etc.), the adsorption of proteins to synthetic surfaces has been the subject of extensive research worldwide. Nonspecific adsorption of proteins to sensing surface presents a key challenge also for affinity biosensors.[176,177] This problem is more severe when complex samples such as blood or cell lysate are to be analyzed.[178,179] Although the molecular mechanism of protein resistance has not been fully understood, research into protein-resistant surfaces has made significant advances. Various surface coatings displaying low fouling or even nonfouling properties (i.e., exhibiting complete resistance to protein binding and cell colonization) have been proposed. For affinity biosensors it is especially important to create surfaces with low fouling background providing also abundant binding sites for immobilization of biomolecular recognition elements.

Hydrophilic polymers such as poly(ethylene glycol) (PEG) and its derivatives have been successfully employed in the design of protein-resistant coatings for SPR sensors. The key factors that influence nonfouling properties of PEG molecules have been considered to be steric-entropy barrier characteristics and a high degree of hydration.[180] Recent measurements of interfacial forces have shown that the protein resistance of PEGylated surfaces correlates with a net repulsive force versus distance curve.[181] An approach utilizing a poly(L-lysine) grafted with poly(ethylene glycol) (PLL-g-PEG) have been used by Pasche et al. to minimize the nonspecific adsorption of proteins.[182,183] In their work, they varied the ratio of the number of lysine monomers and the PEG side chains and, with the optimized surface composition, they observed adsorption from blood serum below 2 ng/cm^2.[182] It was demonstrated that the immobilization of biorecognition elements to PLL-g-PEG surfaces can be performed by introducing biotin to the surface by assembling mixed (PLL-g-PEG/PEGbiotin + PLL-g-PEG) from the corresponding mixed solutions. The resulting biotinylated surfaces have been shown to be highly resistant to nonspecific adsorption

from serum while allowing binding of linkage proteins (e.g., streptavidin or avidin) and subsequent attachment of biotinylated biorecognition elements.[184−186] PEG-containing molecules were also successfully employed as the secondary blocking agents on the surface with covalently immobilized proteins.[187] Oligo(ethylene glycol) (OEG)-terminated alkanethiolates are widely used to form SAMs on gold surfaces of SPR sensors, typically also in combination with alkanethiolates containing various functional groups.[188,189] Several heterobifunctional OEG or PEG surfaces have been employed in affinity biosensors. [190]Although OEG-terminated SAMs have shown high resistance to nonspecific protein adsorption, the real biomedical applicability of these surfaces has been limited, mainly due to the limited oxidative stability of thiolates and the difficulty of integrating them into biomedical devices.[191,192] It has been reported that PEG molecules autoxidize relatively rapidly, especially in the presence of oxygen and transition metal ions.[193] Whitesides and co-workers explored alkanethiolates in SAMs with various functional groups and concluded that inertness of the surface is a general property of a group of surfaces rather than a specific property of ethylene glycol groups. They have also investigated the resistance of SAMs terminated with various groups to bacteria and mammalian cells and found that there was very little correlation between the resistance to the adsorption of protein and the adhesion of cells.[191] On the basis of experimental investigation of SAMs with different functional groups, Whitesides's group concluded that important requirements for protein resistance are (1) hydrophilicity, (2) ability to accept a hydrogen bond, (3) inability to donate to a hydrogen bond, and (4) a net neutral charge.[194] Subsequently, they hypothesized that a zwitterionic SAM combining positively charged and negatively charged groups might offer a new type of protein-resistant surface.[194] Kitano et al. formed a SAM of zwitterionic telomers on a metal surface and demonstrated its ability to reduce the nonspecific adsorption of proteins.[195] Subsequently, Jiang's group extended this material into a dual-functional zwitterionic poly(carboxybetaine methacrylate) (polyCBMA) polymer using reactive carboxyl groups for protein immobilization.[196] They demonstrated a polyCBMA polymer with immobilized antibodies against human chorionic gonadotropin (hCG) that, when exposed to high concentrations of lysozyme and fibrinogen, exhibited nonspecific adsorption of <0.3 ng/cm^2 (Figure 7).[196] Most recently, Jiang's group has investigated bacterial adhesion to the zwitterionic poly(sulfobetaine methacrylate) (polySBMA) and demonstrated that polySBMA surfaces dramatically reduce bacterial adhesion.[197]

Chen et el. showed that oligo(phosphorylcholine) SAMs exhibit strong resistance to protein adsorption, specifically to high concentrations of fibrinogen, lysozyme, and bovine serum albumin.[198]

In the past several few years, numerous SPR biosensors for detection in complex matrices have been reported. The most frequently targeted complex medium is blood serum, which is a key medium for medical diagnostics applications. Most of the reported SPR biosensors were designed to operate in serum diluted by buffer to serum concentrations from 1 to 25%. The detection of antibodies against Epstein−Barr virus (anti-EBNA) in 1% serum was reported by Homola's group.[199] A synthetic peptide, which was used as a biorecognition element, was immobilized on the surface via hydrophobic and electrostatic interactions. Nonspecific

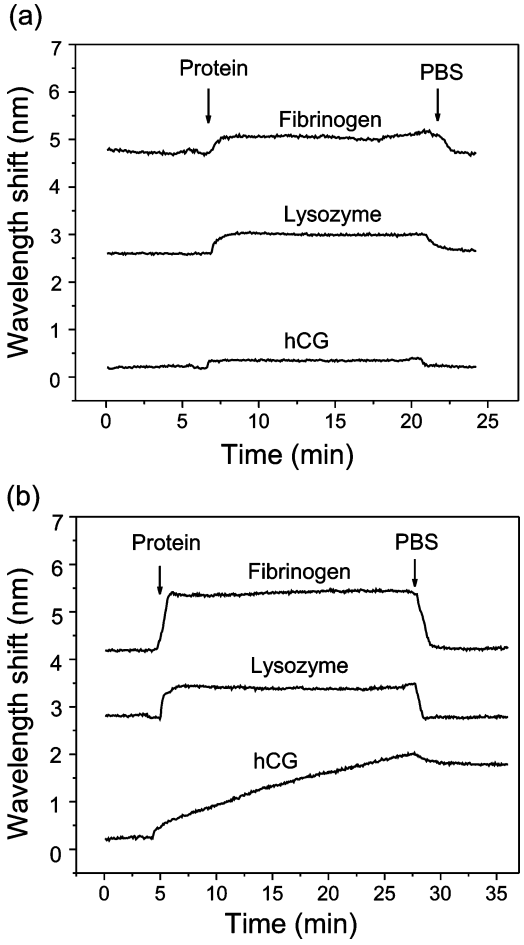

Figure 7. Adsorption of 1 mg/mL fibrinogen, 1 mg/mL lysozyme, and 20 μg/mL hCG from PBS on (a) polyCBMA-grafted surfaces and (b) polyCBMA-grafted surfaces with immobilized hCG antibodies. Reprinted with permission from ref 196. Copyright 2006 American Chemical Society.

adsorption from 1% serum was found to be negligible, and the LOD for anti-EBNA was 0.2 ng/mL.[199] Ayela et al. reported an SPR sensor for the detection of IA-2 autoantibodies also in 1% human serum.[200] In that work various types of mixed SAMs were evaluated in terms of specific and nonspecific binding. It was observed that the nonspecific adsorption from serum to surface coated with EG6-SAM100%COOH was about an order of magnitude lower than the adsorption to a SAM100%COOH-coated surface. Using an EG6-SAM25%COOH-coated surface, their SPR sensor was able to detect antibody at a concentration of 0.2 nM.[200] Cao et al. detected prostate-specific antigen-1−antichymotrypsin (PSA−ACTcomplex) in 10% serum. Their sensor employed a mixed SAM of alkanethiolates terminated with EG6-COOH and EG3-OH groups. The COOH group was biotinylated and used for subsequent immobilization of streptavidin and antibody against the PSA−ACTcomplex. Nonspecific adsorption of albumin, IgG, and fibrinogen on the sensing surface was found to be negligible, and the sensor was demonstrated to be able to detect the PSA−ACT complex at concentrations below 50 ng/mL.[201] Chung et al. demonstrated detection of antibody against human hepatitis B virus (hHBV) in serum dilutions from 5 to 60%.[202] Their sensor employed a thiol monolayer prepared using 11-mercaptoundecanoic acid to which hHBV antigen was coupled using the EDAC/NHS coupling chemistry. The level of nonspecific binding at different concentrations of serum

was measured; serum concentrations of 5, 10, and 20% produced a nonspecific sensor response corresponding to protein adsorption of 20, 26, and 68 ng/cm^2, respectively.[202] Miura's group reported an SPR sensor for the detection of insulin in 10 and 25% serum.[203] The sensing surface of their sensor was constructed using a heterobifunctional oligo(ethylene glycol)−dithiocarboxylic acid derivative (OEG-DCA) containing dithiol and carboxyl end groups to which insulin was covalently bound. The results observed with OEG-DCA SAMs were further compared to those reported using a SAM of monothiol tethered oligo(ethylene glycol)−carboxylic acid (OEG-COOH), and it was concluded that the resistance of the present bare dithiol-tethered OEG-DCA SAM is comparable to or better than that of the monothiol-tethered OEG-COOH SAM.[204] The sensor was able to detect insulin in serum at insulin concentrations down to 6 ng/mL.[203] Although these developments present clear progress toward SPR biosensing in serum, an SPR sensor capable of detecting relevant concentrations of analyte in whole serum has not been demonstrated yet.

4.3. Summary

The past decade has witnessed development of numerous SPR sensors based on excitation of surface plasmons via prism coupling, waveguide coupling, or diffraction coupling and angular, wavelength, intensity, or phase modulation. SPR sensor platforms based on prism coupling remain by far the most common. SPR sensing platforms providing the highest resolutions are typically based on angular[88,127] or wavelength[62] spectroscopy of surface plasmons or phase modulation.[113,115,117] The best SPR sensor platforms with a limited number of sensing channels (<10) provide a refractive index resolution around 10^{-7} RIU. High-throughput SPR sensors with a large number of sensing channels (>100) are usually based on intensity modulation (SPR imaging) and offer an order of magnitude worse performance.[79] One of the prospective approaches to further improving the resolution of SPR sensors involves long-range surface plasmons. SPR sensors based on wavelength spectroscopy of long-range surface plasmons were demonstrated to be able to deliver resolution as low as 3×10^{-8} RIU.[96] However, as the field of long-range surface plasmons extends much farther from the sensing surface than that of conventional surface plasmons, this improvement can be fully harnessed only when large analytes (e.g., bacterial pathogens) are targeted or biorecognition elements are immobilized in a extended coupling matrix.

Various types of biorecognition elements and immobilization methods are available to allow the SPR sensing platforms to be tailored for specific detection of chemical and biological substances. Proteins (e.g., antibodies) and peptides are most frequently immobilized via covalent bonds formed between amino groups of the protein and activated carboxyls on a SAM of alkanethiolates or within a dextran matrix. Oligonucleotides can be efficiently immobilized via interaction between avidin or streptavidin immobilized on the sensing surface and biotinylated oligonucleotide. Small molecules are usually conjugated with a larger protein (BSA), which is subsequently (covalently) immobilized on the sensor surface. High-throughput SPR sensors demand immobilization methods capable of accurate spatially controlled delivery of different biorecognition elements to different areas of the sensing surface. This can be achieved by combining the streptavidin-coated surface with a spatially controlled delivery of biotinylated biorecognition elements by microspotting.[79] An interesting alternative approach is based on the use of a conventional DNA chip and its conversion to a protein chip by incubating the chip with a mixture of proteins conjugated with complementary DNA sequences.[165]

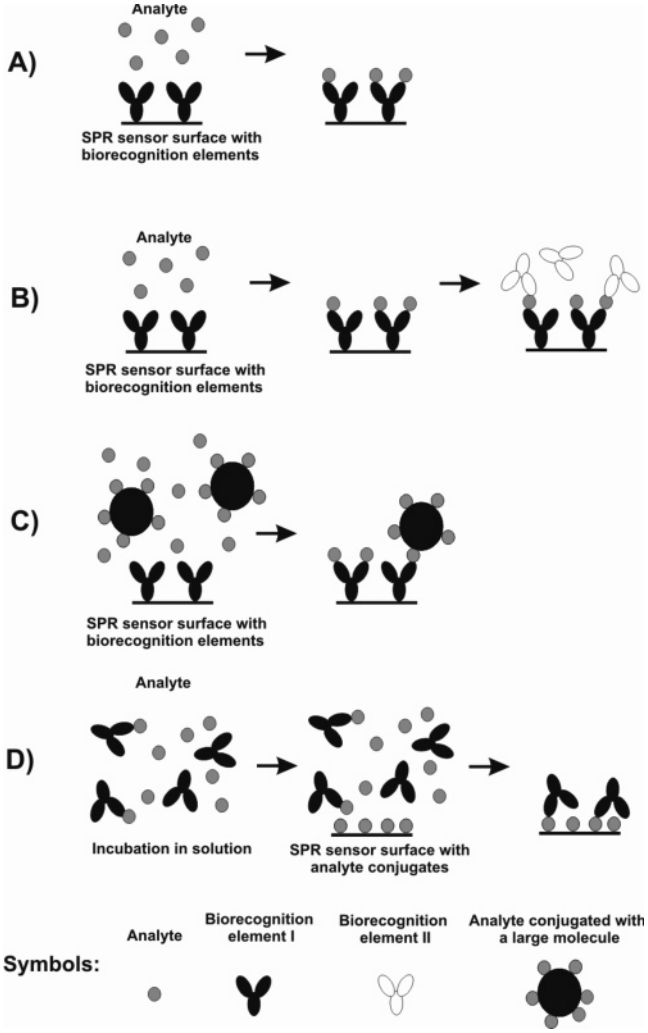

Figure 8. Main detection formats used in SPR biosensors: (A) direct detection; (B) sandwich detection format; (C) competitive detection format; (D) inhibition detection format.

5. Applications of SPR Sensors for Detection of Chemical and Biological Species

SPR biosensors have been applied in numerous important fields including medical diagnostics, environmental monitoring, and food safety and security.

5.1. Detection Formats

Various formats for the detection of chemical and biological analytes have been applied in SPR sensors.[205,206] The format of detection is chosen on the basis of the size of target analyte molecules, binding characteristics of available biomolecular recognition element, range of concentrations of analyte to be measured, and sample matrix.[206] The most frequently used detection formats include (a) direct detection, (b) sandwich detection format, (c) competitive detection format, and (d) inhibition detection format (Figure 8).

In the direct detection mode (Figure 8A), the biorecognition element (e.g., antibody) is immobilized on the SPR

sensor surface. Analyte in solution binds to the antibody, producing a refractive index change detected by the SPR sensor. Direct detection is usually preferred in applications, where direct binding of analyte of concentrations of interest produces a sufficient response. The specificity and LOD can be improved by using the sandwich detection format (Figure 8B), in which the sensor surface with captured analyte is incubated with a second antibody. Smaller analytes (molecular weight < 5000) often do not generate a sufficient change in the refractive index and therefore are measured using either competitive or inhibition detection format. Figure 8C shows an example of the competitive detection format, in which the sensing surface is coated with an antibody interacting with the analyte; when a conjugated analyte is added to the sample, the analyte and its conjugated analogue compete for a limited number of binding sites on the surface. The binding response is inversely proportional to the analyte concentration. In the inhibition detection format (Figure 8D) a fixed concentration of an antibody with affinity to analyte is mixed with a sample containing an unknown concentration of analyte. Then, the mixture is injected in the flow cell of the SPR sensor and passed over a sensor surface to which analyte or its analogue is immobilized. Noncomplexed antibodies are measured as they bind to the analyte molecules immobilized on the sensor surface. The binding response is inversely proportional to the concentration of analyte.

In recent years, various modifications and extensions of these basic detection formats have been developed in order to expand and improve detection capabilities of SPR biosensors.[207]

Several detection formats for the detection of multiple analytes have been reported. Chung et al. modified the sandwich assay approach to allow detection of multiple analytes in a single sensing channel.[208] They immobilized antibodies against two different analytes on the same area of the sensor surface. After incubation of sample with the sensor surface, solutions containing respective antibody were sequentially injected. Sensor response to each antibody was proportional to a concentration of the respective analyte.[208] The same concept was adopted for inhibition detection format by Lechuga's group.[209] They immobilized three analyte derivatives on the sensor surface, and the sensor response to each analyte was determined by incubation of the sensor with a solution containing a respective antibody.[209]

Enhancement of sensor sensitivity through the "labeling" of a secondary antibody in the sandwich detection format by latex particles[210] or gold nanoparticles[211] was demonstrated in the 1990s. In 2005 Mitchell et al. used the labeling approach in the inhibition detection format.[212] They used gold nanoparticles to improve the sensitivity of the SPR sensor for detection of progesterone. In their study, the (primary) antibody mixed with a sample was conjugated with biotin. Upon incubation of the sample with a sensor surface coated with progesterone, streptavidin conjugated with a gold nanoparticle (10 or 20 nm in diameter) was injected. The LOD for progesterone in buffer was established at 23 pg/mL; this corresponds to an improvement by a factor of 17 compared to the inhibition format.[212] In 2003 Sato et al. described amplification of SPR response to DNA based on the use of DNA-carrying hydrogel microspheres.[213] Acrylamide-based microspheres with carboxyl groups were conjugated with DNA probes. Binding of DNA-carrying acrylamide-based microspheres with target DNAs at the sensor surface resulted in a 100-fold increase in sensitivity compared to the sensitivity of nonamplified DNA target hybridization. In 2004 Okamura et al. reported the enhancement of an SPR sensor response by means of hydrogel nanospheres and the same protocol.[214] Their hydrogel nanospheres were prepared by precipitation polymerization of acrylamide, methylenebisacrylamide, and methacrylic acid.[214] Styrene−glycidyl methacrylate (SG) microspheres prepared by soap-free emulsion copolymerization were proposed by Sato et al.[215] They used DNA conjugated with SG microspheres to enhance the signal from hybridization of DNA to a complementary DNA strand immobilized on the SPR sensor surface. They immobilized short ssDNA onto the sensor surface to capture (a longer) target DNA. Subsequently, DNA-carrying microspheres were injected to bind to the free portion of the target DNA.[215] In 2006 Komatsu et al. proposed an amplification method suitable for intensity-modulated SPR sensors based on dye-doped polymer particles.[216] The dye-doped polymer particles can enhance the sensitivity of intensity-modulated SPR sensors by two mechanisms—by the shift in the resonant coupling condition due to the refractive index change induced by the presence of the particles and by absorption of light in the dye-doped particles. In a model experiment, the authors compared sensor responses due to the binding of BSA or BSA conjugated with dye-doped polymer particles to anti-BSA immobilized on the sensor surface. The use of particles was demonstrated to provide a 100-fold improvement in sensor sensitivity.[216] Recently, several methods for enhancing the sensitivity of SPR biosensors based on enzymatic amplification were developed by Corn's group. Goodrich et al. reported an enzymatic amplification method for the detection of DNA molecules that utilizes RNA microarrays in conjunction with the enzyme RNase H.[217] In this method, a single-stranded RNA microarray is exposed to a solution containing both the complementary DNA and RNase H. The DNA binds to its RNA complement on the surface and forms an RNA−DNA heteroduplex. RNase H then binds to this heteroduplex, selectively hydrolyzes the RNA probe, and releases the DNA complement back into solution. The released DNA molecule binds to another RNA probe on the surface, so that a single DNA molecule can initiate the destruction of many surface-bound RNA probes. Eventually, all of the RNA probe molecules are destroyed and removed from the surface. The loss of RNA probe molecules from the surface is detected by the SPR method. Using this approach, DNA solutions were detected at levels down to 10 fM.[217] Another enzymatic amplification approach for the detection of DNA was demonstrated by Lee et al.[218] In the first step of this approach, an ssDNA array is exposed to a solution containing target DNA and enzyme exonuclease III (*Exo*III); the target DNA hybridizes to its complementary ssDNA array elements, and *Exo*III binds to the dsDNA. *Exo*III selectively hydrolyzes the probe DNA strand from the duplex, releasing the target DNA strand back into solution. The released target DNA is then free to bind to another surface-bound ssDNA probe. This cyclic reaction progresses until all ssDNA probes on the surface are destroyed by *Exo*III.[218] Using this approach, a 16-mer ssDNA was detected down to 10−100 pM, which presents a 10^2-10^3 -fold improvement.[218] Fang et al. described an amplification method for the detection of RNA based on poly(A) enzyme chemistry and nanoparticle enhancement.[219] In this method the target RNA is adsorbed from solution onto a single-stranded LNA microarray. Subsequently, poly(A) tails are introduced to the surface-

bound RNAs via the poly(A) polymerase surface reaction. Finally, poly(A) tails are hybridized with T_{30}-DNA-coated Au nanoparticles. This approach was demonstrated to allow detection of RNAs down to 10 fM.[219] Recently, Li et al. reported another enzymatic amplification approach.[220] In the first step of this method, the target protein binds to the aptamer immobilized on the sensor surface. Then, a horseradish peroxidase (HRP)-conjugated antibody to the target protein is introduced to create an aptamer−protein−antibody sandwich, which is subsequently exposed to the substrate 3,3′,5,5′-tetramethylbenzidine (TMB). Reaction of TMB with HRP gives rise to a dark blue precipitate. This methodology was applied in an SPR sensor for detection of human thrombin. The LOD was demonstrated at a concentration of 500 fM, which corresponds to an enhancement factor of $\sim 10^4$.[220]

5.2. Food Quality and Safety Analysis

As the acceptance of SPR biosensor technology in food analysis continues to increase, the number of publications on SPR biosensors for the detection of analytes related to food quality and safety increases.[221−225] The targeted analytes include pathogens, toxins, drug residues, vitamins, hormones, antibodies, chemical contaminants, allergens, and proteins.

5.2.1. Pathogens

In recent years, various pathogens have been targeted by SPR biosensors.[226] In particular, they include bacteria, protozoa, fungi, and parasites.

Escherichia coli O157:H7 was first detected by SPR by Fratamico et al. in 1998.[227] Since then, numerous SPR biosensors for the detection of *E. coli* O157:H7 have been reported. Choi's group used the commercial SPR sensor Multiskop (Optrel, Germany) and monoclonal antibodies immobilized on a protein G-coated sensor surface. The sensor was demonstrated to be able to directly detect *E. coli* O157:H7 at concentrations as low as 10^4 cells/mL.[228] Subsequently, they demonstrated that in conjunction with the immobilization of antibodies via a mixed SAM of alkanethiolates, the same SPR instrument can detect *E. coli* O157:H7 down to 10^2 cells/mL.[229] Taylor et al. detected *E. coli* O157:H7 using a custom-built SPR sensor with wavelength modulation and examined the effect of various treatment methods on sensor performance.[230] A monoclonal antibody was immobilized on a mixed −COOH- and −OH-terminated SAM of alkanethiolates via amine coupling chemistry. Detection of *E. coli* O157:H7 was performed in the sandwich detection format using a secondary polyclonal antibody. Detection limits for detergent-lysed bacteria, heat-killed bacteria, and untreated bacteria were determined to be 10^4, 10^5, and 10^6 colony-forming units (cfu)/mL, respectively.[230] Detection of *E. coli* O157:H7 using a commercially available Spreeta sensor (Texas Instruments Co.) was reported by Meeusen et al.[231] Biotinylated polyclonal antibody against *E. coli* O157:H7 was immobilized on the avidinated gold surface. The SPR biosensor was shown to be capable of detecting *E. coli* O157:H7 in cultures at levels down to 8.7×10^6 cfu/mL in 35 min.[231] Another SPR sensor for the detection of *E. coli* O157:H7 based on the Spreeta sensor was reported by Su and Li.[232] In that work, polyclonal *E. coli* O157:H7 antibodies were immobilized via protein A adsorbed on the sensor surface. The sensor was demonstrated to be able to detect *E. coli* O157:H7 in an aqueous environment at levels down to 10^6 cells/mL.[232] Subramanian et al. demonstrated an SPR biosensor for the detection of *E. coli* O157:H7. They used the commercial SPR sensor SR 7000 (Reichert Analytical Instruments) and attachment of *E. coli* O157:H7 polyclonal antibodies via alkanethiolate SAM and amine coupling chemistry. Detection of *E. coli* O157:H7 was performed in sandwich format. The detection limit for *E. coli* O157:H7 was established at 10^3 cfu/mL.[233] Taylor et al. reported SPR-based detection of *E. coli* O157:H7 in apple juice using a custom-built multichannel SPR sensor with wavelength modulation and sandwich detection format.[234] Biotinylated polyclonal antibodies against *E. coli* O157:H7 were immobilized via streptavidin attached to a mixed SAM of oligo(ethylene glycol) alkanethiolate and biotinylated alkanethiolate. Detection of heat-killed *E. coli* O157:H7 was performed in buffer, in a mixture of four bacterial species, and in apple juice. The effect of the pH of the apple juice on the sensor response was investigated, and SPR responses were higher for bacteria in apple juice at pH 7.4 than in apple juice at pH 3.7. The LOD was 1.4×10^4 cfu/mL in buffer and about 10^5 cfu/mL in apple juice with an adjusted pH of 7.4.[234] Waswa et al. used two commercial SPR sensors—laboratory instrument Biacore 2000[235] and a miniature SPR sensor Spreeta[236]—to detect *E. coli* O157:H7. Immobilization of *E. coli* O157:H7 antibody for the laboratory SPR system was performed by first attaching protein A using a carboxymethylated dextran layer and amine coupling chemistry and subsequent attachment of the antibody.[235] The LOD for *E. coli* O157:H7 in pasteurized milk was determined to be 25 cfu/mL.[235] In the Spreeta sensor, the biotinylated *E. coli* O157:H7 antibody was attached to a layer of neutravidin molecules adsorbed on the gold surface.[236] The detection limit for *E. coli* O157:H7 in milk, apple juice, and ground beef was estimated to be in the range of 10^2-10^3 cfu/mL.[236]

Salmonella enteritidis was detected using a custom-built SPR sensor with wavelength modulation by Koubová et al.[162] In that work, a double layer of antibodies was physisorbed on a bare gold surface and cross-linked with gluteraldehyde. Direct detection of heat-killed, ethanol-soaked *S. enteritidis* at a concentration as low as 10^6 cfu/mL was demonstrated.[162] Bokken et al. demonstrated detection of *Salmonella* groups A, B, D, and E using the commercial SPR sensor Biacore 3000.[237] Antibodies were immobilized in a carboxymethylated dextran layer via amine coupling chemistry, and detection of *Salmonella* serotypes was performed using the sandwich format. *Salmonella* serotypes were detectable at a concentration of 1.7×10^5 cfu/mL even in the presence of other bacteria at 10^8 cfu/mL levels.[237] Choi's group demonstrated the detection of *Salmonella typhimurium* using the commercial SPR sensor Multiskop and monoclonal antibodies immobilized via protein G attached to an alkanethiolate SAM on the sensor surface. The LOD was 10^2 cfu/mL.[238] An SPR sensor for the detection of *Salmonella paratyphi* was demonstrated by the same group.[239] They used the same SPR instrument—a Multiskop—and a similar method for the attachment of monoclonal antibodies via protein G. Detection of *S. paratyphi* was shown down to concentrations of 10^2 cfu/mL.[239] In 2006 detection of *Salmonella* in food matrices was reported by two groups. Taylor et al. reported SPR-based detection of *Salmonella choleraesuis* serotype typhimurium in apple juice using a custom-built multichannel SPR sensor with wavelength modulation and sandwich detection format.[234] Biotinylated polyclonal antibodies against *Salmonella* were immobilized via streptavidin attached to a mixed SAM of oligo(ethylene glycol) alkanethiolate and

biotinylated alkanethiolate. Detection of *Salmonella* was performed in buffer, in a mixture of four bacterial species, and in apple juice. The effect of the pH of the apple juice on the sensor response was investigated, and SPR responses were higher for bacteria in apple juice at pH 7.4 than in apple juice at pH 3.7. The LOD for *S. choleraesuis* was 4.4×10^4 cfu/mL in buffer and about 10^4 cfu/mL in apple juice with an adjusted pH of 7.4.[234] Waswa et al. detected *S. enterica* serovar Enteritidis in milk using the commercial SPR sensor Biacore 2000.[235] In that work, polyclonal *S. enterica* antibody was immobilized by first attaching protein A using a carboxymethylated dextran layer and amine coupling chemistry and subsequent attachment of the antibody to protein A.[235] The LOD for *Salmonella* in pasteurized milk was determined to be 23 cfu/mL.[235] In 2007 Mazumdar et al. also reported the detection of *Salmonella* in milk.[240] They used the commercial SPR sensor Plasmonic and sandwich detection format. Polyclonal capture antibody was immobilized by self-assembly on the hydrophobic sensing surface formed by alkylsilanes. Milk spiked with *S. typhimurium* cells, killed by thimerosal (1%, w/w), was incubated with the sensing surface for 15 min and then switched with a solution containing the second antibody. The LOD for *S. typhimurium* cells in milk was at 10^5 cells/mL.[240]

Listeria monocytogenes was detected by Koubová et al.[162] They used a custom-built SPR sensor with wavelength modulation and a double layer of antibodies adsorbed on a bare gold surface and cross-linked with glutaraldehyde. Heat-killed *Listeria* bacteria were detected at levels down to 10^7 cfu/mL.[162] Leonard et al. used the commercial SPR sensor Biacore 3000 and competitive format to detect the *L. monocytogenes*.[241] A polyclonal anti-goat antibody was immobilized in a carboxymethylated dextran layer using amine coupling chemistry. Solutions of known concentrations of *L. monocytogenes* were incubated with rabbit anti-*Listeria* antibodies. Cells and bound antibodies were then centrifuged out of solution, and the unbound antibodies remaining in solution were detected by the SPR sensor. The LOD was determined to be 10^5 cells/mL.[241] Detection of *L. monocytogenes* in apple juice was reported by Taylor et al.[234] They used a custom-built multichannel SPR sensor with wavelength modulation and sandwich detection format. Biotinylated polyclonal antibodies against *L. monocytogenes* were immobilized via streptavidin attached to a mixed SAM of oligo(ethylene glycol) alkanethiolate and biotinylated alkanethiolate. Detection of *L. monocytogenes* was performed in buffer, in a mixture of four bacterial species, and in apple juice. In the considered range of concentrations of *L. monocytogenes* in apple juice, the sensor response was higher for bacteria in apple juice with an adjusted pH of 7.4 than for those in buffer or natural apple juice with a pH of 3.7. The LOD for *L. monocytogenes* was determined to be about 3×10^3 cfu/mL for detection in both buffer and apple juice with a pH of 7.4.[234]

Campylobacter jejuni was detected by Taylor et al.[234] They used a custom-built multichannel SPR sensor with wavelength modulation and sandwich detection format. Biotinylated polyclonal antibodies against *C. jejuni* were immobilized via streptavidin attached to a mixed SAM of oligo(ethylene glycol) alkanethiolate and biotinylated alkanethiolate. Detection of heat-killed *C. jejuni* was performed for buffer solutions containing only *C. jejuni* as well as a mixture of *C. jejuni* and other bacteria and apple juice spiked with *C. jejuni*. The LOD for *C. jejuni* was 1×10^5 cfu/mL in buffer and about 5×10^4 cfu/mL in apple juice.[234]

Staphylococcus aureus was detected by means of an SPR biosensor by Subramanian et al.[242] They used the commercial SPR sensor SR 7000 and detected *S. aureus* directly or in sandwich detection format. Alkane monothiol and dithiol dendritic tether-based SAMs were examined for subsequent attachment of *S. aureus* antibodies using amine coupling chemistry. The LOD was determined to be 10^7 cfu/mL for direct detection and 10^5 cfu/mL for sandwich format for both sensing surfaces.[242] Balasubramanian et al. reported an SPR-based detection of *S. aureus* using lytic phage as a biorecognition element.[243] In that work a commercial SPR sensor, Spreeta, was used as a detection platform, and lytic phage was immobilized on the sensor surface by direct physical adsorption. The LOD for *S. aureus* in buffer was found to be 10^4 cfu/mL.[243]

Recently, Taylor et al. demonstrated the simultaneous detection of the four above-mentioned bacteria—*E. coli* O157:H7, *C. jejuni*, *S. typhimurium*, and *L. monocytogenes*—on a custom-built multichannel SPR sensor.[234] All bacteria were heat-killed and ultrasonicated prior to detection. Simultaneous detection of individual bacteria in the mixtures showed good agreement with detections of individual bacteria in buffer. Detections of individual bacteria and mixtures were also performed in apple juice samples. LODs for all four cases were established at 10^4, 5×10^4, 5×10^4, and 10^4 cfu/mL for *E. coli* O157:H7, *C. jejuni*, *S. typhimurium*, and *L. monocytogenes*, respectively.[234]

Yersinia enterocolitica was detected by Choi's group,[244] using the commercial SPR sensor Multiskop and monoclonal *Y. enterocolitica* antibodies immobilized via protein G attached to an alkanethiolate SAM on the sensor surface. The LOD for *Y. enterocolitica* in buffer was determined to be 10^2 cfu/mL.[244]

Vibrio cholerae O1 was detected by means of an SPR biosensor by Choi's group.[245] They used the commercial SPR sensor Multiskop and monoclonal antibodies immobilized via protein G attached to an alkanethiolate SAM on the sensor surface. The LOD for *V. cholera* O1 in buffer was determined to be about 4×10^5 cfu/mL.[245]

Protozoan parasite *Cryptosporidium parvum* oocyst, was detected by an SPR biosensor by Kang et al.[246] In that work, the authors used the commercial SPR sensor platform Biacore 2000 and direct detection approach. Immobilization of biotinylated monoclonal antibody against *C. parvum* oocyst was performed on a mixed alkanethiolate SAM with attached streptavidin. The biosensor was able to detect *C. parvum* oocyst in buffer directly at a concentration of 10^6 oocysts/mL. The authors also explored an alternative detection format consisting of the immunoreaction step between the biotinylated antibody and oocysts followed by the binding step of antibody−oocysts complex on the streptavidin-incubated surface. In this format, the LOD for *C. parvum* oocyst in buffer was established at 10^2 oocysts/mL.[246]

Detection of a fungal pathogen, *Fusarium culmorum*, in wheat using an SPR sensor was demonstrated by Zezza et al.[247] Detection of *F. culmorum* was based on extraction of DNA from a sample, amplification of specific DNA fragment of *F. culmorum*, and subsequent detection of the amplicon using the SPR method via hybridization with complementary sequence immobilized on the SPR sensor (Biacore X) surface. The detection limit for the *F. culmorum* amplicon was 0.25 ng/μL. In 30 ng of durum wheat DNA, the smallest

detectable amount of specific *F. culmorum* DNA was 0.06 pg.[247]

5.2.2. Toxins

Toxins implicated in food safety include mainly toxins produced by bacteria, fungi, and algae.

Staphylococcal enterotoxin B (SEB) was detected by an SPR sensor by Nedelkov et al. in 2000.[248,249] They used the commercial SPR sensor Biacore X and SEB antibody immobilized in a carboxymethyldextran layer on the sensor surface via amine coupling chemistry. SEB was detected directly in milk and mushroom samples at levels down to 1 ng/mL. The SPR detection was followed by identification of the bound toxin by matrix-assisted laser desorption/ionization time-of-flight (MALDI-TOF) mass spectrometry.[248,249] In 2002 Homola's group reported detection of SEB using a fiber optic SPR sensor.[250] A double layer of antibodies was physisorbed on the surface of the SPR sensor and cross-linked with glutaraldehyde. SEB was detected directly, and the limit of detection for SEB in buffer was established at 10 ng/mL.[250] Naimushin et al. detected SEB using a prototype of an SPR sensor developed by Texas Instruments Co. and antibodies immobilized on the sensor surface via a gold binding peptide.[251] SEB was detected in buffer and seawater using direct detection or sandwich format with one or two amplification antibodies. The LOD for direct detection was 0.2 nM (5.6 ng/mL) in buffer and 1 nM (28 ng/mL) in seawater. Using a one-step amplification, concentrations of 20 pM (0.6 ng/mL) and 50 pM (1.4 ng/mL) were detected in buffer and seawater, respectively. The use of a second amplification antibody was shown to improve the LOD in buffer to 100 fM (2.8 pg/mL).[251] Homola et al. reported the detection of SEB in buffer and milk.[91] In that work, a custom-built wavelength modulation SPR sensor was employed, and polyclonal SEB antibody was immobilized on a mixed SAM of alkanethiolate using amine coupling chemistry. Detection of SEB was performed directly or using sandwich detection format. The LOD for direct detection of SEB in buffer was 5 ng/mL. Using a secondary antibody the LOD was improved to 0.5 ng/mL for both buffer and milk.[91] In 2003 Medina reported the detection of SEB using an inhibition detection format.[252] Sample containing SEB was incubated with a known concentration of SEB antibody for 20−30 min, and then the mixture was analyzed by the SPR sensor. The LOD for SEB in milk was established at 0.3 ng/mL. The sensing surface was demonstrated to be regenerable for repeated use by 100 mM hydrochloric acid.[252] Detection of SEB in another food matrix was demonstrated by Medina, who detected SEB in ham tissue.[253] In that work the commercial SPR sensor Biacore 1000 was used, and polyclonal antibody was immobilized in a carboxymethyldextran layer on the sensor surface via amine coupling chemistry. The LOD for sandwich detection format was determined to be 2.5 ng/mL in both buffer and ham tissue extract.[253]

Medina also demonstrated detection of Staphylococcal enterotoxin A (SEA) in raw eggs using the commercial SPR sensor Biacore 1000 and competitive detection format.[254] SEA was immobilized in a carboxymethyldextran layer on the sensor surface via amine coupling chemistry. Homogenized raw egg samples were clarified by centrifugation. Anti-SEA was added to the sample, allowing SEA to bind with anti-SEA. The bound complex was separated from the free antibody by centrifugation. The supernatant was injected over the SEA-coated surface. Using this approach, SEA was detected in whole egg at concentrations down to 1 ng/mL.[254]

Domoic acid (DA) was detected using an SPR biosensor by Lotierzo et al.[255] They used the commercial SPR sensor Biacore 3000 and a molecularly imprinted polymer photografted on a gold chip as a biorecognition element. Detection was performed in a competitive binding format in which free DA competed with its conjugate with horseradish peroxidase. The sensor was demonstrated to be able to detect DA in buffer at a concentration as low as 5 ng/mL.[255] In 2005 Yu et al. demonstrated detection of DA using a custom-built SPR and inhibition detection format.[256] DA was immobilized on a mixed SAM of OEG-containing alkanethiolates using amine coupling chemistry. The effect of regeneration and storage on the performance of the SPR sensor was investigated. The LOD of DA in buffer was established at 0.1 ng/mL.[256] Traynor et al. demonstrated SPR-based detection of DA in extracts of shellfish species.[257] They used the commercial SPR sensor Biacore Q, and immobilization of DA in a carboxymethyldextran layer on the sensor surface was performed by amine coupling chemistry. Detection of DA was performed in inhibition format. Detection limits for DA in mussels, oysters, and cockles were determined to be about 1, 4.9, and 7 μg/g, respectively.[257] Stevens et al. detected domoic acid in clam extracts using a portable SPR biosensor employing Spreeta 2000 modules and inhibition detection format.[258] Polyclonal DA antibodies were immobilized on the sensor surface via a gold binding peptide. Detection was performed in buffer and in diluted clam extracts. The sensor was able to detect DA at 3 ng/mL in both buffer and diluted clam extracts.[258]

Aflatoxin B_1 was detected using the commercial SPR sensor Biacore 1000 by Daly et al.[259] In that work, aflatoxin B_1 was conjugated to BSA and immobilized on carboxymethylated dextran using amine coupling chemistry. Detection was performed using inhibition detection format. Detection of aflatoxin B_1 in buffer was demonstrated at levels down to 3 ng/mL.[259] Dunne et al. demonstrated an SPR sensor for aflatoxin B_1 using scFvs as a biorecognition element.[148] Detection was performed in the commercial SPR sensor Biacore 3000 using inhibition detection format. Aflatoxin B_1 derivative was immobilized on the carboxymethylated dextran layer on the sensor surface using amine coupling chemistry. Regeneration protocol was developed enabling at least 75 detection/regeneration cycles. The LOD for aflatoxin B_1 in buffer was 375 pg/mL for monomeric scFv and 190 pg/mL for dimeric scFv.[148]

Detection of deoxynivalenol in buffer and wheat was demonstrated by Tüdös et al.[260] In that work, the commercial SPR system Biacore Q system was used and detection of deoxynivalenol was performed using the inhibition detection format. Deoxynivalenol conjugated to casein was immobilized on a carboxymethylated dextran layer on the sensor surface using amine coupling chemistry. The sensor was demonstrated to detect deoxynivalenol in buffer down to 2.5 ng/mL and showed good agreement with liquid chromatography−tandem mass spectrometry measurements on wheat samples.[260]

5.2.3. Veterinary Drugs

Another important field in which SPR biosensor technology has been increasingly applied is testing for veterinary drug residues (e.g., antibiotics, β-agonists, and antiparasitic drugs) in food.[261]

An SPR sensor for the detection of antibiotics (penicillins and cephalosporins) in milk was demonstrated by Cacciatore et al.[262] Their approach was based on the noncompetitive inhibition of the binding of digoxigenin-labeled ampicillin (DIG-AMPI) to a soluble penicillin-binding protein 2× derivative (PBP 2×*) of *Streptococcus pneumoniae* by other β-lactam antibiotics. Subsequently, the DIG−AMPI/PBP 2×* complex was detected using the commercial SPR platform Biacore 3000 and digoxigenin antibody immobilized on the sensor chip. The LODs for the selected antibiotics in raw milk were established to be below 2 ng/mL for benzylpenicillin, ampicillin, and amoxicillin, 15 ng/mL for cloxacillin, 50 ng/mL for cephalexin, and 25 ng/mL for cefoperazone.[262] Chloramphenicol and chloramphenicol glucuronide residues in various food matrices were detected by Ashwin et al.[263] They used the commercial SPR platform Biacore Q and direct detection format. They detected chloramphenicol in extracts from honey, prawns, and dairy products and chloramphenicol glucuronide in extracts of porcine kidney at concentrations below 0.2 μg/kg.[263] Detection of chloramphenicol and chloramphenicol glucuronide using an SPR sensor and inhibition assay was performed by Ferguson et al.[264] They used the commercial SPR sensor Biacore Q and a chip with immobilized chloramphenicol derivative (Qflex Kit Chloramphenicol, Biacore). A known concentration of drug-specific antibody was mixed with the sample and injected over the surface of a sensor chip on which a chloramphenicol derivative was immobilized. Chloramphenicol and chloramphenicol glucuronide in extracts from food matrices were detected at levels down to 0.005 μg/kg (poultry), 0.02 μg/kg (honey), 0.04 μg/kg (prawn), and 0.04 μg/kg (milk).[264] Dumont et al. demonstrated an SPR sensor for the detection of fenicol antibiotic residues in shrimps.[265] They used the commercial SPR sensor Biacore Q and inhibition detection format. Analyte molecules were immobilized on carboxymethylated dextran using amine coupling chemistry. Chloramphenicol, florefenicol, florefenicol amine, and thiamphenicol were detected in extract from shrimp at levels down to 1, 0.2, 250, and 0.5 ng/mL, respectively.[265] In 2007 Moeller et al. reported an SPR biosensor for the indirect detection of tetracycline in honey and milk.[266] Their approach was based on the resistance mechanism against tetracycline in Gram-negative bacteria—tetracyclines release Tet repressor protein (TetR) from the *tet* operator (*tet*O). Biotinylated single-strain DNA containing the sequence of the tetracycline operator *tet*O1 was immobilized on a streptavidin-coated sensor chip. The repressor protein TetR was attached to the chip-bound operator *tet*O. Injection of a solution containing tetracycline allowed tetracycline to bind to TetR. This resulted in the release of a conformationally changed protein, which was continuously flushed away from the sensor surface. The decrease in surface density was measured using the commercial SPR sensor Biacore 3000. The LOD was estimated to be 1 ng/mL for tetracycline in buffer and 15 ng/mL and 25 μg/kg for tetracycline in raw milk and honey, respectively.[266] Detection of the antibiotic tylosin was demonstrated by Caldow et al.[267] They used the commercially available SPR sensor Biacore Q and inhibition detection format. Immobilization of tylosin on a carboxymethyldextran layer on the sensor surface was performed by amine coupling chemistry. Tylosin was detected in extract from honey at levels down to 2.5 μg/kg.[267]

5.2.4. Vitamins

Vitamin B2 (riboflavin) was detected by Caelen et al. using the commercial SPR sensor platform Biacore Q and inhibition detection format.[268] A riboflavin derivative was immobilized on the carboxymethylated dextran using amine coupling chemistry. A known concentration of riboflavin binding protein was mixed with a sample, and the amount of unreacted protein was measured using the SPR sensor. Riboflavin was detected in milk-based products, and the LOD was established at 70 ng/mL.[268] Haughey et al. reported an SPR sensor for the detection of vitamin B5 (pantothenic acid).[269] They used the commercial SPR sensor Biacore Q and inhibition detection format. Vitamin B5 derivative was immobilized in carboxymethylated dextran using amine coupling chemistry. Detection of vitamin B5 was performed in extracts from various foods (e.g., infant formula, cereal, pet food, egg powder). The LOD was 4.4 ng/mL.[269] An SPR sensor for the detection of vitamin B8 (biotin) and vitamin B9 (folic acid) was demonstrated by Indyk et al.[270] They used the commercial SPR sensor Biacore Q, a biotin sensor chip, and inhibition detection format. In their experiments, they detected biotin and folic acid in infant formulas and milk powders at concentrations as low as 2 ng/mL.[270] SPR-based detection of vitamin B12 (cobalamine) was demonstrated by Indyk et al.[271] They used the commercial SPR sensor Biacore Q and inhibition detection format. Vitamin B12 was immobilized in carboxymethylated dextran layer on the sensor surface using amine coupling chemistry. The LOD for cobalamine in milk or infant formula or an extract from beef was determined to be 0.06 ng/mL.[271]

5.2.5. Hormones

The steroid hormone progesterone in cow's milk was detected by Gillis et al.[272,273] They used the commercial SPR sensor platform Biacore 2000 and inhibition assay. Progesterone derivative was immobilized in the carboxymethylated dextran layer on the sensor surface using amine coupling chemistry. A known concentration of monoclonal antibody was incubated with sample (buffer or cow's milk), and the amount of unreacted antibody was detected by the SPR sensor. In their earlier work in 2002, Gillis et al. established the LOD for progesterone in raw bovine milk at 3.6 ng/mL.[272] Optimization of the assay reported in 2006 allowed Gillis et al. to detect progesterone in buffer and bovine milk down to 60 pg/mL and 0.6 ng/mL, respectively.[273] Mitchell et al. used the commercial SPR sensor Biacore 2000 and inhibition detection format combined with gold nanoparticles and proteins to improve the sensitivity of the detection.[212] Progesterone was immobilized to a dextran layer through covalent immobilization using an OEG linker attached to the progesterone. Detection formats employing gold particles conjugated with streptavidin and attached to biotinylated monoclonal antibody in both label prebinding and sequential binding formats were explored. Prelabeling format allowed detection of progesterone down to 143 pg/mL, and sequential binding formats yielded a LOD of 23.1 pg/mL. Secondary antibody labeling produced an 8-fold signal enhancement and a LOD of 20.1 pg/mL, whereas the use of secondary antibody conjugated with a gold nanoparticle improved the LOD to 8.6 pg/mL.[212]

5.2.6. Diagnostic Antibodies

Detection of *Mycoplasma hyopneumoniae* antibody in pig serum using the SPR method was demonstrated by Kim et

al.[274] They used the commercial Autolab Esprit SPR system and a recombinant 30 kDa fragment of P97 adhesin as an antigen. The performance of the SPR biosensor was compared with that of enzyme-linked immunosorbent assay (ELISA) using 70 pig serum samples. There was found to be a strong positive correlation between these two methods and, in terms of the LOD, the SPR sensor outperformed ELISA by a factor of 10.[274] Classical swine fever virus (CSFV) antibody in pig serum was detected by Cho and Park.[275] They used the commercial Autolab Esprit SPR system and recombinant gp55 protein as an antigen. They used the same immobilization method and methodology as in their previous study.[274] One hundred and seventy pig serum samples were analyzed by the SPR sensor and ELISA. It was determined that the LOD of the SPR sensor was better by a factor of 10 than that of ELISA.[275]

5.2.7. Allergens

Direct detection of peanut allergens by means of SPR sensor was demonstrated by Mohammed et al.[276] They used a miniature commercial SPR sensor Spreeta and peanut-specific antibodies adsorbed on the sensor surface. The LOD for the peanut allergen in buffer was estimated to be 700 ng/mL.[276] Food allergens were also detected by Malmheden Yman et al.[277] They used the commercial Biacore Q SPR instrument and affinity-purified antibodies raised against egg white, protein conalbumin, sesame seed protein, peanut protein, hazelnut protein (corylin), and crab meat, which were immobilized on the carboxymethylated dextran by the amine coupling method. Detection of allergens was performed directly and by sandwich detection format. The second antibody in the sandwich assay was demonstrated to improve both the sensitivity and specificity of the detection. Peanut proteins in chocolate diluted only 10 times before the analysis were detected down to 1 μg/g. Conalbumin in pasta was detected at levels as low as 0.3 μg/g. Sesame seed protein was detected down to 0.125 μg/mL, corresponding to 12.5 μg/g in solid food (e.g., bread). Tropomyosin in pasta was detected at the level of 10 μg/g.[277]

5.2.8. Proteins

Simultaneous detection of three caseins in milk using an SPR method was demonstrated by Dupont and Muller-Renaud.[278] They used the commercial SPR sensor platform Biacore 3000 and sandwich assay format employing two monoclonal antibodies directed against the N- and C-terminal extremities of each of the caseins, respectively. Antibody against C-terminal extremities of each of the caseins was immobilized in a separate sensing channel of the four-channel SPR sensor via carboxymethylated dextran matrix and amine coupling. Three major caseins (α_{s1}, β, and κ) were detected in milk samples. The LODs were estimated at 85 ng/mL for β-casein, 870 ng/mL for α_{s1}-casein, and 470 ng/mL for κ-casein.[278] Indyk et al. detected proteins such as immunoglobulin G, folate-binding protein, lactoferrin, and lactoperoxidase in bovine milk using the commercial SPR biosensor Biacore Q.[279] Respective monoclonal antibodies were immobilized on the dextran matrix using amine coupling chemistry. The detection was performed directly in milk samples diluted in buffer. The LODs were established at 16.8 ng/mL for immunoglobulin G, 0.7 ng/mL for folate-binding protein, 1.1 ng/mL for lactoferrin, and 75 ng/mL for lactoperoxidase.[279]

5.2.9. Chemical Contaminants

Detection of 4-nonylphenol in shellfish using an SPR biosensor was demonstrated by Samsonova et al.[280] They used the commercial SPR platform Biacore Q and inhibition detection format. 9-(*p*-Hydroxyphenyl)nonanoic acid was immobilized on dextran matrix using amine coupling chemistry. Using monoclonal antibodies, a detection limit of 2 ng/mL in buffer was achieved. The detection was performed in <3 min including a 30 s regeneration step. The sensor was regenerated by 100 mM sodium hydroxide in 10% acetonitrile. In shellfish samples, 4-nonylphenol was detected at concentrations down 10 ng/g.[280] A suspected carcinogen, insulin-like growth factor-1 (IGF-1), can occur in milk of cows treated by recombinant bovine somatotropin treatment. Guidi et al. detected IGF-1 using the commercial Biacore SPR sensor platform and inhibition detection format.[281] Recombinant IGF-1 was immobilized to a carboxymethylated dextran matrix via amine coupling chemistry. Polyclonal antibody was incubated with a sample for 2 h, and then the sample was injected in the flow cell of the SPR sensor. On the basis of the reported data, the LOD for IGF-1 in buffer and milk can be estimated to be below 10 ng/mL.[281]

5.3. Medical Diagnostics

Fast, sensitive, and specific detection of molecular biomarkers indicating normal biologic processes, pathogenic processes, or pharmacologic responses to a therapeutic intervention presents an important goal for modern bioanalytics.[282,283] SPR biosensors have been demonstrated to hold promise for the detection of analytes related to medical diagnostics such as cancer markers, allergy markers, heart attack markers, antibodies, drugs, and hormones.

5.3.1. Cancer Markers

The prostate-specific antigen (PSA) is a marker for prostate cancer.[284] Detection of PSA in PBS buffer using the commercial SPR sensor Ibis II has been reported by Besselink et al.[285] In their work, monoclonal antibodies against PSA were immobilized on the sensor surface via amine coupling chemistry. After incubation of the sensing surface with sample containing PSA, the sensor response was amplified with rabbit anti-PSA polyclonal antibodies followed with either biotinylated goat anti-rabbit IgG and streptavidin-coated latex microspheres or goat anti-rabbit IgG-coated colloidal gold. The detection format employing gold particle enhancement provided a LOD as low as 0.15 ng/mL. Huang et al. investigated the detection of PSA using direct and sandwich detection formats and the commercial SPR sensor Biacore 2000.[286] PSA-receptor molecules consisting of a single-domain antigen-binding fragment were covalently immobilized on the sensor surface via a mixed alkanethiolate SAM. PSA concentrations as low as 10 ng/mL were detected in buffer. Sandwich detection format involving a biotinylated secondary antibody and streptavidin-modified gold nanoparticles improved the LOD for PSA below 1 ng/mL. Recently, the determination of a complex of PSA with α_1-antichymotrypsin (PSA−ACT) in both HBS buffer and human serum was demonstrated by Cao et al.[201] using the commercial SPR sensor Biacore 2000. Mixed alkanethiolates were optimized to provide a stable surface for sequential attachment of biotin, streptavidin, and biotinylated antibodies against PSA−ACT. The PSA−ACT complex in HBS buffer and human serum was detected

directly at concentrations as low as 20.7 and 47.5 ng/mL, respectively. The LOD for the PSA−ACT complex was improved by employing sandwich detection format and PSA polyclonal antibody to 10.2 and 18.1 ng/mL for detection in the HBS buffer and serum, respectively.[201]

The quantitation of a pancreatic cancer marker, carbohydrate antigen (CA 19-9) was performed by Chung et al. using a miniature commercial SPR sensor Spreeta.[287] The antibody against CA 19-9 was immobilized on the sensor surface via a SAM of alkanethiolates. The sensor was shown to be able to detect CA 19-9 at a concentration of 410.9 U/mL directly and 66.7 U/mL using a sandwich assay.[287]

Protein vascular endothelial growth factor (VEGF), which plays a role in breast cancer, lung cancer, and colorectal cancer, was detected using an SPR imaging method and RNA aptamer microarray. The adsorption of proteins onto the RNA microarray was detected by the formation of a surface aptamer−protein−antibody complex. The sensor response was amplified using a localized precipitation reaction catalyzed by the enzyme horseradish peroxidase conjugated to the antibody. The sensor was demonstrated to be able to detect VEGF at a concentration of 1 pM.[220]

Yang et al.[288] measured levels of interleukin-8 (IL-8) protein in the saliva of healthy individuals and patients with oropharyngeal squamous cell carcinoma using the commercial SPR sensor Biacore X. The sandwich detection format using two monoclonal antibodies recognizing different epitopes on the IL-8 was used. A monoclonal antibody against IL-8 was immobilized in the dextran layer via amine coupling chemistry. Saliva samples were first centrifuged to clarify the supernatants. The supernatants were then aspirated and separated from the cellular pellet. The detection limit for IL-8 was determined to be 2.5 pM (∼0.02 ng/mL) for detection in buffer and 184 pM (∼1.5 ng/mL) for detection in saliva samples.

Carcinoembryonic antigen (CEA), a marker related to colorectal cancer, was detected by the SPR method of Tang et al.[289] They used the commercial SPR sensor Autolab Springle and protein A adsorbed on the SPR sensor surface for subsequent attachment of carcinoembryonic antibody. The LOD of 0.5 ng/mL was achieved, and the sensor was demonstrated to be regenerable for repeated use.[289]

Tian et al. demonstrated an SPR biosensor for the detection of fibronectin, a glycoprotein implicated in carcinoma development.[212] In that work, a research SPR instrument employing an acousto-optic tunable filter and wavelength modulation was used. Fibronectin antibody was immobilized on the self-assembled alkanethiolate monolayer using amine coupling chemistry. Fibronectin was detected directly, in sandwich detection format, and with additional amplification using colloidal gold. Regenerability of the sensor was demonstrated. The LODs for fibronectin in buffer were established at 2.5, 0.5, and 0.25 μg/mL for direct detection, sandwich detection, and colloidal Au-enhanced detection, respectively.[212]

5.3.2. Antibodies against Viral Pathogens

SPR biosensors for the detection of hepatitis virus specific antibodies were reported by several research groups. In 2003 Rojo et al. described the SPR biosensor-based detection of antibodies against hepatitis G in serum.[150] They used the commercial SPR sensor Biacore 1000 and synthetic peptide as a biorecognition element, which was immobilized in the dextran layer on the sensor surface via amine coupling chemistry. Threshold measurements on sera of chronic hepatitis C patients as well as control samples from healthy patients obtained with the sensor were consistent with those obtained by ELISA. Chung et al. used the commercial SPR sensor Spreeta for the detection of antibodies against human hepatitis B virus (hHBV). The hHBV antigen was immobilized on the SAM of alkanethiolates via amine coupling chemistry. Antibodies against hHBV were detected in 5% serum in PBS. The LOD for direct detection was established at 9.2 nM. Amplification methods based on sandwich detection and avidin-biotinylated antibodies were shown to yield amplification factors of 7 and 14, respectively. Using peroxidase−antiperoxidase complex, 17-fold amplification of the sensor response was obtained and the LOD was lowered to 0.64 nM.[202]

Wittekindt et al. demonstrated an SPR sensor for the detection of antibodies against herpes simplex virus type 1 and type 2 (HSV-1, HSV-2) in human sera.[151] They used the commercial SPR sensor Biacore X and SPR chips coated with streptavidin on which two biotinylated peptides, used as biorecognition elements, were immobilized. Human serum samples (diluted 1:100 in HBS buffer) were tested using the SPR biosensor and immunoblotting (reference method). A good agreement between the SPR biosensor and immunoblotting was obtained (correlation of 83 and 86% for antibodies against HSV-1 and HSV-2, respectively).[151]

Direct detection of antibodies against Epstein−Barr virus (anti-EBNA) in 1% human serum was reported by Homola's group.[152] A short synthetic peptide was used as biorecognition element and was immobilized on the surface of a wavelength-modulated SPR biosensor via hydrophobic and electrostatic interactions. The LOD for anti-EBNA was determined to be 0.2 ng/mL. A procedure for the regeneration of the sensor was developed and demonstrated to allow at least 10 repeated anti-EBNA detection experiments without a significant loss in sensor sensitivity.[152]

Regnault et al. reported the SPR biosensor-based detection of anti-protein S antibodies following Varicella-Zolter virus infection.[290] In that work, protein S was immobilized in the layer of dextran via amine coupling chemistry and the experiments were performed using the commercial SPR sensor Biacore X. A high sensor response was observed to diluted plasma (1:5) of an infected patient, whereas samples from healthy patients generated a minimum response.[290]

Antibodies against human respiratory syncytial virus (RSV) in sera were detected by the commercial SPR biosensor Biacore 2000 by McGill et al.[291] Monoclonal antibodies against the virus glycoproteins (F- and G-glycoproteins) were covalently attached to the dextran matrix via amine coupling chemistry and then used to immobilize the respective virus glycoproteins. Serum samples isolated from patients' respiratory tracts were diluted in HBS buffer (1:10) and filtered. The SPR biosensor was demonstrated to be able to recognize the antigenic differences between the two different genotypes of the virus (G- and F-virus glycoproteins).[291]

Abad et al. demonstrated SPR-based detection of isotype-specific anti-adenoviral antibodies in patients dosed with an adenoviral-based gene therapy vector. The antibodies were detected using the commercial SPR instrument Biacore 3000 and intact virus immobilized in the thin layer of dextran on the surface of the sensor by amine coupling chemistry.[292] Patient serum samples or ascites fluid samples were diluted 1:10 with HEPES prior to the analysis.

5.3.3. Drugs and Drug-Induced Antibodies

Dillon et al. demonstrated the SPR biosensor-based detection of morphine-3-glucuronide (M3G), the main metabolite of heroin and morphine.[293] They used the commercial SPR sensor Biacore 1000 and inhibition detection format. M3G−ovalbumin conjugate was immobilized on the dextran matrix via amine coupling chemistry. Two polyclonal antibodies were produced, purified, and tested for the detection of M3G. Regeneration protocols were developed for both polyclonal antibodies and allowed for approximately 60 cycles for the first antibody and 50 cycles for the second antibody. The LOD for M3G in buffer and in urine (diluted 1:250) was found to be <1 ng/mL for both antibodies.[293]

Detection of the oral anticoagulant warfarin by the SPR method was performed by Fitzpatrick and O'Kennedy.[294] They used the commercial SPR sensor Biacore 3000 and inhibition detection format. 4′-Aminowarfarin or 4′-azowarfarin−BSA was immobilized on a dextran matrix via amine coupling chemistry. Detection of warfarin was performed in plasma ultrafiltrate (diluted 1:100). The sensor was demonstrated to detect warfarin at concentrations down to 4 ng/mL and to be regenerable for more than 70 detection cycles.[294]

Gobi et al. reported SPR sensor-based detection of insulin.[203] In that work the commercial SPR sensor SPR-670 and inhibition format were employed. Insulin was covalently bound to the activated monolayer of heterobifunctional OEG−dithiocarboxylic acid derivative. After 5 min of incubation of sample with a known concentration of monoclonal anti-insulin antibody, the mixture was injected in the SPR sensor and the concentration of the unreacted antibody was measured. A regeneration protocol was developed, and the chip was shown to be reusable for more than 25 detection cycles without an appreciable change in the sensor activity. The LOD for insulin in buffer was 1 ng/mL. The lowest detectable concentration of insulin in the serum samples spiked with insulin was 6 ng/mL.[203]

Rini et al. reported an SPR sensor for threshold measurement of antibodies against granulocyte macrophage colony stimulating factor (GM-CSF) used in therapies for various kinds of cancer.[295] Rini et al. used the commercial SPR instrument Biacore 2000 and SPR chips with GM-CSF antigen immobilized on the carboxymethylated dextran via amine coupling chemistry. Antibodies against GM-CSF were induced in prostate cancer patients by repeated administration of GM-CSF, and their presence was measured in diluted sera (1:5). The SPR measurements showed the presence of GM-CSF reactive antibodies for all prostate cancer patients treated with GM-CSF, which was in agreement with reference ELISA measurements.[295]

An SPR biosensor for the detection of antibody against insulin was demonstrated by Kure at al.[296] Insulin antibodies can cause insulin resistance or hypoglycemia in diabetic patients treated with human insulin. In that work the commercial SPR biosensor Biacore 2000 was employed and purified human insulin, as a biorecognition element, was immobilized on the sensor surface via amine coupling chemistry. In calibration experiment in buffer, monoclonal antibodies against insulin were detected at concentrations as low as 0.6 μg/mL. Serum samples were pretreated to remove insulin and filtered before SPR measurements. Insulin antibodies were detected in eight diabetic patient serum samples and determined to fall in the range of 2.91−16.3 μg/mL. No insulin antibodies were detected in the control group.[296]

5.3.4. Hormones

A marker of pregnancy—human chorionic gonadotropin hormone (hCG)—has been a frequent target of optical biosensor technologies. Jiang's group reported SPR sensor-based detection of hCG exploiting a wavelength-modulated SPR sensor and DNA-directed antibody immobilization method.[165] The immobilization consisted of non-covalent attachment of streptavidin to a biotinylated SAM of alkanethiolates followed with the binding of biotinylated oligonucleotides to available streptavidin binding sites. Antibodies chemically modified with oligonucleotides with a complementary sequence were finally attached to this surface via DNA hybridization. The detection limit for direct detection of hCG in buffer was determined to be 0.5 ng/mL. Recently, detection of hCG in urine was performed using a sequential detection method developed by Chung et al.[208] They used the commercial SPR sensor Spreeta and immobilized two molecular recognition elements (antibody against HCG and antibody against human albumin) in a single sensing channel of Spreeta sensor using SAM of alkanethiolates and amine coupling chemistry. Amplification polyclonal anti-hCG antibodies were used to increase the sensor response. In 10-fold diluted urine, the detection limit for hCG was established to be 46 mIU/mL.[208]

SPR-based detection of 17β-estradiol was demonstrated by Miyashita et al.[297] They used the commercial SPR sensor Biacore X and inhibition detection format. Estradiol−BSA conjugate was immobilized on carboxymethylated dextran layer by amine coupling chemistry. The binding of unreacted antibody to 17β-estradiol conjugates at the surface of the sensor was measured. The 17β-estradiol was detected down to 0.47 nM ($\sim$0.14 ng/mL).[297]

Teramura and Iwata demonstrated an SPR sensor for the detection of α-fetoprotein (AFP) in human plasma.[298] They used a research SPR sensor system with angular modulation and a SAM of tri(ethylene glycol), and carboxyl group-terminated hexa(ethylene glycol) was employed for covalent attachment of monoclonal AFP-antibody. Detection was performed in sandwich detection format. The SPR signal shift was further enhanced by applying a polyclonal antibody against the second antibody. The polyclonal antibody against the second antibody was demonstrated to amplify the sensor response to AFP by a factor of 7. The LOD for AFP in blood plasma was estimated to be in nanograms per milliliter levels.[298]

5.3.5. Allergy Markers

Measurement of immunoglobulin E (IgE) antibody levels plays an important role in the diagnostics of allergies. Imato's group reported direct detection of IgE antibody using an SPR biosensor.[199] In that work, anti-IgE antibody was immobilized on the surface of the commercial SPR sensor SPR 20 by physical adsorption. A sample containing IgE antibody was mixed with an anti-IgE(H) antibody solution to form an anti-IgE(H) complex via the Ce2 domain of the IgE antibody. The solution was introduced in the SPR sensor and the immunocomplex of the IgE−anti-IgE(H) reacted with the anti-IgE(D) antibody immobilized on the sensor chip via the Ce3 domain of the IgE antibody. The LOD for the IgE antibody was about 10 ppb.[199]

The same group reported SPR-based detection of histamine (β-imidazole ethylamine)—a protein involved in allergic reactions. Their SPR sensor was based on the commercial SPR-20 sensor and inhibition detection format. Histamine was immobilized on the sensor surface using a self-assembled alkanethiolate monolayer and amine coupling chemistry. A regeneration protocol was developed, and it was demonstrated that the sensor can be used for more than 10 detection/regeneration cycles. The limit of detection was 3 ppb.[299]

5.3.6. Heart Attack Markers

Detection of a marker of cardiac muscle injury, troponin (cTn I), in serum was demonstrated by Wei et al.[300] In that work, biotinylated antibodies against cTn I were immobilized on the avidin layer created using amine coupling chemistry on an activated SAM of alkanethiolates. cTn I was detected directly and in sandwich detection format. The LODs were determined to be 2.5 and 0.25 ng/mL for direct and sandwich detection format, respectively.[300] Detection of cTn I was also demonstrated by Booksh's group.[301] They used a miniature fiber optic SPR sensor on which human anti-cardiac troponin I was immobilized via a dextran layer and amine coupling chemistry. The LOD for cTnI in buffer was established at 3 ng/mL.[301]

5.3.7. Other Molecular Biomarkers

Detection of antibodies against glucose 6-phosphate isomerase (GPI) in synovial fluids of rheumatoid arthritis and osteoarthritis patients (diluted 1:100 in Hepes) using a Biacore 2000 is presented in the work of Kim et al.[302] Recombinant human GPI proteins produced from *E. coli* were immobilized on the dextran sensor surface via amine coupling chemistry. The synovial fluid samples from rheumatoid arthritis patients showed a significantly higher level of binding to the recombinant GPI proteins than samples from osteoarthritis patients.

SPR-based detection of anti-glutamic acid decarboxylase (GAD) antibodies for diagnosing type I diabetes mellitus was reported by Sim's group.[303,304] They used the commercial SPR sensor Biacore 2000 and biotinylated GAD coupled to streptavidin molecules anchored covalently on a mixed SAM of hydroxyl- and carboxyl-terminated alkanethiolates. Optimization of SAM composition was carried out. The SPR sensor employing an optimized SAM was shown to be able to detect antibody in HBS-EP buffer in sub-micromolar levels.[304]

Detection of c-reactive protein (CRP), a human blood serum marker for inflammatory processes, using SPR biosensor technology was demonstrated by Meyer.[305] They used the commercial SPR sensor Plasmonic and sandwich detection format. Biotinylated monoclonal antiCRP antibody C6 was immobilized on the biotin-coated sensor surface via streptavidin. Buffer spiked with CRP was injected in the SPR sensor cuvette and then replaced by a solution containing the secondary antiCRP antibody C2. The sandwich assay was completed typically within 30−60 min. The LOD for CRP in buffer was determined to be 1 μg/mL.[305]

SPR-based detection of the cystatin C marker of the glomerular filtration rate (GFR), a critical measure of normal kidney function, was demonstrated by Corn's group.[306] They used an SPR imaging instrument with antibodies immobilized on the alkanethiolate-modified sensor surface using carbonyldiimidazole surface reaction. The sensor was shown to be able to detect cystatin C at 1 nM levels.[306]

Hwang et al. reported an SPR sensor for the detection of hepatitis B surface antigen (HBsAg), an early indicator of hepatitis B.[307] In their work, they used the commercial SPR sensor Biacore 3000 and immobilized anti-HBsAg polyclonal antibody to the dextran layer on a sensor chip surface using amine coupling chemistry. HBsAg was detected at concentrations as low as ~1 μg/mL.[307]

5.4. Environmental Monitoring

Analytes of environmental concern[225,308] targeted by SPR biosensors include, in particular, pesticides, aromatic hydrocarbons, heavy metals, phenol, polychlorinated biphenyls, and dioxins.

5.4.1. Pesticides

Following the demonstration of SPR biosensors for the detection of atrazine[309] and simazine[137,138] in the 1990s, various pesticides have been targeted by SPR sensor technology.

Lechuga's group reported a portable SPR sensor for the detection of atrazine in water using inhibition format.[310] An atrazine derivative was immobilized on the alkanethiolate SAM formed on the gold-coated sensor surface. The sample was incubated with polyclonal antibodies, and then the mixture was analyzed by the SPR sensor. The LOD was established at 20 pg/mL. A measurement/regeneration cycle required about 25 min.[310] An alternative approach to the detection of atrazine based on specifically expressed mRNA in *Saccharomyces cerevisiae* bacteria exposed to atrazine was reported by Lim et al.[311] The cells were brought into contact with the analyzed sample and disrupted, and the amount of expressed P450 mRNA was measured by an SPR biosensor with complementary oligonucleotide probes immobilized on the sensor surface using streptavidin−biotin chemistry. The LOD (1 pg/mL) presents a substantial improvement compared to previous works.[18,309]

Lechuga's group demonstrated SPR biosensors for the detection of organophosphate pesticide chlorpyrifos and carbaryl.[312−314] They used inhibition detection format in which a pesticide derivative with BSA was covalently immobilized on a self-assembled alkanethiolate monolayer formed on the SPR sensor surface. Typical limits of detection were around 50 pg/mL for chlorpyrifos[312,314] and 1 ng/mL for carbaryl.[312,313] A protocol for regeneration of the sensing surface was developed, and the sensor was able to perform ~200 detection cycles without degradation in performance.[312] The detection cycle was completed in 20 min. The sensors were tested in ground, river, and drinking water samples without the observation of significant matrix effects. Lechuga's group also demonstrated an SPR sensor for the detection of dichlorodiphenyltrichloroethane (DDT).[315] They used a portable SPR sensor now commercially available from Sensia (Spain) and inhibition detection format. DDT derivative was immobilized on a self-assembled alkanethiolate monolayer on the SPR sensor surface. Two monoclonal antibodies, specific to DDT and specific to DDT and its metabolites, were used in the inhibition detection format. Regeneration of the sensor surface was developed, and 270 detection cycles were performed. The LOD in distilled water was established at 15 pg/mL for the DDT-specific assay and at 31 pg/mL for the DDT group-selective assay. Nearly the same performance was achieved when the sensor was used to analyze river water samples.[315] Detection of three pesticides—DDT, carbaryl, and chlorpyrifos—using a single

channel of an SPR sensor and inhibition detection format was demonstrated by Lechuga's group.[209] DDT, carbaryl, and chlorpyrifos derivatives were attached to carboxylic terminal groups on a SAM of alkanethiolates. A sample was mixed with antibody against one target and injected in the flow cell of the sensor. After the sensor response had been established, a sample mixed with antibody against another target was injected with or without previous regeneration of the sensing surface. The LODs for this multianalyte detection approach were established at 18 pg/mL for DDT, 50 pg/mL for carbaryl, and 52 pg/mL for chlorpyrifos. These detection limits were comparable with those obtained using single-analyte functionalizations.[209]

Miura's group applied the SPR method to the detection of 2,4-dichlorophenoxyacetic acid (2,4-D).[316,317] Initially, they used inhibition detection format and a conjugate of 2,4-D derivative and BSA (2,4-D−BSA) immobilized on the sensor by physisorption. The LOD was established at 0.5 ng/mL.[316] In their later study, they used a SAM of alkanethiolates for covalent attachment of 2,4-D−BSA conjugate on the sensor surface. This functionalization approach led to an improvement in the LOD to 10 ppt.[317] Regeneration of the sensor for up to 30 detection cycles was demonstrated using pepsin.[317]

5.4.2. 2,4,6-Trinitrotoluene (TNT)

SPR biosensors for the detection of TNT, which is a prime constituent of most of landmines and also exhibits toxic, mutagenic, and carcinogenic effects, have been extensively researched by Miura's group. They used inhibition detection format involving various conjugates and antibodies. The conjugates used in their experiments included 2,4,6-trinitrophenol−BSA (TNP−BSA).[318,319] TNP−ovalbumin (TNP-OVA),[318] 2,4,6-trinitrophenyl−keyhole limpet hemocyanin (TNP−KLH),[320] and TNP−β-Alanine−ovalbumin (TNP−β-Ala−OVA).[321] The antibodies (monoclonal and polyclonal) were homemade[321] or commercial. Most of their sensors delivered a LOD below 10 pg/mL (10 ppt);[318,320−322] the best LOD (1 ppt) was achieved using the immunoreaction between a homemade polyclonal anti-2,4,6-trinitrophenyl−keyhole limpet hemocyanine antibody with a physically immobilized TNP−OVA.[318] The sensor surface was regenerated by pepsin. The detection cycle was typically completed in <20 min. The inhibition-based SPR biosensors of TNT were found to exhibit low cross-sensitivity to other similar compounds such as 1,4-DNT, 1,3-DNB, 2A-4,6-DNT, and 4A-4,6-DNT.[323] Larsson et al. studied the effect of composition of molecular coatings on the performance of the SPR biosensor for the detection of TNT.[324] They used the commercial SPR platform Biacore2000 and inhibition detection format. Two types of thiols, OEG-alkylthiols terminated with a hydroxyl group and a TNT analogue (2,4-dinitrobenzene), were self-assembled on the surface of an SPR chip. The ratio of TNT analogues and hydroxyl-terminated OEG-thiols was optimized to provide highly selective and sensitive biochips with minimum nonspecific binding. The LOD for TNT in buffer was demonstrated to be <10 pg/mL.[324]

5.4.3. Aromatic Hydrocarbons

An SPR biosensor for the detection of 2-hydroxybiphenyl (HBP, a metabolite of BaP) was demonstrated by Miura's group. The sensor was based on the inhibition immunoassay format. An antibody against HBP was mixed with a sample and, after incubation, the unreacted antibody was detected using an SPR biosensor functionalized with an HBP conjugate. HBP−BSA was immobilized on the surface of the SPR sensor by physical adsorption.[325,326] The LOD using the commercial SPR biosensor SPR-20 was demonstrated to be 0.1 ppb (ng/mL). Most recently, this detection approach was combined with a portable SPR sensor, and the LOD of 0.1 ppb (ng/mL) was reproduced also on this sensor platform. A simple regeneration procedure using a pepsin solution allowed more than 30 measurement cycles without appreciable deterioration of sensor response. The measurement cycle was completed in 20 min. The same group also demonstrated detection of benzo[*a*]pyrene (BaP). They used the commercial SPR biosensor SPR-20 and inhibition assay. BAP molecules were attached to the sensor surface either by immobilizing BaP−BSA conjugate on the sensor via physical adsorption[327,328] or by immobilizing BaP analogue on the sensor surface with a mixed SAM of alkanethiolates.[329] The biomolecular coating incorporating a BaP analogue was determined to yield a more sensitive sensor with a LOD for BaP in buffer as low as 0.05 ppb.[329] In 2005, Kawazumi et al. reported the simultaneous detection of benzo[*a*]pyrene and 2-hydroxybiphenyl using a compact, portable SPR instrument.[52] They employed inhibition detection format and BSA−BaP and BSA−HBP conjugates immobilized on the surface of a dual-channel SPR sensor via physical adsorption. The sensor was shown to be able to detect BaP and HBP in buffer down to parts per billion levels.[52]

5.4.4. Heavy Metals

An SPR sensor for direct detection of Cu^{2+} ions was reported by Ock et al.[330] Their sensor employed a thin polymer layer containing squarylium dye (SQ), which changes its refractive index absorption properties when interacting with Cu^{2+} ions. Owing to anomalous dispersion accompanied with this absorption, a substantial refractive index change can be observed when SQ dye is exposed to Cu^{2+} ions. The sensor responded to Cu^{2+} in buffer at levels as low as 1×10^{-12} M.[330] Another SPR sensor for the detection of heavy metals was demonstrated by Wu et al., who used a Biacore X instrument with rabbit metallothinein coupled to the dextran matrix on the sensor surface.[286] Metallothinein is a protein that can be found in cells of many organisms and is known to bind to metals (especially cadmium and zinc). Model experiments in which metallothein was used as a receptor demonstrated the potential of this sensor to directly detect Cd, Zn, and Ni in buffer at concentrations down to 100 ng/mL. Forzani et al. demonstrated another approach to the direct detection of Cu^{2+} and Ni^{2+} ions. In their work they used a differential SPR sensor coated by properly selected peptides specifically binding metal ions. Detection limits for Cu^{2+} and Ni^{2+} in deionized water were 32 and 178 pM, respectively.[153]

5.4.5. Phenols

An SPR biosensor for the detection of bisphenol A (BPA) was developed by Soh et al.[332] They used the commercial SPR-20 sensor and inhibition detection format. The sensor surface was modified with a thiol monolayer on which BPA molecules were immobilized through BPA succinimidyl ester. Using a monoclonal antibody, detection of BPA in buffer at concentrations as low as 10 ng/mL was achieved.[332] Detection time was approximately 30 min, and the sensor was demonstrated to be regenerable using 0.01 M hydrochloric acid. Another SPR biosensor for the detection of BPA

Table 1. Overview of SPR Biosensors for Food Quality and Safety Analysis

analyte	sensor system	detection matrix	limit of detection	detection format	ref
Escherichia coli O157:H7					
	Multiskop	buffer	10^4 cells/mL	direct	228
	Multiskop	buffer	10^2 cells/mL	direct	229
	custom-built	detergent-lysed bacteria	10^4 cfu/mL	sandwich	230
		heat-killed bacteria	10^5 cfu/mL		
		untreated bacteria	10^6 cfu/mL		
	Spreeta	BPV solution	8.7×10^6 cfu/mL	direct	231
	Spreeta	aqueous solution	10^6 cells/mL	direct	232
	SR 7000	PBST solution	10^3 cfu/mL	sandwich	233
	custom-built	heat-killed bacteria in buffer	1.4×10^4 cfu/mL	sandwich	234
		apple juice, pH 7.4	10^5 cfu/mL		
	Biacore 2000	pasteurized milk	25 cfu/mL	direct	235
	Spreeta	milk; apple juice; ground beef	10^2-10^3 cfu/mL	direct	236
Salmonella spp.					
S. enteritidis	custom-built	heat-killed bacteria in buffer	10^6 cfu /mL	direct	162
S. group A, B, D, E	Biacore 3000	HBS-EP solution	1.7×10^5 cfu/mL	sandwich	237
S. typhimurium	Multiskop	buffer	10^2 cfu/mL	direct	238
S. paratyphi	Multiskop	buffer	10^2 cfu/mL	direct	239
	Plasmonic	milk	10^5 cells/mL	sandwich	240
S. choleraesuis	custom-built	buffer	4.4×10^4 cfu/mL	sandwich	234
		apple juice, pH 7.4	10^4 cfu/mL		
S. enterica	Biacore 2000	pasteurized milk	23 cfu/mL	direct	235
Lysteria monocytogenes					
	custom-built	heat-killed bacteria in buffer	10^7 cfu /mL	direct	162
	Biacore 3000	PBS solution	10^5 cells/mL	competitive	241
	custom-built	apple juice, pH 7.4; buffer	3×10^3 cfu/mL	sandwich	234
Campylobacter jejuni					
	custom-built	heat-killed bacteria in buffer	1×10^5 cfu/mL	sandwich	234
		apple juice, pH 7.4	5×10^4 cfu/mL		
Staphylococcus aureus					
	SR 7000	PBST soluiton	10^5 cfu/mL	sandwich	242
			10^7 cfu/mL	direct	
	Spreeta	buffer	10^4 cfu /mL	direct	243
mixture of *E. coli*, *C. jejuni*, *S. typhimurium*, and *L. monocytogenes*					
	cutom-built	heat-killed bacteria in buffer; apple juice	$10^4-5 \times 10^4$ cfu/mL	sandwich	234
Yersinia enterocolitica					
	Multiskop	buffer	10^2 cfu/mL	direct	244
Vibrio cholerae O1					
	Multiskop	buffer	4×10^5 cfu/mL	direct	245
Cryptosporidium parvum					
	Biacore 2000	buffer	10^6 oocyst/mL	direct	246
			10^2 oocyst/mL		246
Fusarium culmorum					
	Biacore X	wheat	0.25 ng/μL	direct, PCR amplicon	247
Staphylococcal enterotoxins					
SEB	Biacore X	milk	1 ng/mL	direct	248, 249
	fiber optic	buffer	10 ng/mL	direct	250
	Spreeta	buffer	5.6 ng/mL	direct	251
		seawater	28 ng/mL	direct	
		buffer	0.6 ng/mL	sandwich	
		seawater	1.4 ng/mL	sandwich	
	custom-built	buffer; milk	5 ng/mL	direct	91
		buffer; milk	0.5 ng/mL	sandwich	
	Biacore 1000	milk	0.3 ng/mL	inhibition	252
	Biacore 1000	buffer; ham tissue extract	2.5 ng/mL	sandwich	253
SEA	Biacore 1000	raw eggs	1 ng/mL	competitive	254
domoic acid					
	Biacore 3000	buffer	5 ng/mL	competitve	255
	custom-built	buffer	0.1 ng/mL	inhibition	256
	Biacore Q	shellfish species extract	1−7 μg/g	inhibiton	257
	Spreeta	buffer; clam extracts	3 ng/mL	inhibition	258
aflatoxin B_1					
	Biacore 1000	buffer	3 ng/mL	inhibition	259
	Biacore 3000	buffer	190 pg/mL	inhibition	148
deoxynivalenol					
	Biacore Q	buffer	2.5 ng/mL	inhibition	260

Table 1 (Continued)

analyte	sensor system	detection matrix	limit of detection	detection format	ref
antibiotics					
benzylpenicillin, ampicillin, amoxicillin	Biacore 3000	raw milk	2 ng/mL	inhibition	262
Row70cloxacillin			15 ng/mL		
cephalexin			50 ng/mL		
cefoperazon			25 ng/mL		
chloramphenicol, chloramphenicol glucuronide	Biacore Q	honey extract; prawn; dairy products; porcine kidney	0.2 μg/kg	direct	263
	Biacore Q	poultry	0.005 μg/kg	inhibition	264
		honey	0.02 μg/kg		
		prawn	0.04 μg/kg		
		milk	0.04 μg/kg		
chloramphenicol	Biacore Q	shrimps	1 ng/mL	inhibition	265
florephenicol			0.2 ng/mL		
florephenicol amine			250 ng/mL		
thiamphenicol			0.5 ng/mL		
tetracycline	Biacore 3000	buffer	1 ng/mL		
		raw milk	15 ng/mL	indirect	266
		honey	25 μg/kg		
tylosin	Biacore Q	honey extract	2.5 μg/kg	inhibition	267
vitamins					268
B2 (riboflavin)	Biacore Q	milk-based products	70 ng/mL	inhibition	
B5 (pantothenic acid)	Biacore Q	various foods	4.4 ng/mL	inhibition	269
B8 (biotin), B9 (folic acid)	Biacore Q	milk powder; infant formulas	2 ng/mL	inhibition	270
B12 (cobalamine)	Biacore Q	milk; infant formulas	0.06 ng/mL	inhibition	271
hormones					
progesterone	Biacore 2000	buffer	60 pg/mL	inhibition	273
		milk	0.6 ng/mL		
	Biacore 2000	buffer	8.6 pg/mL	imhibition, amplification	212
diagnostic antibodies					
Mycoplasma hyopneumoniae	Autolab Esprit SPR	pig serum		direct	274
classical swine fever virus	Autolab Esprit SPR	pig serum		direct	275
allergens					
peanut allergens	Spreeta	buffer	700 ng/mL	direct	276
peanut proteins	Biacore Q	chocolate	1 μg/g	direct sandwich	277
conalbumin		pasta	0.3 μg/g		
seasame seed protein		bread	12.5 μg/g		
tropomyosin		pasta	10 μg/g		
proteins					
β-casein	Biacore 3000	milk	85 ng/mL	sandwich	278
α_{s1}-casein			870 ng/mL		
κ-casein			470 mg/mL		
IgG	Biacore Q	milk	16.8 ng/mL	direct	279
folate-binding protein			0.7 ng/mL		
lactoferrin			1.1 ng/mL		
lactoperoxidase			75 ng/mL		
chemical contaminants					
4-nonylphenol	Biacore Q	buffer	2 ng/mL	inhibition	280
		shellfish	10 ng/g		
IGF-1	Biacore	buffer, milk	10 ng/mL	inhibition	281

was demonstrated by Matsumoto's group.[334] Their sensor also used inhibition detection format and BPA−OVA conjugate immobilized on the sensor surface by physical adsorption. The sensor was shown to be able to detect BAP at 1 ng/mL (1 ppb) levels.[334]

Imato's group developed an SPR biosensor for the detection of 2,4-dichlorophenol based on competitive detection format.[333] They used the commercial SPR sensor SPR-20 functionalized with monoclonal antibodies against 2,4-dichlorophenol immobilized on the sensor surface via gold binding peptide and protein G. Detection was based on the competition between the analyte present in sample and added BSA−2,4-dichlorophenol conjugate. The LOD was established at 20 ng/mL.[333]

5.4.6. Polychlorinated Biphenyls

Karube's group demonstrated the detection of PCB 3,3′,4,4′,5-pentachlorobiphenyl using the commercial SPR sensor Biacore 2000 and competitive detection format.[333] In their work, the sample was mixed with a conjugate of PCB−HRP and flowed across the sensor surface with polyclonal antibodies immobilized in the dextran matrix. The presence of PCB was detected as a decrease in the binding of PCB−HRP conjugate. The LOD was determined to be 2.5 ng/mL. The sensor surface was regenerable using 0.1 M hydrochloric acid. The detection was completed in 15 min.[335]

5.4.7. Dioxins

Karube's group also demonstrated an SPR biosensor for the detection of 2,3,7,8-TCDD.[335] They used the commercial SPR sensor Biacore 2000 and competitive detection format. Monoclonal antibody was immobilized in the dextran layer on the sensor chip by amine coupling chemistry. The sample was mixed with a of 2,3,7,8-TCDD−HRP conjugate and injected into the sensor. A LOD of 0.1 ng/mL was attained, and the sensor was shown to be regenerable using 0.1 M hydrochloric acid.[335] Detection was completed in 15 min.

Table 2. Overview of SPR Biosensors for Medical Diagnostic

analyte	sensor system	detection matrix	limit of detection	detection format	ref
cancer markers					
prostate-specific antigen (PSA)	Ibis II	3% BSA in PBS	0.15 ng/mL	sandwich	285
	Biacore 2000	buffer	10 ng/mL	direct	286
			1 ng/mL	sandwich	
PSA−ACT complex (α_1-antichymotrypsin)	Biacore 2000	HBS buffer	20.7 ng/mL	direct	201
		HBS buffer	10.2 ng/mL	sandwich	
		human serum	47.5 ng/mL	direct	
		human serum	18.1 ng/L	sandwich	
carbohydrate antigen (CA 19-9)	Spreeta	buffer	410.9 U/mL	direct	287
		buffer	66.7 U/mL	sandwich	
vascular endothelial growth factor (VEGF)	cutom-built SPRI	buffer	1 pM	sandwich	220
interleukin-8 (IL-8)	Biacore X	buffer	2.5 pM (∼0.02 ng/mL)	sandwich	288
		human saliva	184 pM (∼1.5 ng/mL)		
carcinoembryonic antigen (CEA)	Autolab Springle	buffer	0.5 ng/mL	direct	289
fibronectin	custom-built	buffer	2.5 μg/mL	direct	212
		buffer	0.5 μg/mL	sandwich	
		buffer	0.25 μg/mL	amplification	
antibodies against viral pathogens					
hepatitis virus specific	Biacore 1000	human serum		direct	150
	Spreeta	5% serum in PBS	9.2 nM	direct	202
			4.4 nM	sandwich	
			0.64 nM	amplified	
anti-hepatits simplex virus	Biacore X	serum in HBS (1:100)		direct	151
anti-EBNA	custom-built	1% human serum	0.2 ng/mL	direct	152
anti-protein S	Biacore X	plasma 1:5		direct	290
anti-RSV	Biacore 2000	HBS Buffer		direct	291
anti-adenoviral	Biacore 3000	ascites fluid in Hepes (1:10)		direct	292
drugs and drug-induced antibodies					
morphine-3-glucuronide	Biacore 1000	urine in buffer (1:250)	1 ng/mL	inhibition	293
warfarin	Biacore 3000	plasma (1:100)	4 ng/mL	inhibition	294
insulin	SPR-670	buffer	1 ng/mL	inhibition	203
		serum	6 ng/mL	inhibition	
anti-GM-CSF	Biacore 2000	serum (1:5)		direct	295
anti-insulin	Biacore 2000	buffer	0.6 μg/mL	direct	296
		serum	2.91 μg/mL	direct	
hormones					
hCG	custom-built	buffer	0.5 ng/mL	direct	165
	Spreeta	urine	46 mIU/mL	sandwich	208
17β-estradiol	Biacore X	HBS-EP buffer	0.47 nM (∼0.14 ng/mL)	inhibition	297
α-fetoprotein	custom-built	plasma	ng/mL	sandwich	298
allergy markers					
IgE	SPR 20	buffer	10 ppb	direct	199
histamine	SPR 20	buffer	3 ppb	inhibition	299
heart attack markers					
troponin (cTn I)		serum	2.5 ng/mL	direct	300
		serum	0.25 ng/mL	sandwich	
	custom fiber-optic	buffer	3 ng/mL	direct	301
other molecular biomarkers					
Glc-6-P isomerase	Biacore 2000	synovial fluids in Hepes (1:100)		direct	302
anti-GAD	Biacore 2000	HBS-EP buffer	$<\mu$M	direct	303, 304
c-reactive protein	Plasmonic	buffer	1 μg/mL	sandwich	305
cystatin C	custom-built SPRI	buffer	1 nM	direct	306
HBsAg	Biacore 3000	buffer	1 μg/mL	direct	307

5.5. Summary

Over the past 5 years, more than 100 SPR biosensors for the detection of a variety of chemical and biological analytes were demonstrated. Most of these biosensors are based on prism coupling and angular or wavelength spectroscopy of surface plasmons. Commercial SPR systems have played an important role in the development of detection applications due to their increasing spread and the availability of special SPR platforms and kits dedicated to specific applications (e.g., Biacore Q for food analysis). Data collected in Tables 1−3 illustrate recent applications of SPR biosensors and achieved levels of performance. The performance figures should be compared with caution as performance of an SPR biosensor is a result of a multitude of factors (performance of optical platform, characteristics of the employed biorecognition element, suitability and degree of optimization of the immobilization method, detection format, and methodology), and thus low performance of one part of the biosensor (e.g., optical platform) can be compensated for by high performance of another component (e.g., biorecognition elements).

Clearly, analytes implicated in food safety have received the most attention (Table 1). Bacterial pathogens such as *E. coli* and *Salmonella* were the most frequently targeted analytes. Detection limits below 10^2 bacteria/mL were reported. A great deal of research has been devoted to the

Table 3. Overview of SPR Biosensors for Environmental Monitoring

analyte	sensor system	detection matrix	limit of detection	detection format	ref
pesticides					
atrazine	Sensia	water	20 pg/mL	inhibition	310
			1 pg/mL		311
chlorpyrifos	custom-built	water	50 pg/mL	inhibition	312, 314
carbaryl	custom-built	water	1 ng/mL	inhibition	312, 313
DDT	Sensia	water	15 pg/mL	inhibition	315
DDT		water	18 pg/mL	inhibition	209
carbaryl			50 pg/mL		
chloropyrifos			52 pg/mL		
2,4-dichlorophenoxyacetic acid	SPR-20	buffer	0.5 ng/mL	inhibition	316
	custom-built	buffer	10 ppt	inhibition	317
2,4,6-trinitrotoluene (TNT)					
	Biacore 2000	buffer	10 pg/mL	inhibition	318, 320−322
	Biacore 2000	buffer	10 pg/mL	inhibition	324
aromatic hydrocarbons					
2-hydroxybiphenyl	SPR-20	buffer	0.1 ng/mL	inhibition	325, 326
benzo[*a*]pyrene	SPR-20	buffer	0.01 ng/mL	inhibition	327, 328
	SPR-20	buffer	0.05 ng/mL	inhibition	329
heavy metals					
Cu^{2+} ions	custom-built	buffer	∼pM	direct	330
Cd, Zn, Ni	Biacore X	buffer	∼μM	direct	331
Cu^{2+}	custom-built	deionized water	32 pM	direct	153
Ni^{2+}			178 pM		
phenols					
bisphenol A	SPR-20	buffer	10 ng/mL	inhibition	332
	Spreeta	buffer	1 ng/mL	inhibition	334
2,4-dichlorphenol	SPR-20	buffer	20 ng/mL	competitive	333
PCB	Biacore 2000	buffer	2.5 ng/mL	competitive	335
2,3,7,8-TCDD	Biacore 2000	buffer	0.1 ng/mL	competitive	335

development of SPR biosensors for other significant groups of analytes such as Staphylococcal enterotoxins (best demonstrated LODs < 1 ng/mL) and antibiotics (best LODs < 1−10 ng/mL depending on the substance). Several analytes have been detected also in complex food matrices. In the field of medical diagnostics (Table 2), the most attention has been paid to the development of SPR sensors for the detection of cancer markers (best LODs < 1−100 ng/mL) and antibodies (best LODs < 1−100 ng/mL). However, most of the detection experiments were performed in buffers rather than in clinical samples. The development of SPR biosensors for environmental monitoring (Table 3) has focused mainly on the detection of pesticides. The best LODs ranged from 1 to 100 pg/mL, depending on the analyte. Detection experiments were performed in buffers or real-world water samples.

6. Conclusions

In the past 5 years, SPR biosensor technology has made substantial advances in terms of both sensor hardware and biospecific coatings. SPR biosensors have been applied for the detection of a variety of chemical and biological analytes. We envision that the performance of SPR biosensor technology will continue to evolve and that advanced SPR sensor platforms combined with novel biospecific surfaces with high resistance to the nonspecific binding will lead to robust SPR biosensors enabling rapid, sensitive, and specific detection of chemical and biological analytes in complex samples in the field. These biosensors will benefit numerous important sectors such as medical diagnostics, environmental monitoring, and food safety and security.

7. Abbreviations

ATR, attenuated total reflection; CCD, charge-coupled device; DNA, deoxyribonucleic acid; ELISA , enzyme-linked immunosorbent assay; LED, light-emitting diode; LOD, limit of detection; MALDI-TOF, matrix-assisted laser desorption/ionization time-of-flight mass spectrometry; RIU, refractive index unit; RNA, ribonucleic acid; scFvs, single-chain antibody fragment; SAM, self-assembled monolayer; SP, surface plasmon; SPR, surface plasmon resonance; WDM, wavelength division multiplexing.

8. Acknowledgment

I gratefully acknowledge the financial support of the Grant Agency of the Academy of Sciences of the Czech Republic (IAA400500507, KAN200670701).

9. References

(1) Cush, R.; Cronin, J. M.; Stewart, W. J.; Maule, C. H.; Molloy, J.; Goddard, N. J. *Biosens. Bioelectron.* **1993**, *8*, 347.
(2) Buckle, P. E.; Davies, R. J.; Kinning, T.; Yeung, D.; Edwards, P. R.; Pollard-Knight, D.; Lowe, C. R. *Biosens. Bioelectron.* **1993**, *8*, 355.
(3) Clerc, D.; Lukosz, W. *Sens. Actuators B* **1997**, *40*, 53.
(4) Brandenburg, A.; Gombert, A. *Sens. Actuators B* **1993**, *17*, 35.
(5) Lukosz, W.; Clerc, D.; Nellen, P. M. *Sens. Actuators A* **1990**, *25*, 181.
(6) Heideman, R. G.; Lambeck, P. V. *Sens. Actuators B* **1999**, *61*, 100.
(7) Heideman, R. G.; Kooyman, R. P. H.; Greve, J. *Sens. Actuators B* **1993**, *10*, 209.
(8) Ymeti, A.; Kanger, J. S.; Greve, J.; Besselink, G. A. J.; Lambeck, P. V.; Wijn, R.; Heideman, R. G. *Biosens. Bioelectron.* **2005**, *20*, 1417.
(9) Schmitt, K.; Schirmer, B.; Hoffmann, C.; Brandenburg, A.; Meyrueis, P. *Biosens. Bioelectron.* **2007**, *22*, 2591.
(10) Gauglitz, G.; Brecht, A.; Kraus, G.; Mahm, W. *Sens. Actuators B* **1993**, *11*, 21.
(11) Schmitt, H.-M.; Brecht, A.; Piehler, J.; Gauglitz, G. *Biosens. Bioelectron.* **1997**, *12*, 809.
(12) Gordon, J. G.; Ernst, S. *Surf. Sci.* **1980**, *101*, 499.
(13) Nylander, C.; Liedberg, B.; Lind, T. *Sens. Actuators* **1982**, *3*, 79.
(14) Ligler, F. S.; Taitt, C. A. R. *Optical Biosensors: Present and Future*; Elsevier: Amsterdam, The Netherlands, 2002.
(15) Malhotra, B. D.; Turner, A. P. F. *Perspectives in Biosensors*; JAI: Amsterdam, The Netherlands, 2003.

(16) Gorton, L. *Biosensors and Modern Biospecific Analytical Techniques*, 1st ed.; Elsevier: Amsterdam, The Netherlands, 2005.
(17) Vo-Dinh, T. *Nanotechnology in Biology and Medicine: Methods, Devices, and Applications*; CRC Press: Boca Raton, FL, 2007.
(18) Nakamura, H.; Karube, I. *Anal. Bioanal. Chem.* **2003**, *377*, 446.
(19) Ince, R.; Narayanaswamy, R. *Anal. Chim. Acta* **2006**, *569*, 1.
(20) Bally, M.; Halter, M.; Voros, J.; Grandin, H. M. *Surf. Interface Anal.* **2006**, *38*, 1442.
(21) Rebecca, L.; Rich, D. G. M. *J. Mol. Recognit.* **2006**, *19*, 478.
(22) Rebecca, L.; Rich, D. G. M. *J. Mol. Recognit.* **2005**, *18*, 431.
(23) Rebecca, L.; Rich, D. G. M. *J. Mol. Recognit.* **2005**, *18*, 1.
(24) Rebecca, L.; Rich, D. G. M. *J. Mol. Recognit.* **2003**, *16*, 351.
(25) Rebecca, L.; Rich, D. G. M. *J. Mol. Recognit.* **2002**, *15*, 352.
(26) Rebecca, L.; Rich, D. G. M. *J. Mol. Recognit.* **2001**, *14*, 273.
(27) Homola, J.; Yee, S. S.; Gauglitz, G. *Sens. Actuators B* **1999**, *54*, 3.
(28) Homola, J. *Anal. Bioanal. Chem.* **2003**, *377*, 528.
(29) Boozer, C.; Kim, G.; Cong, S.; Guan, H.; Londergan, T. *Curr. Opin. Biotechnol.* **2006**, *17*, 400.
(30) Phillips, K. S.; Cheng, Q. *Anal. Bioanal. Chem.* **2007**, *387*, 1831.
(31) Homola, J. *Surface Plasmon Resonance Based Sensors*; Springer: Berlin, Germany, 2006.
(32) Wood, R. W. *Proc. Phys. Soc. London* **1902**, *18*, 269.
(33) Fano, U. *J. Opt. Soc. Am.* **1941**, *31*, 231.
(34) Otto, A. Z. *Phys.* **1968**, *216*, 398.
(35) Kretschmann, E.; Raether, H. Z. *Naturforsch* **1968**, *2135*−*2136*, 2135.
(36) Boardman, A. D. *Electromagnetic Surface Modes*; Wiley: Chichester, U.K., 1982.
(37) Raether, H. *Springer Trends Mod. Phys.* **1988**, *111*, 1.
(38) Pitarke, J. M.; Silkin, V. M.; Chulkov, E. V.; Echenique, P. M. *Rep. Prog. Phys.* **2007**, *70*, 1.
(39) Ishimaru, A.; Jaruwatanadilok, S.; Kuga, Y. *Prog. Electromagn. Res.*−*Pier* **2005**, *51*, 139.
(40) Stegeman, G. I.; Burke, J. J.; Hall, D. G. *Opt. Lett.* **1983**, *8*, 383.
(41) Burke, J. J.; Stegeman, G. I.; Tamir, T. *Phys. Rev. B* **1986**, *33*, 5186.
(42) Sarid, D. *Phys. Rev. Lett.* **1981**, *47*, 1927.
(43) Hutley, M. C. *Diffraction Gratings*; Academic Press: London, U.K., 1982.
(44) Matsubara, K.; Kawata, S.; Minami, S. *Appl. Spectrosc.* **1988**, *42*, 1375.
(45) Zhang, L. M.; Uttamchandan, D. *Electron. Lett.* **1988**, *24*, 1469.
(46) Brockman, J. M.; Nelson, B. P.; Corn, R. M. *Annu. Rev. Phys. Chem.* **2000**, *51*, 41.
(47) Ho, C.; Robinson, A.; Miller, D.; Davis, M. *Sensors* **2005**, *5*, 4.
(48) Tumolo, T.; Angnes, L.; Baptista, M. S. *Anal. Biochem.* **2004**, *333*, 273.
(49) de Feijter, J. A.; Benjamins, J.; Veer, F. A. *Biopolymers* **1978**, *17*, 1759.
(50) Snyder, A. W.; Love, J. D. *Optical Waveguide Theory*; Chapman and Hall: London, U.K., 1983.
(51) O'Brien, M. J.; Perez-Luna, V. H.; Brueck, S. R. J.; Lopez, G. P. *Biosens. Bioelectron.* **2001**, *16*, 97.
(52) Kawazumi, H.; Gobi, K. V.; Ogino, K.; Maeda, H.; Miura, N. *Sens. Actuators B* **2005**, *108*, 791.
(53) Piliarik, M.; Vaisocherová, H.; Homola, J. *Biosens. Bioelectron.* **2005**, *20*, 2104.
(54) Berger, C. E. H.; Beumer, T. A. M.; Kooyman, R. P. H.; Greve, J. *Anal. Chem.* **1998**, *70*, 703.
(55) Fu, E.; Chinowsky, T.; Foley, J.; Weinstein, J.; Yager, P. *Rev. Sci. Instrum.* **2004**, *75*, 2300.
(56) Kukanskis, K.; Elkind, J.; Melendez, J.; Murphy, T.; Miller, G.; Garner, H. *Anal. Biochem.* **1999**, *274*, 7.
(57) Goddard, N. J.; Pollardknight, D.; Maule, C. H. *Analyst* **1994**, *119*, 583.
(58) Sjölander, S.; Urbanitzky, C. *Anal. Chem.* **1991**, *63*, 2338.
(59) Stenberg, E.; Persson, B.; Roos, H.; Urbaniczky, C. J. *Colloid Interface Sci.* **1991**, *143*, 513.
(60) Chinowsky, T. M.; Jung, L. S.; Yee, S. S. *Sens. Actuators B* **1999**, *54*, 89.
(61) Tobiška, P.; Homola, J. *Sens. Actuators B* **2005**, *107*, 162.
(62) Nenninger, G. G.; Piliarik, M.; Homola, J. *Meas. Sci. Technol.* **2002**, *13*, 2038.
(63) Thirstrup, C.; Zong, W.; Borre, M.; Neff, H.; Pedersen, H. C.; Holzhueter, G. *Sens. Actuators B* **2004**, *100*, 298.
(64) Dostálek, J.; Homola, J.; Miler, M. *Sens. Actuators B* **2005**, *107*, 154.
(65) Ran, B.; Lipson, S. G. *Opt. Express* **2006**, *14*, 5641.
(66) Thomsen, V.; Schatzlein, D.; Mercuro, D. *Spectroscopy* **2003**, *18*, 112.
(67) Sepulveda, B.; Calle, A.; Lechuga, L. M.; Armelles, G. *Opt. Lett.* **2006**, *31*, 1085.
(68) Jordan, C. E.; Frutos, A. G.; Thiel, A. J.; Corn, R. M. *Anal. Chem.* **1997**, *69*, 4939.
(69) Jordan, C. E.; Corn, R. M. *Anal. Chem.* **1997**, *69*, 1449.
(70) Nelson, B. P.; Frutos, A. G.; Brockman, J. M.; Corn, R. M. *Anal. Chem.* **1999**, *71*, 3928.
(71) Nelson, B. P.; Grimsrud, T. E.; Liles, M. R.; Goodman, R. M.; Corn, R. M. *Anal. Chem.* **2001**, *73*, 1.
(72) Fu, E.; Foley, J.; Yager, P. *Rev. Sci. Instrum.* **2003**, *74*, 3182.
(73) Wark, A. W.; Lee, H. J.; Corn, R. M. *Anal. Chem.* **2005**, *77*, 3904.
(74) Zybin, A.; Grunwald, C.; Mirsky, V. M.; Kuhlmann, J.; Wolfbeis, O. S.; Niemas, K. *Anal. Chem.* **2005**, *77*, 2393.
(75) Shumaker-Parry, J. S.; Campbell, C. T. *Anal. Chem.* **2004**, *76*, 907.
(76) Shumaker-Parry, J. S.; Aebersold, R.; Campbell, C. T. *Anal. Chem.* **2004**, *76*, 2071.
(77) Campbell, C. T.; Kim, G. *Biomaterials* **2007**, *28*, 2380.
(78) Piliarik, M.; Katainen, J.; Homola, J. *Optical Sensing Technology and Applications*; Prague, Czech Republic; SPIE: Bellingham, WA, 2007; p 658515.
(79) Piliarik, M.; Vaisocherová, H.; Homola, J. *Sens. Actuators B* **2007**, *121*, 187.
(80) http://www.gwctechnologies.com.
(81) http://www.lumera.com.
(82) http://www.ibis-spr.nl/.
(83) http://www.genoptics-spr.com/.
(84) Lofas, S.; Malmqvist, M.; Ronnberg, I.; Stenberg, E.; Liedberg, B.; Lundstrom, I. *Sens. Actuators B* **1991**, *5*, 79.
(85) Liedberg, B.; Lundstrom, I.; Stenberg, E. *Sens. Actuators B* **1993**, *11*, 63.
(86) Karlsson, R.; Stahlberg, R. *Anal. Biochem.* **1995**, *228*, 274.
(87) Nice, E. C.; Catimel, B. *Bioessays* **1999**, *21*, 339.
(88) http://www.biacore.com.
(89) Pedersen, H. C.; Thirstrup, C. *Appl. Opt.* **2004**, *43*, 1209.
(90) Pedersen, H. C.; Zong, W. Y.; Sorensen, M. H.; Thirstrup, C. *Opt. Eng.* **2004**, *43*, 2505.
(91) Homola, J.; Dostálek, J.; Chen, S. F.; Rasooly, A.; Jiang, S. Y.; Yee, S. S. *Int. J. Food Microbiol.* **2002**, *75*, 61.
(92) Homola, J.; Lu, H. B.; Yee, S. S. *Electron. Lett.* **1999**, *35*, 1105.
(93) Homola, J.; Lu, H. B. B.; Nenninger, G. G.; Dostálek, J.; Yee, S. S. *Sens. Actuators B* **2001**, *76*, 403.
(94) Dostálek, J.; Vaisocherová, H.; Homola, J. *Sens. Actuators B* **2005**, *108*, 758.
(95) Nenninger, G. G.; Tobiška, P.; Homola, J.; Yee, S. S. *Sens. Actuators B* **2001**, *74*, 145.
(96) Slavík, R.; Homola, J. *Sens. Actuators B* **2007**, *123*, 10.
(97) Melendez, J.; Carr, R.; Bartholomew, D. U.; Kukanskis, K.; Elkind, J.; Yee, S.; Furlong, C.; Woodbury, R. *Sens. Actuators B* **1996**, *35*, 212.
(98) Elkind, J. L.; Stimpson, D. I.. A. A. S. D. U. B.; Melendez, J. L. *Sens. Actuators B* **1999**, *54*, 182.
(99) Chinowsky, T. M.; Quinn, J. G.; Bartholomew, D. U.; Kaiser, R.; Elkind, J. L. *Sens. Actuators B* **2003**, *91*, 266.
(100) Naimushin, A.; Soelberg, S.; Bartholomew, D.; Elkind, J.; Furlong, C. *Sens. Actuators B* **2003**, *96*, 253.
(101) Naimushin, A. N.; Spinelli, C. B.; Soelberg, S. D.; Mann, T.; Stevens, R. C.; Chinowsky, T.; Kauffman, P.; Yee, S.; Furlong, C. E. *Sens. Actuators B* **2005**, *104*, 237.
(102) http://www.ti.com/.
(103) http://www.optrel.de/.
(104) http://www.reichertspr.com/.
(105) http://www.plasmonic.de/.
(106) http://www.ecochemie.nl/.
(107) http://dkktoa.net/index.html.
(108) http://www.biosuplar.com/.
(109) http://www.sensia.es/.
(110) Nikitin, P. I.; Beloglazov, A. A.; Kochergin, V. E.; Valeiko, M. V.; Ksenevich, T. I. *Sens. Actuators B* **1999**, *54*, 43.
(111) Nikitin, P. I.; Grigorenko, A. N.; Beloglazov, A. A.; Valeiko, M. V.; Savchuk, A. I.; Savchuk, O. A.; Steiner, G.; Kuhne, C.; Huebner, A.; Salzer, R. *Sens. Actuators A* **2000**, *85*, 189.
(112) Notcovich, A. G.; Zhuk, V.; Lipson, S. G. *Appl. Phys. Lett.* **2000**, *76*, 1665.
(113) Wu, C.-M.; Jian, Z.-C.; Joe, S.-F.; Chang, L.-B. *Sens. Actuators B* **2003**, *92*, 133.
(114) Alieva, E. V.; Konopsky, V. N. *Sens. Actuators B* **2004**, *99*, 90.
(115) Naraoka, R.; Kajikawa, K. *Sens. Actuators B* **2005**, *107*, 952.
(116) Ho, H. P.; Lam, W. W.; Wu, S. Y. *Rev. Sci. Instrum.* **2002**, *73*, 3534.
(117) Wu, S. Y.; Ho, H. P.; Law, W. C.; Lin, C. L.; Kong, S. K. *Opt. Lett.* **2004**, *29*, 2378.
(118) Ho, H. P.; Law, W. C.; Wu, S. Y.; Lin, C. L.; Kong, S. K. *Biosens. Bioelectron.* **2005**, *20*, 2177.
(119) Ho, H. P.; Law, W. C.; Wu, S. Y.; Liu, X. H.; Wong, S. P.; Lin, C. L.; Kong, S. K. *Sens. Actuators B* **2006**, *114*, 80.
(120) Yuan, W.; Ho, H. P.; Wong, C. L.; Kong, S. K.; Lin, C. L. *IEEE Sensors J.* **2007**, *7*, 70.
(121) Brockman, J. M.; Fernandez, S. M. *Am. Lab.* **2001**, *33*, 37.

(122) Baggio, R.; Carven, G. J.; Chiulli, A.; Palmer, M.; Stern, L. J.; Arenas, J. E. *J. Biol. Chem.* **2005**, *280*, 4188.
(123) Adam, P.; Dostálek, J.; Homola, J. *Sens. Actuators B* **2006**, *113*, 774.
(124) Adam, P.; Dostálek, J.; Telezhnikova, O.; Homola, J. 2007; p 65851Y.
(125) Vala, M.; Dostálek, J.; Homola, J. 2007; p 658522.
(126) Unfricht, D. W.; Colpitts, S. L.; Fernandez, S. M.; Lynes, M. A. *Proteomics* **2005**, *5*, 4432.
(127) Telezhnikova, O.; Homola, J. *Opt. Lett.* **2006**, *31*, 3339.
(128) Chien, F. C.; Lin, C. Y.; Yih, J. N.; Lee, K. L.; Chang, C. W.; Wei, P. K.; Sun, C. C.; Chen, S. J. *Biosens. Bioelectron.* **2007**, *22*, 2737.
(129) Van Gent, J.; Lambeck, P. V.; Kreuwel, H. J. M.; Gerritsma, G. J.; Sudholter, E. J. R.; Reinhoudt, D. N.; Popma, T. J. A. *Appl. Opt.* **1990**, *29*, 2843.
(130) Jorgenson, R. C.; Yee, S. S. *Sens. Actuators B* **1993**, *12*, 213.
(131) Homola, J. *Sens. Actuators B* **1995**, *29*, 401.
(132) Slavík, R.; Homola, J.; Čtyrok, J. *Sens. Actuators B* **1999**, *54*, 74.
(133) Slavík, R.; Homola, J.; Čtyrok, J.; Brynda, E. *Sens. Actuators B* **2001**, *74*, 106.
(134) Piliarik, M.; Homola, J.; Maniková, Z.; Čtyrok, J. *Sens. Actuators B* **2003**, *90*, 236.
(135) Chiu, M. H.; Wang, S. F.; Chang, R. S. *Opt. Lett.* **2005**, *30*, 233.
(136) Lin, H. Y.; Tsai, W. H.; Tsao, Y. C.; Sheu, B. C. *Appl. Opt.* **2007**, *46*, 800.
(137) Mouvet, C.; Harris, R.; Maciag, C.; Luff, B.; Wilkinson, J.; Piehler, J.; Brecht, A.; Gauglitz, G.; Abuknesha, R.; Ismail, G. *Anal. Chim. Acta* **1997**, *338*, 109.
(138) Harris, R. D.; Luff, B. J.; Wilkinson, J. S.; Piehler, J.; Brecht, A.; Gauglitz, G.; Abuknesha, R. A. *Biosens. Bioelectron.* **1999**, *14*, 377.
(139) Dostálek, J.; Čtyrok, J.; Homola, J.; Brynda, E.; Skalsk, M.; Nekvindová, P.; Spirková, J.; Škvor, J.; Schrofel, J. *Sens. Actuators, B* **2001**, *76*, 8.
(140) Huang, J. G.; Lee, C. L.; Lin, H. M.; Chuang, T. L.; Wang, W. S.; Juang, R. H.; Wang, C. H.; Lee, C. K.; Lin, S. M.; Lin, C. W. *Biosens. Bioelectron.* **2006**, *22*, 519.
(141) Harris, R. D.; Wilkinson, J. S. *Sens. Actuators B* **1995**, *29*, 261.
(142) Lavers, C. R.; Wilkinson, J. S. *Sens. Actuators B* **1994**, *22*, 75.
(143) Ctyroky, J.; Homola, J.; Skalsky, M. *Electron. Lett.* **1997**, *33*, 1246.
(144) Skorobogatiy, M.; Kabashin, A. V. *Appl. Phys. Lett.* **2006**, 89.
(145) Debackere, P.; Scheerlinck, S.; Bienstman, P.; Baets, R. *Opt. Express* **2006**, *14*, 7063.
(146) Wang, T. J.; Lin, W. S.; Liu, F. K. *Biosens. Bioelectron.* **2007**, *22*, 1441.
(147) Tomizaki, K. Y.; Usui, K.; Mihara, H. *ChemBioChem* **2005**, *6*, 782.
(148) Dunne, L.; Daly, S.; Baxter, A.; Haughey, S.; O'Kennedy, R. *Spectrosc. Lett.* **2005**, *38*, 229.
(149) Scholler, N.; Garvik, B.; Quarles, T.; Jiang, S.; Urban, N. *J. Immunol. Methods* **2006**, *317*, 132.
(150) Rojo, N.; Ercilla, G.; Haro, I. *Curr. Protein Pept. Sci.* **2003**, *4*, 291.
(151) Wittekindt, C.; Fleckenstein, B.; Wiesmuller, K.; Eing, B. R.; Kuhn, J. E. *Virol. J. Methods* **2000**, *87*, 133.
(152) Vaisocherová, H.; Mrkvová, K.; Piliarik, M.; Jinoch, P.; Steinbachová, M.; Homola, J. *Biosens. Bioelectron.* **2007**, *22*, 1020.
(153) Forzani, E. S.; Zhang, H. Q.; Chen, W.; Tao, N. J. *Environ. Sci. Technol.* **2005**, *39*, 1257.
(154) Win, M. N.; Klein, J. S.; Smolke, C. D. *Nucleic Acids Res.* **2006**, *34*, 5670.
(155) Wang, Z.; Wilkop, T.; Xu, D.; Dong, Y.; Ma, G.; Cheng, Q. *Anal. Bioanal. Chem.* **2007**, *389*, 819.
(156) Jayasena, S. D. *Clin. Chem.* **1999**, *45*, 1628.
(157) Zhang, S. G. *Nat. Mater.* **2004**, *3*, 7.
(158) Lofas, S.; Johnsson, B.; Edstrom, A.; Hansson, A.; Lindquist, G.; Hillgren, R. M. M.; Stigh, L. *Biosens. Bioelectron.* **1995**, *10*, 813.
(159) Knoll, W.; Liley, M.; Piscevic, D.; Spinke, J.; Tarlov, M. J. *Adv. Biophys.* **1997**, *34*, 231.
(160) Jung, L. S.; Nelson, K. E.; Stayton, P. S.; Campbell, C. T. *Langmuir* **2000**, *16*, 9421.
(161) Nelson, K. E.; Gamble, L.; Jung, L. S.; Boeckl, M. S.; Naeemi, E.; Golledge, S. L.; Sasaki, T.; Castner, D. G.; Campbell, C. T.; Stayton, P. S. *Langmuir* **2001**, *17*, 2807.
(162) Koubová, V.; Brynda, E.; Karasová, L.; Škvor, J.; Homola, J.; Dostálek, J.; Tobiška, P.; Rosick, J. *Sens. Actuators, B* **2001**, *74*, 100.
(163) Busse, S.; Scheumann, V.; Menges, B.; Mittler, S. *Biosens. Bioelectron.* **2002**, *17*, 704.
(164) Zhen, G. L.; Falconnet, D.; Kuennemann, E.; Voros, J.; Spencer, N. D.; Textor, M.; Zurcher, S. *Adv. Funct. Mater.* **2006**, *16*, 243.
(165) Ladd, J.; Boozer, C.; Yu, Q.; Chen, S.; Homola, J.; Jiang, S. *Langmuir* **2004**, *20*, 8090.
(166) Rusmini, F.; Zhong, Z.; Feijen, J. *Biomacromolecules* **2007**, *8*, 1775.
(167) Oshannessy, D. J.; Brighamburke, M.; Peck, K. *Anal. Biochem.* **1992**, *205*, 132.
(168) Johnson, C. P.; Jensen, I. E.; Prakasam, A.; Vijayendran, R.; Leckband, D. *Bioconjugate Chem.* **2003**, *14*, 974.
(169) Wegner, G. J.; Lee, N. J.; Marriott, G.; Corn, R. M. *Anal. Chem.* **2003**, *75*, 4740.
(170) Lata, S.; Reichel, A.; Brock, R.; Tampe, R.; Piehler, J. *J. Am. Chem. Soc.* **2005**, *127*, 10205.
(171) Tinazli, A.; Tang, J.; Valiokas, R.; Picuric, S.; Lata, S.; Piehler, J.; Liedberg, B.; Tampe, R. *Chemistry* **2005**, *11*, 5249.
(172) Valiokas, R.; Klenkar, G.; Tinazli, A.; Tampe, R.; Liedberg, B.; Piehler, J. *ChemBioChem* **2006**, *7*, 1325.
(173) Vaisocherová, H.; Zítová, A.; Lachmanová, M.; Štčpánek, J.; Rosenberg, I.; Králíková, S.; Liboska, R.; Rejman, D.; Homola, J. *Biopolymers* **2006**.
(174) Hermanson, G. T. *Bioconjugate Techniques*; Academic Press: San Diego, CA, 1996.
(175) Shumaker-Parry, J. S.; Zareie, M. H.; Aebersold, R.; Campbell, C. T. *Anal. Chem.* **2004**, *76*, 918.
(176) Joos, T. O.; Schrenk, M.; Hopfl, P.; Kroger, K.; Chowdhury, U.; Stoll, D.; Schorner, D.; Durr, M.; Herick, K.; Rupp, S.; Sohn, K.; Hammerle, H. *Electrophoresis* **2000**, *21*, 2641.
(177) Calvo, K. R.; Liotta, L. A.; Petricoin, E. F. *Biosci. Rep.* **2005**, *25*, 107.
(178) Huang, R. P. *Frontiers Biosci.* **2003**, *8*, D559.
(179) Figeys, D. *Proteomics* **2002**, *2*, 373.
(180) Blattler, T. M.; Pasche, S.; Textor, M.; Griesser, H. J. *Langmuir* **2006**, *22*, 5760.
(181) Pasche, S.; Textor, M.; Meagher, L.; Spencer, N. D.; Griesser, H. J. *Langmuir* **2005**, *21*, 6508.
(182) Pasche, S.; De Paul, S. M.; Voros, J.; Spencer, N. D.; Textor, M. *Langmuir* **2003**, *19*, 9216.
(183) Pasche, S.; Textor, M.; Meagher, L.; Spencer, N. D.; Griesser, H. J. *Langmuir* **2005**, *21*, 6508.
(184) Huang, N. P.; Voros, J.; De Paul, S. M.; Textor, M.; Spencer, N. D. *Langmuir* **2002**, *18*, 220.
(185) Fei, X.; Guoliang, Z.; Marcus, T.; Wolfgang, K. *Biointerphases* **2006**, *1*, 73.
(186) Marie, R.; Dahlin, A. B.; Tegenfeldt, J. O.; Hook, F. *Biointerphases* **2007**, *2*, 49.
(187) Frederix, F.; Bonroy, K.; Reekmans, G.; Laureyn, W.; Campitelli, A.; Abramov, M. A.; Dehaen, W.; Maes, G. *J. Biochem. Biophys. Methods* **2004**, *58*, 67.
(188) Feng, C. L.; Zhang, Z.; Forch, R.; Knoll, W.; Vancso, G. J.; Schonherr, H. *Biomacromolecules* **2005**, *6*, 3243.
(189) Mancebo, H. S.; Lee, G.; Flygare, J.; Tomassini, J.; Luu, P.; Zhu, Y.; Peng, J.; Blau, C.; Hazuda, D.; Price, D.; Flores, O. *Genes Dev.* **1997**, *11*, 2633.
(190) Harbers, G. M.; Emoto, K.; Greef, C.; Metzger, S. W.; Woodward, H. N.; Mascali, J. J.; Grainger, D. W.; Lochhead, M. J. *Chem. Mater.* **2007**, *19*, 4405.
(191) Ostuni, E.; Chapman, R. G.; Liang, M. N.; Meluleni, G.; Pier, G.; Ingber, D. E.; Whitesides, G. M. *Langmuir* **2001**, *17*, 6336.
(192) Bearinger, J. P.; Terrettaz, S.; Michel, R.; Tirelli, N.; Vogel, H.; Textor, M.; Hubbell, J. *A. Nat. Mater.* **2003**, *2*, 259.
(193) Li, L.; Chen, S.; Jiang, S. *J. Biomater. Sci., Polym. Ed.* **2007**, *18*, 1415.
(194) Holmlin, R. E.; Chen, X. X.; Chapman, R. G.; Takayama, S.; Whitesides, G. M. *Langmuir* **2001**, *17*, 2841.
(195) Kitano, H.; Kawasaki, A.; Kawasaki, H.; Morokoshi, S. *J. Colloid Interface Sci.* **2005**, *282*, 340.
(196) Zhang, Z.; Chen, S.; Jiang, S. *Biomacromolecules* **2006**, *7*, 3311.
(197) Cheng, G.; Zhang, Z.; Chen, S. F.; Bryers, J. D.; Jiang, S. Y. *Biomaterials* **2007**, *28*, 4192.
(198) Chen, S.; Liu, L.; Jiang, S. *Langmuir* **2006**, *22*, 2418.
(199) Vaisocherová, H.; Mrkvová, K.; Piliarik, M.; Jinoch, P.; Steinbachová, M.; Homola, J. *Biosens. Bioelectron.* **2007**, *22*, 1020.
(200) Ayela, C.; Roquet, F.; Valera, L.; Granier, C.; Nicu, L.; Pugniere, M. *Biosens. Bioelectron.* **2007**, *22*, 3113.
(201) Cao, C.; Kim, J. P.; Kim, B. W.; Chae, H.; Yoon, H. C.; Yang, S. S.; Sim, S. J. *Biosens. Bioelectron.* **2006**, *21*, 2106.
(202) Chung, J. W.; Kim, S. D.; Bernhardt, R.; Pyun, J. C. *Sens. Actuators B* **2005**, *111*, 416.
(203) Gobi, K. V.; Iwasaka, H.; Miura, N. *Biosens. Bioelectron.* **2007**, *22*, 1382.
(204) Lahiri, J.; Isaacs, L.; Tien, J.; Whitesides, G. M. *Anal. Chem.* **1999**, *71*, 777.
(205) Habauzit, D.; Chopineau, J.; Roig, B. *Anal. Bioanal. Chem.* **2007**, *387*, 1215.
(206) Shankaran, D. R.; Gobi, K. V. A.; Miura, N. *Sens. Actuators B* **2007**, *121*, 158.
(207) Seydack, M. *Biosens. Bioelectron.* **2005**, *20*, 2454.
(208) Chung, J. W.; Bernhardt, R.; Pyun, J. C. *Immunol. J. Methods* **2006**, *311*, 178.

(209) Mauriz, E.; Calle, A.; Manclus, J. J.; Montoya, A.; Lechuga, L. M. *Anal. Bioanal. Chem.* **2007**, *387*, 1449.
(210) Kubitschko, S.; Spinke, J.; Bruckner, T.; Pohl, S.; Oranth, N. *Anal. Biochem.* **1997**, *253*, 112.
(211) Lyon, L. A.; Musick, M. D.; Smith, P. C.; Reiss, B. D.; Pena, D. J.; Natan, M. *J. Sens. Actuators B* **1999**, *54*, 118.
(212) Mitchell, J. S.; Wu, Y.; Cook, C. J.; Main, L. *Anal. Biochem.* **2005**, *343*, 125.
(213) Sato, Y.; Ikegaki, S.; Suzuki, K.; Kawaguchi, H. *J. Biomater. Sci. Polym. Ed.* **2003**, *14*, 803.
(214) Okumura, A.; Sato, Y.; Kyo, M.; Kawaguchi, H. *Anal. Biochem.* **2005**, *339*, 328.
(215) Sato, Y.; Sato, Y.; Okumura, A.; Suzuki, K.; Kawaguchi, H. *J. Biomater. Sci. Polym. Ed.* **2004**, *15*, 297.
(216) Komatsu, H.; Miyachi, M.; Fujii, E.; Citterio, D.; Yamada, K.; Sato, Y.; Kurihara, K.; Kawaguchi, H.; Suzuki, K. *Sci. Technol. Adv. Mater.* **2006**, *7*, 150.
(217) Goodrich, T. T.; Lee, H. J.; Corn, R. M. *Anal. Chem.* **2004**, *76*, 6173.
(218) Lee, H. J.; Li, Y.; Wark, A. W.; Corn, R. M. *Anal. Chem.* **2005**, *77*, 5096.
(219) Fang, S. P.; Lee, H. J.; Wark, A. W.; Corn, R. M. *J. Am. Chem. Soc.* **2006**, *128*, 14044.
(220) Li, Y.; Lee, H. J.; Corn, R. M. *Anal. Chem.* **2007**, *79*, 1082.
(221) Patel, P. D. *J. AOAC Int.* **2006**, *89*, 805.
(222) Lazcka, O.; Campo, F. J. D.; Munoz, F. X. *Biosens. Bioelectron.* **2007**, *22*, 1205.
(223) Leonard, P.; Hearty, S.; Brennan, J.; Dunne, L.; Quinn, J.; Chakraborty, T.; O'Kennedy, R. *Enzyme Microb. Technol.* **2003**, *32*, 3.
(224) Mello, L. D.; Kubota, L. T. *Food Chem.* **2002**, *77*, 237.
(225) Baeumner, A. J. *Anal. Bioanal. Chem.* **2003**, *377*, 434.
(226) Bergwerff, A. A.; Van Knapen, F. *J. AOAC Int.* **2006**, *89*, 826.
(227) Fratamico, P. M.; Strobaugh, T. P.; Medina, M. B.; Gehring, A. G. *Biotechnol. Tech.* **1998**, *12*, 571.
(228) Oh, B. K.; Kim, Y. K.; Bae, Y. M.; Lee, W. H.; Choi, J. W. *J. Microb. Biotechnol.* **2002**, *12*, 780.
(229) Oh, B. K.; Lee, W.; Lee, W. H.; Choi, J. W. *Biotechnol. Bioprocess Eng.* **2003**, *8*, 227.
(230) Taylor, A. D.; Yu, Q. M.; Chen, S. F.; Homola, J.; Jiang, S. Y. *Sens. Actuators B* **2005**, *107*, 202.
(231) Meeusen, C. A.; Alocilja, E. C.; Osburn, W. N. *Trans. ASAE* **2005**, *48*, 2409.
(232) Su, X. L.; Li, Y. *Trans. ASAE* **2005**, *48*, 405.
(233) Subramanian, A.; Irudayaraj, J.; Ryan, T. *Biosens. Bioelectron.* **2006**, *21*, 998.
(234) Taylor, A. D.; Ladd, J.; Yu, Q. M.; Chen, S. F.; Homola, J.; Jiang, S. Y. *Biosens. Bioelectron.* **2006**, *22*, 752.
(235) Waswa, J. W.; Debroy, C.; Irudayaraj, J. *J. Food Process Eng.* **2006**, *29*, 373.
(236) Waswa, J.; Irudayaraj, J.; DebRoy, C. *LWT−Food Sci. Technol.* **2007**, *40*, 187.
(237) Bokken, G.; Corbee, R. J.; van Knapen, F.; Bergwerff, A. A. *FEMS Microbiol. Lett.* **2003**, *222*, 75.
(238) Oh, B. K.; Kim, Y. K.; Park, K. W.; Lee, W. H.; Choi, J. W. *Biosens. Bioelectron.* **2004**, *19*, 1497.
(239) Oh, B. K.; Lee, W.; Kim, Y. K.; Lee, W. H.; Choi, J. W. *J. Biotechnol.* **2004**, *111*, 1.
(240) Mazumdar, S. D.; Hartmann, M.; Kampfer, P.; Keusgen, M. *Biosens. Bioelectron.* **2007**, *22*, 2040.
(241) Leonard, P.; Hearty, S.; Quinn, J.; O'Kennedy, R. *Biosens. Bioelectron.* **2004**, *19*, 1331.
(242) Subramanian, A.; Irudayaraj, J.; Ryan, T. *Sens. Actuators B* **2006**, *114*, 192.
(243) Balasubramanian, S.; Sorokulova, I. B.; Vodyanoy, V. J.; Simonian, A. L. *Biosens. Bioelectron.* **2007**, *22*, 948.
(244) Oh, B. K.; Lee, W.; Chun, B. S.; Bae, Y. M.; Lee, W. H.; Choi, J. W. *Colloids Surf. A* **2005**, *257-58*, *369*.
(245) Jyoung, J. Y.; Hong, S. H.; Lee, W.; Choi, J. W. *Biosens. Bioelectron.* **2006**, *21*, 2315.
(246) Kang, C. D.; Lee, S. W.; Park, T. H.; Sim, S. J. *Enzyme Microb. Technol.* **2006**, *39*, 387.
(247) Zezza, F.; Pascale, M.; Mule, G.; Visconti, A. J. *Microbiol. Methods* **2006**, *66*, 529.
(248) Nedelkov, D.; Rasooly, A.; Nelson, R. W. *Int. J. Food Microbiol.* **2000**, *60*, 1.
(249) Nedelkov, D.; Nelson, R. W. *Appl. Environ. Microbiol.* **2003**, *69*, 5212.
(250) Slavík, R.; Homola, J.; Brynda, E. *Biosens. Bioelectron.* **2002**, *17*, 591.
(251) Naimushin, A. N.; Soelberg, S. D.; Nguyen, D. K.; Dunlap, L.; Bartholomew, D.; Elkind, J.; Melendez, J.; Furlong, C. E. *Biosens. Bioelectron.* **2002**, *17*, 573.
(252) Medina, M. B. *J. Rapid Methods Autom. Microbiol.* **2005**, *13*, 37.
(253) Medina, M. B. *J. Rapid Methods Autom. Microbiol.* **2003**, *11*, 225.
(254) Medina, M. B. *J. Rapid Methods Autom. Microbiol.* **2006**, *14*, 119.
(255) Lotierzo, M.; Henry, O. Y. F.; Piletsky, S.; Tothill, I.; Cullen, D.; Kania, M.; Hock, B.; Turner, A. P. F. *Biosens. Bioelectron.* **2004**, *20*, 145.
(256) Yu, Q. M.; Chen, S. F.; Taylor, A. D.; Homola, J.; Hock, B.; Jiang, S. Y. *Sens. Actuators B* **2005**, *107*, 193.
(257) Traynor, I. M.; Plumpton, L.; Fodey, T. L.; Higgins, C.; Elliott, C. T. *J. AOAC Int.* **2006**, *89*, 868.
(258) Stevens, R. C.; Soelberg, S. D.; Eberhart, B. T. L.; Spencer, S.; Wekell, J. C.; Chinowsky, T. M.; Trainer, V. L.; Furlong, C. E. *Harmful Algae* **2007**, *6*, 166.
(259) Daly, S. J.; Keating, G. J.; Dillon, P. P.; Manning, B. M.; O'Kennedy, R.; Lee, H. A.; Morgan, M. R. A. *J. Agric. Food Chem.* **2000**, *48*, 5097.
(260) Tudos, A. J.; Lucas-van den Bos, E. R.; Stigter, E. C. A. *J. Agric. Food Chem.* **2003**, *51*, 5843.
(261) Haughey, S. A.; Baxter, C. A. *J. AOAC Int.* **2006**, *89*, 862.
(262) Cacciatore, G.; Petz, M.; Rachid, S.; Hakenbeck, R.; Bergwerff, A. A. *Anal. Chim. Acta* **2004**, *520*, 105.
(263) Ashwin, H. M.; Stead, S. L.; Taylor, J. C.; Startin, J. R.; Richmond, S. F.; Homer, V.; Bigwood, T.; Sharman, M. *Anal. Chim. Acta* **2005**, *529*, 103.
(264) Ferguson, J.; Baxter, A.; Young, P.; Kennedy, G.; Elliott, C.; Weigel, S.; Gatermann, R.; Ashwind, H.; Stead, S.; Sharman, M. *Anal. Chim. Acta* **2005**, *529*, 109.
(265) Dumont, V.; Huet, A. C.; Traynor, I.; Elliott, C.; Delahaut, P. *Anal. Chim. Acta* **2006**, *567*, 179.
(266) Moeller, N.; Mueller-Seitz, E.; Scholz, O.; Hillen, W.; Bergwerff, A. A.; Petz, M. *Eur. Food Res. Technol.* **2007**, *224*, 285.
(267) Caldow, M.; Stead, S. L.; Day, J.; Sharman, M.; Situ, C.; Elliott, C. *J. Agric. Food Chem.* **2005**, *53*, 7367.
(268) Caelen, I.; Kalman, A.; Wahlstrom, L. *Anal. Chem.* **2004**, *76*, 137.
(269) Haughey, S. A.; O'Kane, A. A.; Baxter, G. A.; Kalman, A.; Trisconi, M. J.; Indyk, H. E.; Watene, G. A. *J. AOAC Int.* **2005**, *88*, 1008.
(270) Indyk, H. E.; Evans, E. A.; Caselunghe, M. C. B.; Persson, B. S.; Finglas, P. M.; Woollard, D. C.; Filonzi, E. L. *J. AOAC Int.* **2000**, *83*, 1141.
(271) Indyk, H. E.; Persson, B. S.; Caselunghe, M. C. B.; Moberg, A.; Filonzi, E. L.; Woollard, D. C. *J. AOAC Int.* **2002**, *85*, 72.
(272) Gillis, E. H.; Gosling, J. P.; Sreenan, J. M.; Kane, M. *J. Immunol. Methods* **2002**, *267*, 131.
(273) Gillis, E. H.; Traynor, I.; Gosling, J. P.; Kane, M. *J. AOAC Int.* **2006**, *89*, 838.
(274) Kim, T. J.; Cho, H. S.; Park, N. Y.; Lee, J. I. *J. Vet. Med. Ser. B: Infect. Dis. Vet. Public Health* **2006**, *53*, 87.
(275) Cho, H. S.; Park, N. Y. *J. Vet. Med. Sci.* **2006**, *68*, 1327.
(276) Mohammed, I.; Mullett, W. M.; Lai, E. P. C.; Yeung, J. M. *Anal. Chim. Acta* **2001**, *444*, 97.
(277) Malmheden Yman, I.; Eriksson, A.; Johansson, M. A.; Hellenas, K. E. *J. AOAC Int.* **2006**, *89*, 856.
(278) Dupont, D.; Muller-Renaud, S. *J. AOAC Int.* **2006**, *89*, 843.
(279) Indyk, H. E.; Filonzi, E. L.; Gapper, L. W. *J. AOAC Int.* **2006**, *89*, 898.
(280) Samsonova, J. V.; Uskova, N. A.; Andresyuk, A. N.; Franek, M.; Elliott, C. T. *Chemosphere* **2004**, *57*, 975.
(281) Guidi, A.; Laricchia-Robbio, L.; Gianfaldoni, D.; Revoltella, R.; Del Bono, G. *Biosens. Bioelectron.* **2001**, *16*, 971.
(282) Pejcic, B.; De Marco, R.; Parkinson, G. *Analyst* **2006**, *131*, 1079.
(283) Andreescu, S.; Sadik, O. A. *Pure Appl. Chem.* **2004**, *76*, 861.
(284) Healy, D. A.; Hayes, C. J.; Leonard, P.; McKenna, L.; O'Kennedy, R. *Trends Biotechnol.* **2007**, *25*, 125.
(285) Besselink, G. A.; Kooyman, R. P.; van Os, P. J.; Engbers, G. H.; Schasfoort, R. B. *Anal. Biochem.* **2004**, *333*, 165.
(286) Wu, L. P.; Li, Y. F.; Huang, C. Z.; Zhang, Q. *Anal. Chem.* **2006**, *78*, 5570.
(287) Chung, J. W.; Bernhardt, R.; Pyun, J. C. *Sens. Actuators B* **2006**, *118*, 28.
(288) Yang, C. Y.; Brooks, E.; Li, Y.; Denny, P.; Ho, C. M.; Qi, F. X.; Shi, W. Y.; Wolinsky, L.; Wu, B.; Wong, D. T. W.; Montemagno, C. D. *Lab Chip* **2005**, *5*, 1017.
(289) Tang, D. P.; Yuan, R.; Chai, Y. Q. *Bioprocess Biosyst. Eng.* **2006**, *28*, 315.
(290) Regnault, V.; Boehlen, F.; Ozsahin, H.; Wahl, D.; de Groot, P. G.; Lecompte, T.; de Moerloose, P. *J. Thromb. Haemostasis* **2005**, *3*, 1243.
(291) McGill, A.; Greensill, J.; Marsh, R.; Craft, A. W.; Toms, G. L. *J. Med. Virol.* **2004**, *74*, 492.
(292) Abad, L. W.; Neumann, M.; Tobias, L.; Obenauer-Kutner, L.; Jacobs, S.; Cullen, C. *Anal. Biochem.* **2002**, *310*, 107.
(293) Dillon, P. P.; Daly, S. J.; Manning, B. M.; O'Kennedy, R. *Biosens. Bioelectron.* **2003**, *18*, 217.
(294) Fitzpatrick, B.; O'Kennedy, R. *J. Immunol. Methods* **2004**, *291*, 11.

(295) Rini, B.; Wadhwa, M.; Bird, C.; Small, E.; Gaines-Das, R.; Thorpe, R. *Cytokine* **2005**, *29*, 56.
(296) Kure, M.; Katsura, Y.; Kosano, H.; Noritake, M.; Watanabe, T.; Iwaki, Y.; Nishigori, H.; Matsuoka, T. *Intern. Med.* **2005**, *44*, 100.
(297) Miyashita, M.; Shimada, T.; Miyagawa, H.; Akamatsu, M. *Anal. Bioanal. Chem.* **2005**, *381*, 667.
(298) Teramura, Y.; Iwata, H. *Anal. Biochem.* **2007**, *365*, 201.
(299) Li, Y.; Kobayashi, M.; Furui, K.; Soh, N.; Nakano, K.; Imato, T. *Anal. Chim. Acta* **2006**, *576*, 77.
(300) Wei, J.; Mu, Y.; Song, D.; Fang, X.; Liu, X.; Bu, L.; Zhang, H.; Zhang, G.; Ding, J.; Wang, W.; Jin, Q.; Luo, G. *Anal. Biochem.* **2003**, *321*, 209.
(301) Masson, J. F.; Obando, L.; Beaudoin, S.; Booksh, K. *Talanta* **2004**, *62*, 865.
(302) Kim, J. Y.; Lee, M. H.; Jung, K. I.; Na, H. Y.; Cha, H. S.; Ko, E. M.; Kim, T. *J. Exp. Mol. Med*. **2003**, *35*, 310.
(303) Lee, J. W.; Sim, S. J.; Cho, S. M.; Lee, J. *Biosens. Bioelectron*. **2005**, *20*, 1422.
(304) Choi, S. H.; Lee, J. W.; Sim, S. *J. Biosens. Bioelectron.* **2005**, *21*, 378.
(305) Meyer, M. H. F.; Hartmann, M.; Keusgen, M. *Biosens. Bioelectron.* **2006**, *21*, 1987.
(306) Lee, H. J.; Nedelkov, D.; Corn, R. M. *Anal. Chem*. **2006**, *78*, 6504.
(307) Hwang, S. Y.; Yoo, C. H.; Jeon, J. Y.; Choi, S. C.; Lee, E. K. *Biotechnol. Bioprocess Eng*. **2005**, *10*, 309.
(308) Rodriguez-Mozaz, S.; de Alda, M. J. L.; Barcelo, D. *Anal. Bioanal. Chem*. **2006**, *386*, 1025.
(309) Minunni, M.; Mascini, M. *Anal. Lett*. **1993**, *26*, 1441.
(310) Farre, M.; Martinez, E.; Ramon, J.; Navarro, A.; Radjenovic, J.; Mauriz, E.; Lechuga, L.; Marco, M. P.; Barcelo, D. *Anal. Bioanal. Chem*. **2007**, *388*, 207.
(311) Lim, T. K.; Oyama, M.; Ikebukuro, K.; Karube, I. *Anal. Chem*. **2000**, *72*, 2856.
(312) Mauriz, E.; Calle, A.; Manclus, J. J.; Montoya, A.; Escuela, A. M.; Sendra, J. R.; Lechuga, L. M. *Sens. Actuators B* **2006**, *118*, 399.
(313) Mauriz, E.; Calle, A.; Abad, A.; Montoya, A.; Hildebrandt, A.; Barcelo, D.; Lechuga, L. M. *Biosens. Bioelectron*. **2006**, *21*, 2129.
(314) Mauriz, E.; Calle, A.; Lechuga, L. M.; Quintana, J.; Montoya, A.; Manclus, J. *J. Anal. Chim. Acta* **2006**, *561*, 40.
(315) Mauriz, E.; Calle, A.; Manclus, J. J.; Montoya, A.; Hildebrandt, A.; Barcelo, D.; Lechuga, L. M. *Biosens. Bioelectron*. **2007**, *22*, 1410.
(316) Gobi, K. V.; Tanaka, H.; Shoyama, Y.; Miura, N. *Sens. Actuators B* **2005**, *111*, 562.
(317) Kim, S. J.; Gobi, K. V.; Tanaka, H.; Shoyama, Y.; Miura, N. *Chem. Lett*. **2006**, *35*, 1132.
(318) Shankaran, D. R.; Matsumoto, K.; Toko, K.; Miura, N. *Electrochemistry* **2006**, *74*, 141.
(319) Shankaran, D. R.; Gobi, K. V.; Sakai, T.; Matsumoto, K.; Imato, T.; Toko, K.; Miura, N. *IEEE Sensors J.* **2005**, *5*, 616.
(320) Shankaran, D. R.; Kawaguchi, T.; Kim, S. J.; Matsumoto, K.; Toko, K.; Miura, N. *Anal. Bioanal. Chem*. **2006**, *386*, 1313.
(321) Matsumoto, K.; Torimaru, A.; Ishitobi, S.; Sakai, T.; Ishikawa, H.; Toko, K.; Miura, N.; Imato, T. *Talanta* **2005**, *68*, 305.
(322) Shankaran, D. R.; Matsumoto, K.; Toko, K.; Miura, N. *Sens. Actuators B* **2006**, *114*, 71.
(323) Kumbhat, S.; Shankaran, D. R.; Kim, S. J.; Gobi, K. V.; Joshi, V.; Miura, N. *Chem. Lett*. **2006**, *35*, 678.
(324) Larsson, A.; Angbrant, J.; Ekeroth, J.; Mansson, P.; Liedberg, B. *Sens. Actuators B* **2006**, *113*, 730.
(325) Gobi, K.; Tanaka, H.; Shoyama, Y.; Miura, N. *Biosens. Bioelectron*. **2004**, *20*, 350.
(326) Kim, S. J.; Gobi, K. V.; Harada, R.; Shankaran, D. R.; Miura, N. *Sens. Actuators B* **2006**, *115*, 349.
(327) Miura, N.; Sasaki, M.; Gobi, K. V.; Kataoka, C.; Shoyama, Y. *Biosens. Bioelectron*. **2003**, *18*, 953.
(328) Gobi, K.; Miura, N. *Sens. Actuators B* **2004**, *103*, 265.
(329) Gobi, K. V.; Kataoka, C.; Miura, N. *Sens. Actuators B* **2005**, *108*, 784.
(330) Ock, K.; Jang, G.; Roh, Y.; Kim, S.; Kim, J.; Koh, K. *Microchem. J*. **2001**, *70*, 301.
(331) Wu, C.-M.; Lin, L.-Y. *Biosens. Bioelectron.* **2004**, *20*, 864.
(332) Soh, N.; Watanabe, T.; Asano, Y.; Imato, T. *Sensor Mater.* **2003**, *15*, 423.
(333) Soh, N.; Tokuda, T.; Watanabe, T.; Mishima, K.; Imato, T.; Masadome, T.; Asano, Y.; Okutani, S.; Niwa, O.; Brown, S. *Talanta* **2003**, *60*, 733.
(334) Matsumoto, K.; Sakai, T.; Torimaru, A.; Ishitobi, S. J. *Fac. Agric. Kyushu Univ.* **2005**, *50*, 625.
(335) Shimomura, M.; Nomura, Y.; Zhang, W.; Sakino, M.; Lee, K. H.; Ikebukuro, K.; Karube, I. *Anal. Chim. Acta* **2001**, *434*, 223.

CR068107D